NTNU

Norwegian University of
Science and Technology

An experimental and numerical study of bolt and nut assemblies under tension loading

Stian Johansen

Espen Waldeland

Civil and Environmental Engineering

Submission date: June 2016

Supervisor: Arild Holm Clausen, KT

Co-supervisor: Arne Aalberg, KT

Eirik Løhre Grimsmo, KT

Norwegian University of Science and Technology

Department of Structural Engineering

Department of Structural Engineering
Faculty of Engineering Science and Technology
NTNU- Norwegian University of Science and Technology

ACCESSIBILITY

OPEN

MASTER THESIS 2016

SUBJECT AREA:	DATE:	NO. OF PAGES:
Computational Mechanics	10.06.2016	21+122+35

TITLE:

An experimental and numerical study of bolt and nut assemblies under tension loading

En eksperimentell og numerisk studie av strekkbelastede konstruksjonsbolter

BY:

Stian Johansen

Espen Waldeland

SUMMARY:
The purpose of this master thesis is to investigate how the nut position affects the failure mode of single tensile loaded bolts under quasi-static conditions. A ductile bolt fracture is preferable from an engineering perspective, as opposed to thread stripping which is typically regarded as a brittle fracture mode. It is advantageous with large deformation of bolts in extreme load cases, because this is easier to detect upon inspection.

Various partially threaded bolt and nut types were investigated in experimental tests. Different nut positions were tested for a range of bolt and nut configurations. Experimental tests showed that thread stripping was more likely to occur when the nut was positioned close to the unthreaded part of the bolt. It was also registered that the use of a high nut or two regular nuts resulted in bolt fracture regardless of the nut position. One Vickers hardness test of each bolt and nut type were also performed.

In addition to experimental testing, finite element models were used to investigate how material and geometrical factors influenced the failure modes. Another objective was to investigate if a 3D model including the helical shape of the threads gave better prediction of the failure modes, compared with an axisymmtric model. All models were able to predict both bolt fracture and thread stripping with reasonable accuracy.

Finite element modeling revealed that material and geometrical factors highly influenced the failure mode of tensile loaded bolts. The 3D helix model was more accurate in predicting the correct physical behaviour because of more accurate geometry, however with a massive increase in computational cost. Anyhow, the axisymmetric model gave reasonable results with only a fraction of the computational cost.

RESPONSIBLE TEACHER: Arild Holm Clausen

SUPERVISOR(S): Arild Holm Clausen, Erik Løhre Grimsmo, Arne Aalberg

CARRIED OUT AT:SIMLab, Department of Structural Engineering, NTNU

MASTER THESIS 2016

Stian Johansen and Espen Waldeland

An experimental and numerical study of bolt and nut assemblies under tension loading

(En eksperimentell og numerisk studie av strekkbelastede konstruksjonsbolter)

This master thesis is a continuation of a master's thesis carried out by E.S. Skavhaug and S.I. Østhus in the spring term of 2015. They found that the failure mode of a bolt loaded in tension may be thread stripping or net failure of the threaded part of the shank, depending on the grip length between the unthreaded shank and the nut. Failure by thread stripping is undesired because this is a more brittle mode. The intention with the present thesis is to look at some features that were not investigated in the previous work, for instance different bolt and nut types, pre-tensioning of bolt and class (strength) of material in the bolt and nut.

The experimental programme of this master thesis involves tests on single bolts with nuts, where the number of threads between the nut and the unthreaded shank is varied. The test matrix should comprise bolts of class 8.8, pre-tensioned not pre-tensioned bolts, different loading rates and different types of nuts. Material tests on the bolts are also required as input for finite element (FE) simulations of the experimental tests.

Some keywords for activities related to this master thesis project may include:

- Literature survey: Behaviour of bolted connections (articles, codes, text books).
- Material tests: Uniaxial tension tests. Identification of parameters for numerical model.
- Single-bolt tests: Survey exploring the effect of different parameters.
- Numerical analyses: Preparation of FE model. FE simulations of tests.

The candidates may agree with the supervisors to pay particular attention to specific parts of the investigation, or include other aspects than those already mentioned.

The thesis is to be organized as a research report, recognizing the guidelines provided by Department of Structural Engineering.

Supervisors: Arild Holm Clausen, Erik Løhre Grimsmo, Arne Aalberg

The report is to be handed in not later than 10 June 2016.

NTNU, 12 January 2016

Arild Holm Clausen

Preface

This master thesis has been performed at the Norwegian University of Science and Technology (NTNU) for the research group Structural Impact Laboratory (SIMLab) at the Department of Structural Engineering. All experimental tests performed for this thesis has been carried out at the Department of Structural Engineering.

In addition to be the final work for the five years study of Civil Engineering, this master thesis has given good knowledge of structural steel bolts, mechanics and the theory of the Finite Element Method. It has also given great experience in practical use of finite element modeling.

We would like express our gratitude to our supervisors Professor Arild H. Clausen and PhD candidate Erik L. Grimsmo for their daily guidance and vital feedback. Their outstanding knowledge and experience has been important, and the result would not have been the same without. We would also like to thank PhD candidate Petter H. Holmstrøm for valuable help in the art of Python scripting and troubleshooting. In addition, we would like to thank Associate Professor David Morin and PhD candidate Sindre N. Olufsen for helpful guidance and debugging in Abaqus. Furthermore, we would like to thank Senior Engineer Trond Auestad for his guidance in the laboratory and Researcher Egil Fagerholt for guidance in use of DIC.

Trondheim, Friday 10^{th} June, 2016

Stian Johansen

Espen Waldeland

Abstract

The purpose of this master thesis is to investigate how the nut position affects the failure mode of single tensile loaded bolts under quasi-static conditions. A ductile bolt fracture is preferable from an engineering perspective, as opposed to thread stripping which is typically regarded as a brittle fracture mode. It is advantageous with large bolt deformations in cases of extreme loads, because this is easier to detect upon inspection.

Various partially threaded bolt and nut types were investigated in experimental tests. Different nut positions were tested for a range of bolt and nut configurations. Experimental tests showed that thread stripping was more likely to occur when the nut was positioned close to the unthreaded part of the bolt. It was also registered that the use of a high nut or two regular nuts resulted in bolt fracture regardless of the nut position. One *Vickers hardness test* of each bolt and nut type were also performed.

In addition to experimental testing, finite element models were used to investigate how material and geometrical factors influenced the failure modes. Another objective was to investigate if a 3D model including the helical shape of the threads gave better prediction of the failure modes, compared with an axisymmtric model. All models were able to predict both bolt fracture and thread stripping with reasonable accuracy.

Finite element modeling revealed that material and geometrical factors highly influenced the failure mode of tensile loaded bolts. The 3D helix model was more accurate in predicting the correct physical behaviour because of more accurate geometry, however with a massive increase in computational cost. Anyhow, the axisymmetric model gave reasonable results with only a fraction of the computational cost.

Sammendrag

Hensikten med denne masteroppgaven er å studere hvordan mutterposisjonen påvirker bruddformen for strekkbelastede bolter under kvasi-statiske forhold. Fra et ingeniørperspektiv er det ønskelig med et duktilt boltebrudd, i motsetning til gjengestripping som ofte er ansett som en sprø bruddform. I ekstreme lasttilfeller er det fordelaktig med store boltedeformasjoner, fordi det er lettere å oppdage ved inspeksjon i etterkant.

Ulike delgjengde bolt- og muttertyper ble strekktestet i laboratorium. Forskjellige mutterplasseringer ble testet for et utvalg av bolt- og mutterkonfigurasjoner.
Strekkforsøkene viste at gjengestripping forekom oftere når mutteren var plassert nærmere den ugjengede delen av skaftet på bolten. Det ble også avdekket at bruk av en høy mutter eller to vanlige muttere ga boltebrudd uavhengig av mutterplassering. I tillegg ble én *Vickers hardhetstest* gjennført for hver type bolt og mutter.

Det ble også gjennomført elementmetodesimuleringer for å undersøke hvordan geometri og materialparametere påvirket bruddformen. Et annet mål med elementmetodesimuleringene var å studere om en 3D modell med heliksformede gjenger beskriver riktig bruddform med bedre forutsigbarhet enn en aksesymmetrisk modell. Alle modellene klarte å gjenskape både gjengestripping og boltebrudd med rimelig nøyaktighet.

Elementmetodesimuleringene avslørte at material og geometri har stor påvirkning på bruddformen. 3D modellen med heliksform klarte bedre å gjennskape fysisk oppførsel på grunn av dens korrekte geometri, men analysetiden var svært lang. En aksesymmetrisk modell ga derimot tilfredstillende resultater, med bare en brøkdel av analysetiden.

Contents

List of Tables

List of Figures

1. *Introduction*

This master thesis is written in conjunction with the work of PhD candidate Erik Løhre Grimsmo for the research group SIMLab at NTNU. It is a continuation of the work carried out by Skavhaug and Østhus [35] in their master thesis the spring of 2015.

The reader is expected to have good knowledge of mechanics and the theory of Finite Element Method (FEM), in addition to basic knowledge of steel bolt design.

1.1 Background

Structural elements are often connected together using steel bolts. Bolt and nut connections are a basic assembly method used in mechanical structures due to easy installation and replacement. Connections is often a critical part of structures and to better understand how and why bolted connections fail, a better understanding of the mechanics of threaded assemblies is vital.

If a bolted assembly is loaded beyond its tension capacity, fracture occurs either in the threads or the bolt cross-section. Thread failure is typically considered as a brittle failure mode, and can be difficult to detect upon inspections. The threads are hidden inside the nut, and the bolt can appear unaffected. On the other hand, bolt fracture gives a more ductile behaviour and is easier to detect because of evident deformation.

Several master thesis carried out at SIMLab revealed that thread stripping often was the failure mode for bolts. This was the result for Frich [22], Kolberg and Willand [27] and Skavhaug and Østhus [35]. It was observed that thread stripping often occurred when the nut was placed in certain positions on the threaded part of the bolt. The distance from the start of the threads to the underside of the nut is defined as the threaded length, L_t, see Figure 3.1a.

For short threaded lengths, the failure mode tended to be thread stripping. Necking occurred in the transition zone between the threaded and unthreaded part of the bolt, because of stress accumulation due to cross-sectional reduction and sharp edges in this area. Threads of the bolt will contract as a result of necking, and thus lowering the overlap of mating threads. Thread stripping will occur when the remaining threads gets overloaded.

On the other hand, for large thread lengths, fracture of the bolt cross-sections occurred. The zone of necking was located far under the nut such that all threads are fully in contact throughout deformation.

1.2 Scope of thesis

This thesis is a continuation of the work by Skavhaug and Østhus [35], and its objective is twofold.

The main objective is to study various bolt and nut types to investigate whether thread stripping is valid in general for short thread lengths.

Subsequently, a comprehensive part of this thesis has been devoted to develop a full 3D FE model including the helical geometry of the threads. Axisymmtric models are commonly used because they are less complex and have low computational cost. The purpose of the 3D model is to see if a full model is more accurate when helical threads are included. Detailed investigation of the fracture modes and stress distribution in the bolt and nut will not be considered.

Structure

The thesis is divided into eight chapters:

- Chapter 2: Literature review of previous work, including both experiments and comparisons of axisymmetric contra 3D FE models.
- Chapter 3: Most of the underlying theory used in this thesis is presented.
- Chapter 4: Description of the laboratory work and experimental test program of bolted assemblies and material tests, along with results.
- Chapter 5: Detailed description for determination of material parameters.
- Chapter 6: A presentation and review of the FE models, in addition with results from the parameter study.
- Chapter 7: Comments and discussions of the results from experimental tests and FE analysis.
- Chapter 8: Concluding remarks and suggestions for further work.

2. *Literature review*

Research of threaded assemblies focus on capacity and failure modes from simplified axisymmetric models. Owing to the improvement of computational power and FEM technology, more comprehensive and complex models has been studied in recent years. This chapter presents some of the work carried out in the research of threaded assemblies.

2.1 Chen and Shih " A study of the helical effect on the thread connection by three dimensional finite element analysis"

Chen and Shih [9] performed numerical tests on 1-inch 8UNC, 12UNF and 16UNF threaded assemblies (common bolt types in US and Canada). Their goal was to investigate the helical effect by the use of a 3D model compared to a axisymmetric model. It was observed that the helical effect had negligible influence on the load distribution over the threads. The axisymmetric model gave a good estimation of the load distribution for the 8UNC and 12UNF assembly, but for the 16UNF assembly the axisymetrical model were 12% higher than the 3D model.

It was also observed that the coefficient of friction did not alter the load distribution considerably, although the load distribution was marginally smoother with higher coefficients.

2.2 Sun and Liao "The effect of helix on the nonlinear analysis of threaded connection"

In this article Sun and Liao [36] investigated an ISO M14 bolt and nut assembly with different pitches, i.e the distance from the crest of one thread to the next. Their goal was to investigate whether an axisymmetric FE assumption is accurate. A 3D model was generated by rotating an axisymmetric cross-section with one pitch height helically around the bolt axis, as seen in Figure 2.1b. To avoid geometrical singularities a small hole in the middle was constructed. They compared different elastic load scenarios and found good agreement between the axisymmetric model and the 3D model, as illustrated in Figure 2.1a.

Furthermore, it was also observed that increased pitches influenced the stress distribution. Higher pitches resulted in larger stress concentrations for the threads close to the nut bearing surface. For shorter pitches the stress concentration was more homogeneous.

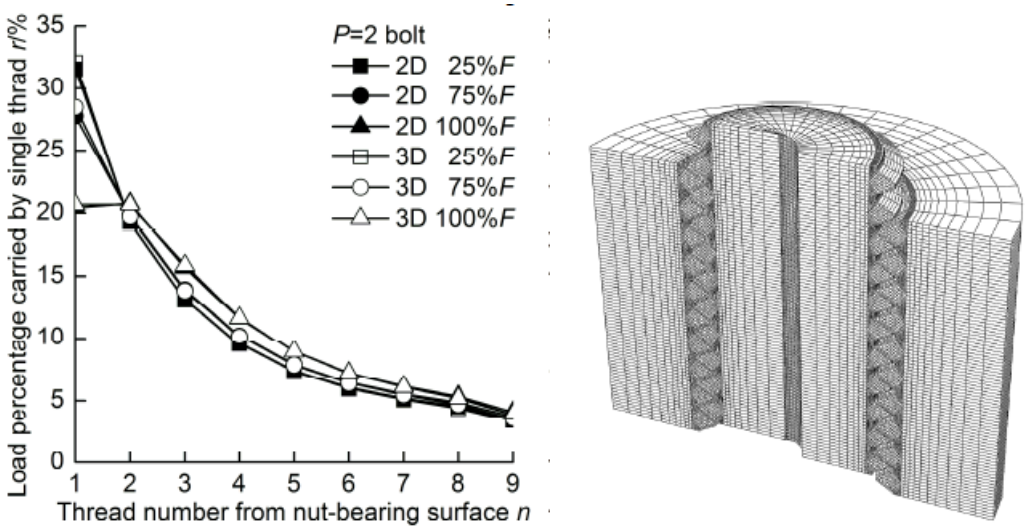

(a) Axial load distribution in threads

(b) Cross-section of 3D FE model

Figure 2.1: Figures from Sun and Liao [36]

2.3 Skavhaug and Østhus "Tension-loaded bolted connections in steel structures "

Skavhaug and Østhus [35] performed experimental tests on single ISO M16 bolts, both fully and partially threaded. A main focus was to investigate how the nut position affects the failure mode of tension loaded bolts. Their experiments showed that bolts with three threads or less between the nut and the unthreaded part of the bolt experienced thread stripping.

FE simulations with an axisymmetric model uncovered that distinctions in nut geometry and material strength had great influence on the fracture mode. This was prevailing for simulations with a low number of free threads between the nut and the unthreaded part of the bolt. Deviations of the nut geometry was investigated considering the bell mouth shape of the nut. The bell mouth shape reduces the height of the outermost threads, and thereby reduces the shear area. Reduction of shear area was additionally assisted when necking initiated close to the underside of the nut. For simulations with only two free threads this altered the fracture mode from bolt fracture to thread stripping, compared to their initial model, as seen in Figure 2.2b.

They also investigated the yield strength of the nut based on results from *Vickers hardness tests*. There was a considerable deviation in the hardness of the nut compared to the bolt. The nut had approximately 77% of the bolt hardness. Based on this, material properties with reduced yield strength was implemented for the nut in FE simulations. The reduction had a great impact, as can been seen in Figure 2.2a. NSR is abbreviation of nut strength reduction.

From their results, it is clear that variation of the nut geometry and material properties influence failure modes of bolted assemblies.

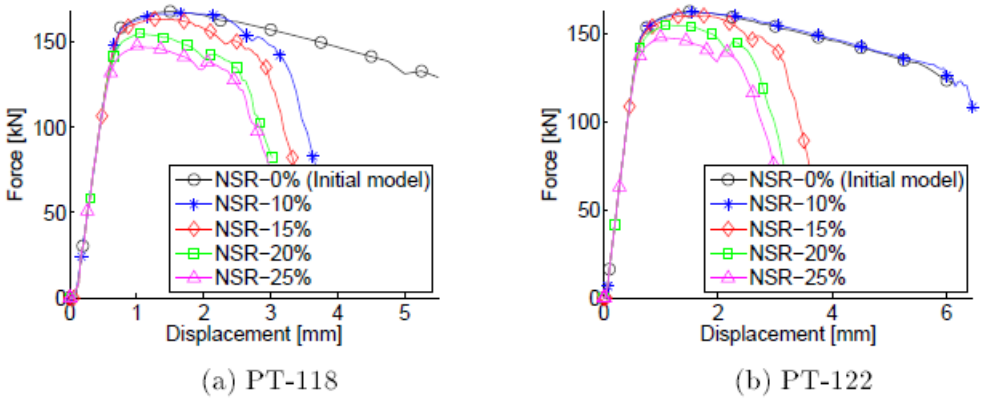

(a) Nut strength reduction for grip length 118 mm og 122 mm

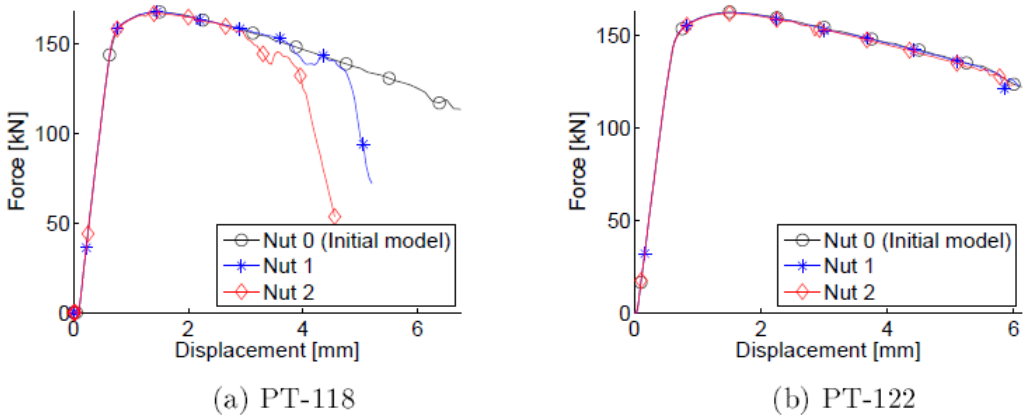

(b) Influence of bell mouth shape for grip length 118 mm og 122 mm

Figure 2.2: Parameter studies of nut strength reduction and bell mouth shape by Skavhaug and Østhus [35]

3. *Theory*

This chapter presents the most important theory applied in this thesis.

3.1 Analytical design of threaded assemblies

Failure of threaded fasteners subjected to static tensile force can be divided into three types of failure modes [8]:

- **Bolt fracture**
- **Bolt thread stripping**
- **Nut thread stripping**

Alexander [7] presented factors that influences the failure mode, and proposed equations for the capacity of each failure mode:

- **Bolt fracture**

$$F_{bf} = \sigma_b \cdot A_s \tag{3.1}$$

- **Bolt thread stripping**

$$F_{bs} = \sigma_b \cdot AS_s \cdot C_1 \cdot C_2 \cdot 0.6 \tag{3.2}$$

- **Nut thread stripping**

$$F_{ns} = \sigma_n \cdot AS_n \cdot C_1 \cdot C_3 \cdot 0.6 \tag{3.3}$$

where σ_b and σ_n are the ultimate stress of the bolt and nut, C_1, C_2, and C_3 are material factors, A_s is the cross-sectional area in the threaded part, AS_b and AS_n are the shear area of the bolt and nut. The shear area is defined by the overlapping (mating) threads, as illustrated in Figure 3.1b.

The factor 0.6 is included to represent the ultimate shear stress, i.e. τ_b, as the threads fail by shear.

$$0.6 \cdot \sigma_b \simeq \tau_b \qquad\qquad \frac{1}{\sqrt{3}} \simeq 0.6$$

The capacity of the threaded assemblies depends on geometrical and material factors. Geometrical factors include the tensile stress area, A_s, and the shear area for bolt and nut, AS_s and AS_n. As seen in Eq. 3.1, the ultimate bolt tensile force is proportional to the tensile area.

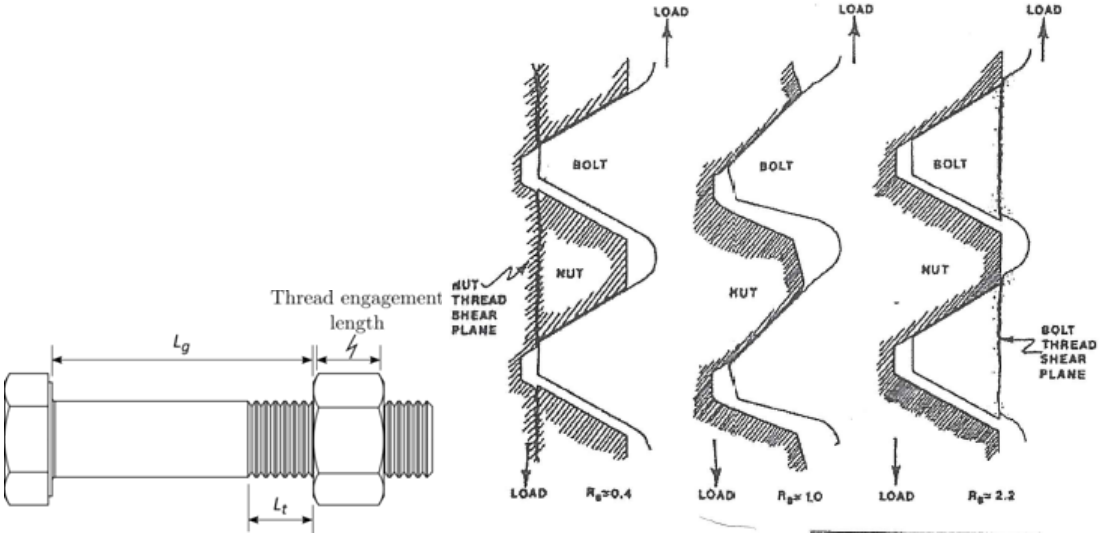

(a) Definitions of grip length, L_g, threaded length, L_t, and threaded engagement, LE [23]

(b) Shear area [7]

Figure 3.1: Definitions used for analytical design of threaded assemblies

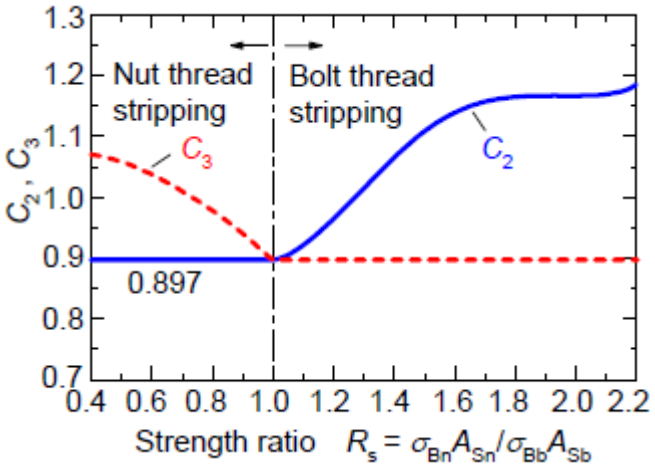

Figure 3.2: Factors C_2 and C_3 used in Alexanders formulas
Modified from [25]

Calculation of the shear area involves several important geometrical aspects. One of them is that nuts are often formed with a countersink in each end to ease installation. Alexander found out through experimental studies that the countersinks reduce the length of engagement, LE. The bolt shear area is also affected by the bell mouth shape of the nut, which can be seen in Figure 6.2a. Nut threads is sheared off by the mating threads of the bolt who all have equal height. Bolt threads will be sheared off by threads with different heights due to the bell mouth shape of the nut. This results in different shear areas for the nut and bolt.

According to Alexander [7], several features influence the failure modes. One vital parameter is the length of the engagement, LE, which is slightly shorter than the nut because of the countersinks. If the length of engagement is long and the material of the nut and bolt corresponds with each other, bolt fracture occurs. If the length of engagement is short thread stripping occurs. Whether thread stripping happens in the bolt or nut depends on their relative strength.

Another important geometrical feature is the nut dilation, i.e. the radial expansion of the nut. This is a result of the contact pressure between threads, which gives a force component in the radial direction. The dilation expansion of the nut reduces the overlap of mating threads and lowers the shear area. Alexander included this effect in the factor C_1.

The relative material strength of the bolt and nut influence the degree of thread bending. Alexander introduced the factors C_2 and C_3 to incorporate this into the design equations. Figure 3.2 shows how the different strength factors depends on the strength ratio, R_s. Further details for C_1,C_2 and C_3 can be found in Appendix A.

3.2 Material mechanics

For a finite element analysis to predict realistic response a material model with proper parameters is essential. Inaccurate material properties can produce unnatural response which could lead to misinterpretation. To understand how the material behave a full examination of the material is needed. A stress-strain relationship from a tensile test in commonly used to characterize different material parameters. This chapter presents background theory for the material model and determination of material properties.

3.2.1 Elasticity

The first phase of the material response is the elastic domain. It is assumed that the deformations are infinitesimal, and a linear elastic behavior is assumed. Metals are in general assumed to be isotropic, such that elasticity can be described with two parameters; Young's modulus, E, and Poisson's ratio, ν. The total strain can be decomposed into two parts; an elastic part,ϵ^e, and a plastic part, ϵ^p, viz.:

$$\epsilon = \epsilon^e + \epsilon^p \tag{3.4}$$

Hooke's law describes the linear elastic stress-strain behavior, and can be simplified into Eq. 3.5 for isotropic materials.

$$\sigma = E\epsilon^e \tag{3.5}$$

where σ is stress and ϵ^e is the elastic strain.

In the elastic domain the deformation is reversible and path independent. An unloading in the elastic domain will bring the specimen back to its initial configuration without any permanent deformation. The elastic behavior takes place right up to the yield limit. Typical yield limit for steel is in the range of 0.001 to 0.005 [28], depending on the strength of the material. Beyond this limit is the plastic domain.

3.2.2 Plasticity

All deformation after the yield limit will produce permanent deformation, i.e. plastic deformation. The theory of plasticity consists of three parts; a yield function, a plastic flow rule and a hardening law. The next sections presents an overview of the different parts.

Yield function

The extension of the elastic domain is defined by a yield function. The yield function, Φ, is in general defined as [12]:

$$\Phi(\sigma, \sigma_y) = \sigma - \sigma_y \tag{3.6}$$

where σ_y is the yield stress and σ is the equivalent stress. For isotropic materials the Von Mises stress is often used as the equivalent stress [12]:

$$\sigma = \sqrt{\frac{1}{2}((\sigma_1 - \sigma_2)^2 + (\sigma_2 - \sigma_3)^2 + (\sigma_1 - \sigma_3)^2)} \tag{3.7}$$

For a uniaxial stress state prior to necking, $\sigma_2 = \sigma_3 = 0$, and Eq. 3.7 simplifies to:

$$\sigma = \sqrt{\frac{1}{2}((\sigma_1)^2 + (\sigma_1)^2)} = \sigma_1 \tag{3.8}$$

It should be noted that the stress can never exceed the current yield stress. This means that the stress either lies within the elastic domain or on the yield limit. Thus, any stress state must satisfy:

$$\Phi(\sigma, \sigma_y) \leq 0 \tag{3.9}$$

Plastic flow rule

In the elastic domain *Hooke's law* gives the relationship between stress and strain. A stress-strain relationship is also needed in the plastic domain, but since plastic deformation is irreversible and path dependent an incremental approach is used. For an associated model the incremental plastic strain rate tensor, $\dot{\epsilon}^p$, can be written as [12]:

$$\dot{\epsilon}^p = \partial\dot{\gamma}\frac{\partial\Phi}{\partial\sigma} \tag{3.10}$$

where $\partial\dot{\gamma}$ is a plastic multiplier. When combining Eq 3.10 with the *Von Mises yield criterion* the plastic strain tensor, also known as the Prandtl-Reuss tensor, can be written as [12]:

$$\dot{\epsilon}^p = \dot{\gamma}\sqrt{\frac{3}{2}}\frac{\sigma}{||\sigma||} \tag{3.11}$$

The equivalent plastic strain rate, $\dot{p}$, can be written as:

$$\dot{p} = \sqrt{\frac{2}{3}\dot{\epsilon}^p : \dot{\epsilon}^p} = \sqrt{\frac{2}{3}}||\dot{\epsilon}^p|| \tag{3.12}$$

and the Von Mises equivalent plastic strain ϵ^p as:

$$\epsilon^p = \int_0^t \dot{p}\, dt \tag{3.13}$$

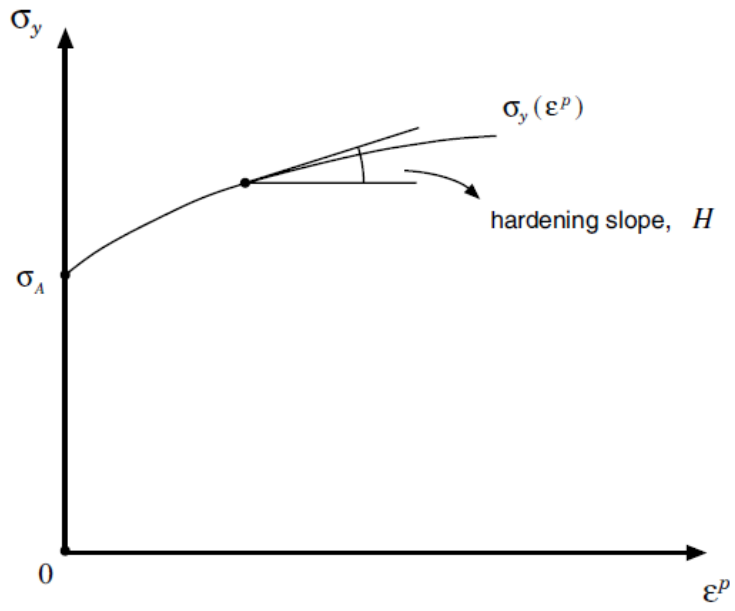

Figure 3.3: One dimensional material hardening curve [12]

Hardning law

For metals the growth of plastic strain is accompanied by an evolution of the stress. This phenomenon is called work hardening. Isotropic hardening can be incorporated in the yield function by making the yield stress a function of the plastic strain, ϵ^p. Figure 3.3 shows a typical hardening curve. The yield function can now be rewritten as:

$$\Phi(\sigma, \sigma_y(\epsilon^p)) \tag{3.14}$$

In numerical analysis the hardening curve is often implemented as a data set obtained from curve fitting. *Voce law* [26], Eq. 3.15, is often used for metals:

$$\sigma(\epsilon^p) = \sum_{i=1}^{n} Q_i(1 - exp(C_i \times \epsilon^p)) \tag{3.15}$$

where n is the number of terms used to fit the observed data, and Q_i and C_i are constants. In case of strain rate effects due to dynamic loading, *Voce law* can be extended by multiplying with a new term [24]:

$$\sigma(\epsilon^p) = \left(\sum_{i=1}^{n} Q_i(1 - exp(C_i \times \epsilon^p))\right)\left(1 + \frac{\dot{\varepsilon}}{\dot{\varepsilon_0}}\right)^q \tag{3.16}$$

where $\dot{\varepsilon}$ is the strain rate, and $\dot{\varepsilon_0}$ and q are material constants defining strain rate sensitivity.

3.2.3 Fracture criterion

To provoke fracture in FE models a fracture criterion is essential. The *Extended Cockcroft-Latham criterion* (ECL), based on total strain energy per unit volume, has been employed. When an element has reached a critical fracture energy, it will be removed from the analysis. The criterion is given by [24]:

$$W_C = \int_0^{\epsilon^f} \left\langle \phi \frac{\sigma_I}{\bar{\sigma}} + (1-\phi) \frac{\sigma_I - \sigma_{III}}{\bar{\sigma}} \right\rangle^{\gamma} \sigma \, d\epsilon^f \tag{3.17}$$

where W_c is a fracture parameter, ϵ^f is the plastic strain at fracture, and σ_I and σ_{III} is the first and third principal stress, respectively. According to Gruben et al. [24], ϕ controls the relative influence of both major principle stress and maximum shear stress, and γ governs the strength of the stress-state dependence. ϕ and γ were set as 0.355 and 1.55, respectively. ϕ and γ was calibrated for a Docol 600DL steel by Gruben et al.

By setting ϕ and γ equal to 1, the classical *Cockcroft-Latham criterion* (CL) is obtained. The principal difference between the classical and extended version is that the extended criterion seems better suited for shear fractures [24]. From Figure 5.5 it can be seen that the fracture strain in ECL is smaller for lower values of triaxiality: the fracture strain diverges when triaxiality tends toward -1/3 (pure compression), and gives higher fracture strain for triaxiality equal to 0 (pure shear). Triaxiality equal to 1/3 (pure tension) gives the same fracture strain in both versions.

From a single uniaxial tensile test it is possible to calculate the fracture parameter because $\sigma_I = \sigma_1$ and $\sigma_{III} = 0$ when ϕ and γ are known. The complete criterion can be obtained by finding the fracture strain, ϵ^f, as a function of stress triaxiality, σ^*. To obtain the complete criterion, under the assumption of plane stress, it can be rewritten as:

$$W_c = \int_0^{\epsilon_f} \left\langle \frac{\phi\left(3\sigma^* \sqrt{3+\mu^2} - 3 - \mu\right) + 6}{3\sqrt{3+\mu^2}} \right\rangle^{\gamma} \sigma \, d\epsilon^f \tag{3.18}$$

where W_C is known from uniaxile testing, σ^* is the stress triaxiality, μ is the lode parameter, and σ is von Mises equivalent stress. σ can be approximated by using *Voce law*, Eq. 3.15, and the W_C-number is calculated from:

$$W_c = \int_0^{\epsilon_f} \sigma_I \, d\epsilon^p \tag{3.19}$$

3.3 Data processing

From the experimental tests the following quantities has been extracted:

$$\sigma = s(1+e); \qquad \epsilon = ln(1+e) \qquad \epsilon^p = \epsilon - \frac{\sigma}{E} \tag{3.20}$$

where s and e are the engineering stress and strain, and σ and ϵ are the true stress and strain.

When describing material behaviour beyond necking, it may be advantageous to use diameter reduction in zone of necking rather than global longitudinal strain. This may give a more precise description of the local material behaviour, since most of the deformation is located in this section. The following derivation is not valid in the elastic domain where Poisson ratio applies. By assuming plastic strain in radial direction the following relationship arises:

$$\epsilon^p = \int_{d_0}^{d} \epsilon^p = \int_{d_0}^{d} \frac{\delta d}{d} = ln(d) - ln(d_0) = \ln\left(\frac{d}{d_0}\right) \tag{3.21}$$

Further, assuming plastic volume conservation of a circular-cross section, the longitudinal strain can be expressed by the change in diameter:

$$\epsilon^p_{volume} = \epsilon^p_l + 2\epsilon^p_{radial} = 0 \quad \Rightarrow \quad \epsilon^p_l = -2\epsilon^p_{radial} = -2\ln\left(\frac{d}{d_0}\right) \tag{3.22}$$

3.4 Digital Image Correlation (DIC)

Digital Image Correlation (DIC) is an optical technique for tracking displacement and measuring strain. DIC allows for measurements both in space and in the plane at the surface. The method is based on an optical comparison of consecutive high resolution photos taken of the specimen during testing. The specimen is painted with a mottled pattern, which allows displacement and strain to be calculated. Calculations are based on a mesh of virtual elements tracking the movement of the mottled painting. This technique also works for a chess pattern, which has been used in this thesis. The optical technique is based on tracing the movement of pixels, and further details can be found in Egil Fagerholts thesis [13].

The main advantage with DIC is that it enables tracking of local strain beyond necking. This is not possible by use of conventional extensometers. DIC can also measure strain over a large surface, as opposed to the small area covered by the extensometer. Displacement between two points of interest can be obtained by placing a virtual vector in a reference photo. The elongation of this vector can then be found by:

$$e_t = \frac{L_t}{L_0} - 1 \tag{3.23}$$

where e_t is the elongation of the vector at time t, L_t is the length of the vector at time t and L_0 is the initial length. Since DIC is based on movements of pixels, the elongation has to be converted from pixels to mm. This is easily done by a known pixel to mm ratio.

3.5 Finite element method

To analyze and validate experimental data the finite element program Abaqus V 6.14 has been utilized. Necessary theory used throughout modeling of the threaded assemblies is presented in this chapter.

Explicit integration scheme

In cases of bolt fracture and thread stripping it is desirable to use an explicit integration scheme, that is based on direct step-by-step integration in the time domain. A dynamic explicit method is based on solving the equation of motion, Eq.3.24, in time step t_{n+1} from known previous quantities in time step t_n:

$$\mathbb{M}\ddot{U}(t) + \mathbb{C}\dot{U}(t) + \mathbb{K}U(t) = \mathbb{R}^{ext}(t) \tag{3.24}$$

where:

$\mathbb{M}$ is the mass matrix

$\mathbb{C}$ is the damping matrix

$\mathbb{K}$ is the stiffness matrix

$\mathbb{R}^{ext}(t)$ is the external load vector

U(t) is the displacement

$\dot{U}(t)$ is the velocity

$\ddot{U}(t)$ is the acceleration

The classical *Central difference explicit method* [10][11] is derived from the Taylor series expansions of the displacement in t_{n+1} and t_{n-1}:

$$u_{n+1} = u_n + \Delta t \dot{u}_n + \frac{\Delta t^2}{2}\ddot{u}_n + \frac{\Delta t^3}{6}\dddot{u}_n + ... \tag{3.25}$$

$$u_{n-1} = u_n - \Delta t \dot{u}_n + \frac{\Delta t^2}{2}\ddot{u}_n - \frac{\Delta t^3}{6}\dddot{u}_n + ... \tag{3.26}$$

Subtracting Eq. 3.26 from Eq. 3.25 gives an expression for the velocity in t_n:

$$u_{n+1} - u_{n-1} = 2\Delta t \dot{u}_n \quad \Rightarrow \quad \dot{u}_n = \frac{u_{n+1} - u_{n-1}}{2\Delta t} \tag{3.27}$$

Likewise adding Eq. 3.25 to Eq. 3.26 gives an expression for the acceleration in t_n:

$$u_{n+1} + u_{n-1} = 2u_n + \Delta t^2 \ddot{u}_n \quad \Rightarrow \quad \ddot{u}_n = \frac{u_{n+1} - 2u_n + u_{n-1}}{\Delta t^2} \tag{3.28}$$

Substituting these two expressions for velocity and acceleration, Eq. (3.27) and (3.28), into the equation of motion gives:

$$\frac{\mathbb{M}}{\Delta t^2}(u_{n+1} - 2u_n + u_{n-1}) + \frac{\mathbb{C}}{2\Delta t}(u_{n+1} - u_{n-1}) + \mathbb{K}u_n = \mathbb{R}^{ext}(t) \tag{3.29}$$

When rearranging the expression, and collecting all terms with u_{n+1} on the left, a compact equation for the future displacement arises:

$$\left(\frac{\mathbb{M}}{\Delta t^2} + \frac{\mathbb{C}}{2\Delta t}\right) u_{n+1} = \mathbb{R}^{ext}(t) - \left(\frac{\mathbb{M}}{\Delta t^2} - \frac{\mathbb{C}}{2\Delta t}\right) u_{n-1} - \left(\mathbb{K} - \frac{\mathbb{M}}{\Delta t^2}\right) u_n \tag{3.30}$$

This expression can be written more compact in a way that easily gives the future displacement:

$$\mathbb{K}^{eff} u_{n+1} = \mathbb{R}^{eff} \quad \Rightarrow \quad u_{n+1} = \left(\mathbb{K}^{eff}\right)^{-1} \mathbb{R}^{eff} \tag{3.31}$$

where:

$$\mathbb{K}^{eff} = \left(\frac{\mathbb{M}}{\Delta t^2} + \frac{\mathbb{C}}{2\Delta t}\right)$$

$$\mathbb{R}^{eff} = \mathbb{R}^{ext}(t) - \left(\frac{\mathbb{M}}{\Delta t^2} - \frac{\mathbb{C}}{2\Delta t}\right) u_{n-1} - \left(\mathbb{K} - \frac{\mathbb{M}}{\Delta t^2}\right) u_n$$

By employing the *Central difference method* and Eq. (3.31) there is no need for equilibrium iterations. This makes every time step computational inexpensive, and the only information needed is the initial condition given by u_n and $\dot{u}_n$. For the first step, the term u_{n-1} is unknown. By rewriting and combining Eq. (3.27) and Eq. (3.28) an expression for the previous displacement arises [32]:

$$u_{n-1} = u_n + \Delta t^2 \ddot{u}_n - 2\Delta t \dot{u}_n \tag{3.32}$$

where Eq. (3.24) in time step t_n gives $\ddot{u}_n = \frac{1}{\mathbb{M}}\left(\mathbb{R}^{ext}(t) - \mathbb{C}\dot{u}_n - \mathbb{K}u_n\right)$. All initial conditions is now known for the iterative solutions progress.

Although this method is quite inexpensive, it can easily be modified to not contain the stiffness matrix $\mathbb{K}$ on the left side in Eq. (3.31). In nonlinear analysis the stiffness will change during deformation, and $\mathbb{K}^{eff}$ needs to be established and factorized for each time step when calculating u_{n+1}. By removing $\mathbb{K}$ from $\mathbb{K}^{eff}$, there is no need to establish, nor factorize $\mathbb{K}^{eff}$ in each time step. By simple modifications of the classical *Central difference method*, the half step method arises [32]. This method will further reduce the computational work, but the derivation is omitted due to similarities with the derivation of the central difference method.

Conditional stability

The main drawback with the explicit method is the conditional stability. To obtain a converging solution the time step has to be smaller than a critical time step [10]:

$$\Delta t_{cr} < \frac{L_e}{C_d} \qquad\qquad C_d = \sqrt{\frac{E}{\rho}} \tag{3.33}$$

where L_e is the characteristic length of the smallest element in the whole FE model. C_d is the dilatational wave speed which is defined by the Young's modulus ,E, and the mass density, ρ.

Because of this criteria it is preferable to use an explicit method for short analysis in time. It is also preferable when the expected response is of high frequency, and when the equilibrium path is discontinuously. This is typical for cracking in reinforced concrete, crashing and fracture modeling. In such cases the time step has to be small to be able to detect sudden changes in stiffness and response discontinuities. Thread stripping is highly dominated by contact and material failure, and the time step should be small to be able to track the response in the analysis.

Computational efficiency

Since the time step is very small, applying real time from experiments in the analysis is practically impossible due to the long analysis time. To circumvent this either mass or time scaling can be employed. From Eq. (3.33) it is clear that increasing the mass will increase the critical time step. This method is preferable where some elements are smaller than the rest, whereas time scaling is preferred if the elements have approximately the same size. Time scaling is performed by increasing the deformation speed, and thus reducing total analysis time.

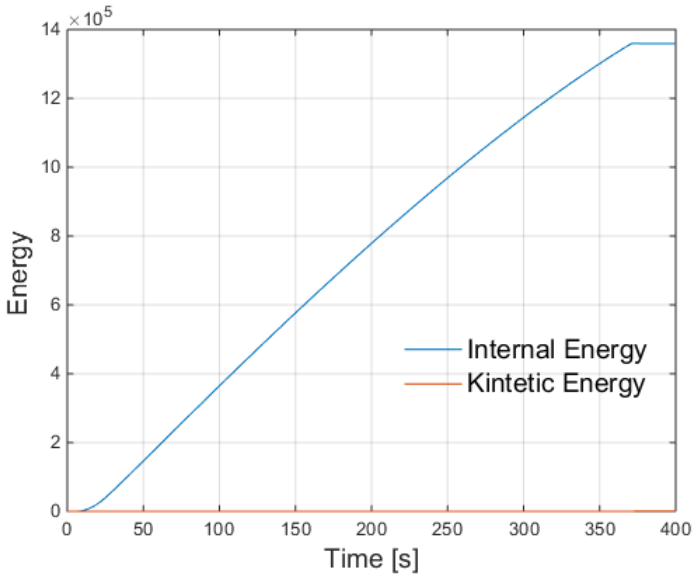

Figure 3.4: Comparison of internal and kinteic energy used for energy balance check. Note that the kinetic energy is neglectable compared to the internal energy.

Carefulness has to be exerted when applying time or mass scaling, because the response may be influenced by inertia forces. To control this, an energy balance check should be performed. The kinetic energy should be less than 1-5 % of the internal energy. A typical energy plot from analysis is illustrated in Figure 3.4.

Another careful aspect is nonlinear material behaviour, e.g. yielding and hardening. In the case of numerical instability a lot of energy can be absorbed by energy dissipating material behaviour. This would be easy to detect in static analysis because the response will grow without limit. It may not happen in nonlinear analysis, and the solution can look credible even though the error is significant. The way to handle this problem is to perform an energy balance check [33]. It should be controlled that the sum of all energy components always are constant, with an error of less than 1 %:

$$E_{internal} + E_{viscous} + E_{friction} + E_{kinetic} - E_{external} = constant \tag{3.34}$$

When this condition is met, all the energy added, $E_{external}$, is physically absorbed for sure. Energy control was performed for every simulation performed.

4. *Experimental tests*

This chapter presents the methods and setup used for the experimental tests. The objective has been to study how the nut position on the threaded parts of bolts affects the failure mode. Various types of partially threaded M16 bolt and nut assemblies were tested. Results from the experimental tests are presented in the end of this chapter.

4.1 Geometry and bolt marking

Table 4.1: Bolt test program

Bolt type	**Strength class**	**Test speed [mm/min]**	**Nut type**	**Grip length [mm]**	**Number of tests**
SB	8.8	0.8	ISO 4032	81	5
SB	8.8	0.8	ISO 4032	89	5
SB	8.8	0.8	ISO 4032	101	5
SB	8.8	60	ISO 4032	101	5
SB	8.8	0.8	2 × ISO 4032	81	3
SB	8.8	0.8	ISO 4033	81	3
SB	8.8	0.8	ISO 4033	89	3
SB	8.8	0.8	ISO 4033	101	3
HR	8.8	0.8	NS-EN 14399	81	3
HR	8.8	0.8	NS-EN 14399	85	5
HR	8.8	0.8	NS-EN 14399	87	5
HR	8.8	0.8	NS-EN 14399	89	5
HR	8.8	0.8	NS-EN 14399	101	3
HR	8.8	60	NS-EN 14399	87	5
					= 58 tests

Table 4.1 presents an overview of the bolts tested in this thesis. All tested bolts were partially threaded of type M16 with a length of 120 mm. Bolt marked with SB are manufactured according to the standard ISO 4014 [15]. Bolts marked HR, which are pre-tensioned bolts, follows the requirements of NS-EN 14399 [19]. While working in the laboratory it was advantageous to standardize the marking of the bolts. The label had the form:

SB-NS-88-81-1 (with positioning (XX)-(YY)-(1)-(2)-(3))

The explanation of the different positions is as follows:

- (XX): SB is abbreviation for Structural Bolt. HR denotes High Strength Bolt, and refers to pre-tensioning bolts.
- (YY): NS refers to Normal Speed on the test machine. HS is analogously used for High Speed. The machine velocity is discussed later.

- (1): This position presents the strength class of the bolt. 88 refers to 8.8.
- (2): This number is the grip length in mm, see Figure 4.1. One test series includes the letter D, which refers to the use of two nuts. Test series that are marked with the letter H are tested with high nuts, i.e. ISO 4033.
- (3): Test number in the test series.

The nut position were measured as the distance from the underside of the bolt head to the under side of the nut, as illustrated in Figure 4.1. This distance is also referred to as the grip length, and the threads between the nut and unthreaded part of the bolt are referred to as free threads. The unthreaded length of the bolt was the same in all tests.

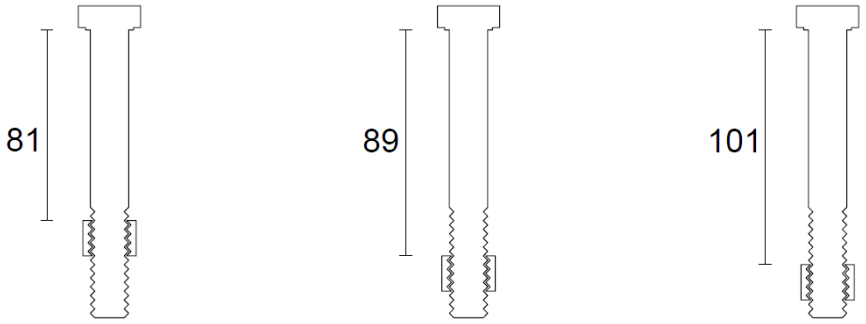

Figure 4.1: Definition of grip length

All SB-bolt tested had nuts with hardness 8 and follows the requirements of NS-EN ISO 4032 [17]. The nuts used with pre-tensioning bolts had hardness 10 and follows the requirements of NS-EN 14399 [19]. High nuts had hardness 8, and were in accordance with requirements of NS-EN ISO 4033 [16]. See Appendix A for more detailed illustration of bolt and nut geometry.

4.2 Setup and testing procedure

In this section the test setup and testing procedure is presented. The principle of collecting data for DIC analysis is subsequently described.

4.2.1 Test setup

Figure 4.2 depicts the test setup. The bolt assembly was placed in a Instron machine with a 250 kN load cell.

Figure 4.2: Test rig for bolt tests

As illustrated in Figure 4.3, the bolt was inserted into two thick purpose made steel plates. The steel plates were in contact with the bolt head and the nut, and transferred the tensile force from the machine to the bolt assembly. Vertical movement of the bolt was unrestricted. Figure 4.3a shows the how the bolted assembly was placed in the machine. The lower part was clamped, while the upper part was moving upward with constant velocity.

Two different velocities were tested. To ensure quasi-static behaviour and negligible dynamic effects the deformation rate was set to 0.8 mm/min. One test was carried out with a deformation rate of 0.4 mm/min without changes in response or fracture mode. Thus 0.8 mm/min seemed reasonable. In addition, to investigate and compare the response of quasi-static behaviour and dynamic behaviour some test series was performed with a deformation rate of 60 mm/min.

During quasi-static deformation the sampling rate for displacement and force was 10 Hz. Similarly, the sampling rate was 1000 Hz for the high speed test series.

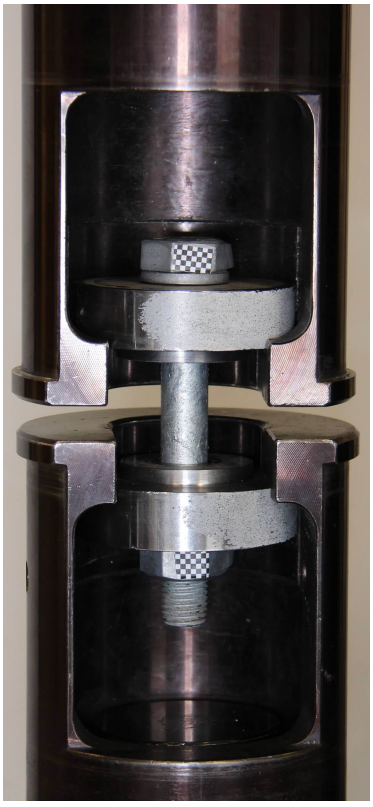

(a) Photo of bolt and bushes mounted in test machine

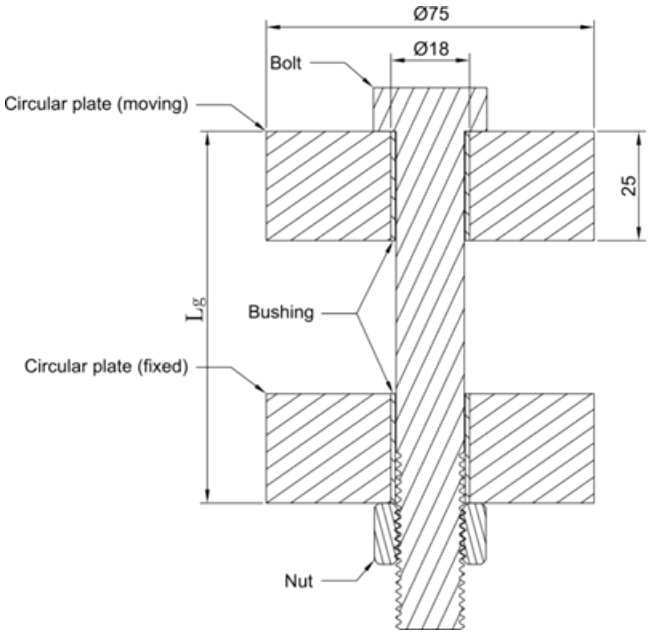

(b) Cross-section of test specimen, steel plates and bushes [23]

Figure 4.3: Test setup for bolt tests

4.2.2 Test procedure

Before every test the dimensions of the bolt and nut were measured and compared with the requirements of respective standards. Length and diameters of the unthreaded and threaded part of the bolt was measured. The height and diameter, in addition with the width across flats and width across corners was measured for the nut. No remarkable deviations in geometry was detected. Average values from these measurements were employed in FE-simulations.

When the bolt setup was placed in the test machine, the grip length was adjusted by rotating the nut. The test rig was hinged in both ends and it was necessary to level the bolt in a vertical position to ensure uniaxial load conditions.

Some of the test specimens were cut with a saw through the cross section after testing. This allowed for further inspections of the fracture mode.

4.2.3 DIC

Figure 4.4: Bolt with chess pattern used for DIC analysis

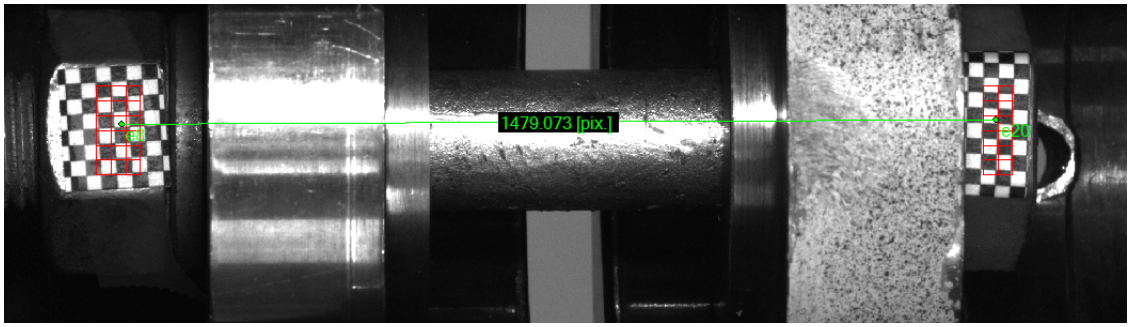

Figure 4.5: Measuring of bolt elongation by a vector in DIC

The test setup for DIC is also illustrated in Figure 4.2. A digital camera was placed in front of the test rig. Before each test a piece of paper with squared chess pattern was taped at the bolt and nut, as depicted in Figure 4.4. These two areas are recognized by the DIC software, which uses them to calculate the displacement with a virtual vector, as shown in Figure 4.5. DIC was used to measure displacement, because the same displacement vector was found in FE-simulations. The displacement from the test rig would not be equivalent to FE deformation because of elastic deformation of the test rig itself.

In the quasi-static tests the camera was programmed with a frequency of 1 Hz, and subsequently with 15 Hz in the dynamic tests. This produced a sufficient number of pictures as basis for displacement measurements.

(a) Test machine with camera in front

(b) Fastening of test specimen

Figure 4.6: Test rig for material tests

4.3 Material tests

A material test program was conducted to determine the mechanical properties of the bolts and nuts. The goal was to calibrate necessary material parameters in the material model presented in Section 3.2. Further calibration details is covered in Chapter 5.

The tensile tests of the bolted assemblies was in a quasi-static strain rate domain, and strain rate effects were assumed to be negligible. One could argue for some local strain rate effects in the threads, but this was not investigated. Further discussions is covered in Chapter 5.

4.3.1 Test setup

An Instron machine with 250 kN load cell was also used for the material tests. However, the threads were screwed directly into the base of the machine. The tensile force was transfered from the machine via two steel clamps around the bolt head, as depicted in Figure 4.6. The displacement rate was constant, with a velocity of 0.8 mm/min. Force and displacement were sampled at at rate of 10 Hz.

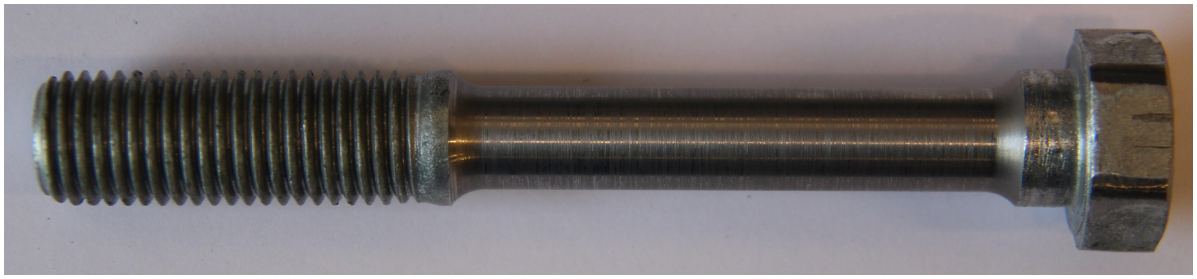

(a) Material test specimen

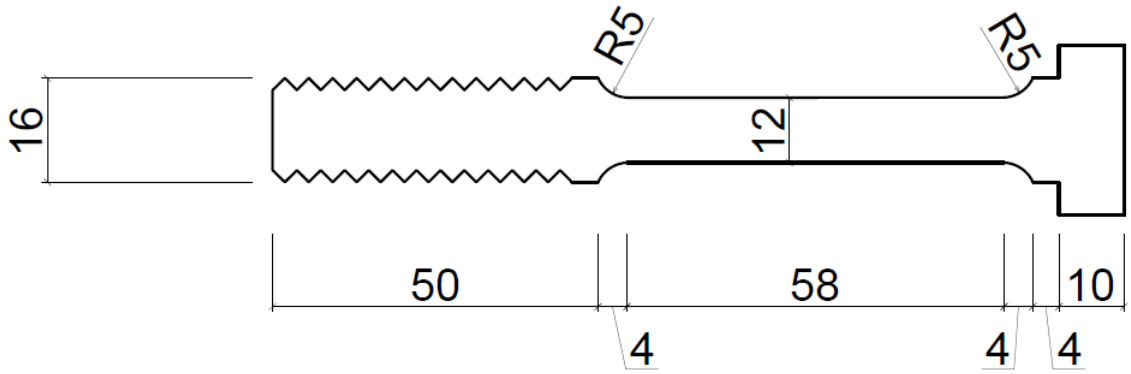

(b) CAD drawing of material test specimen with dimensions

Figure 4.7: Specimen manufactured for material tests

Table 4.2: Material test progam

Bolt type	Strength class	Test speed [mm/min]	Number of tests
SB	8.8	0.8	2
HR	8.8	0.8	2

4.3.2 Test procedure

Tensile tests were performed on purpose-made test specimens, as seen in Figure 4.7a. All dimensions of the specimens geometry is illustrated in Figure 4.7b. The reduced diameter of the unthreaded part ensures necking and fracture to occur in this section of the test specimen. 12 mm is less than the diameter of the thread valley, at the same time as it conserves as much as possible of the bolt diameter. This should provide the best depiction of the material. Initially, control measurements of the test specimens geometry was carried out. No remarkable deviations were detected.

The number of tests performed on each of the test specimens is presented in Table 4.2. As expected, there was negligible variations in material response, and only two tests per bolt type were conducted.

Labeling of the test specimens follows the same procedure as the bolt marking:
SB-NS-1 (with positioning (XX)-(YY)-(NUM)
with explanation as follows:

- (XX): SB is short for Structural Bolt. HR is short for High Strength Bolt, and refers to pre-tensioning bolts.
- (YY): NS refers to Normal Speed on the test machine. HS is analogously used for High Speed.
- (NUM): Test number in the test series.

4.3.3 DIC

DIC was utilized to trace the diameter reduction to determine material parameters. Each of the test specimens were painted with a mottled pattern as depicted in Figure 4.8.

As seen in Figure 4.6, a camera was placed in front of the test specimen. The HUP-profile in the backgruound was used to create a clear background. This would help the DIC software to trace the cross sectional reduction. Pictures were taken with a frequency of 1 Hz.

Figure 4.8: Painted material test specimen

4.4 *Vickers hardness test*

Vickers hardness test is a common method for testing hardness of metals and alloys, based on indentation with a pyramid-shaped diamond into the surface. The area of indentation is calculated by examining the surface under microscope [29]. Hardness is given as load, F, over a given recession, A. The unit is Pascal, but must not be mistaken for pressure because the area of the recession is not normal to the load. From a Vickers Hardness test, it is possible to estimate the yield stress from the proportionality: $\sigma_y \simeq 3\times$ HV, where HV is the hardness [34].

Test were carried out for one SB-bolt, one HR-bolt, one HR-nut, one regular nut and one high nut. These were cut in two before they were sent to SINTEF Materials and Chemistry for testing. The results are presented in Figure 4.9 and Figure 4.10, with the hardness marked above the indentation. Table 4.3 presents results from the hardness tests.

The tests revealed insignificant variation of the hardness over the cross-section of the bolts and nuts. This could imply that the material properties should be consistent over the cross-section for each component. When examining the relative hardness of different bolt and nut compositions, larger deviations were registered especially for the SB-bolt and regular nut. The relative hardness of this assembly was 77 %, and the lowest hardness values were registered in the nut threads. According to Alexander [7], a difference in strength could lead to a change of failure mode towards thread failure. This is consistent with the results observed for tests of SB-bolt with regular nut, which all failed by thread stripping. Anyhow, it is difficult to state if this was valid for all because of limited amount of testing.

Table 4.3: *Vickers hardness* values

	HR-bolt	HR-nut	SB-bolt	Regular nut	High nut
Average hardness [HV]	297.7	315.0	308.4	239.3	286.0
Max deviation [%]	3.3	1.6	2.1	6.8	1.4
HV nut / HV HR-bolt [%]	-	105.8 %	-	-	-
HV nut / HV SB-bolt [%]	-	-	-	77.6	92.7

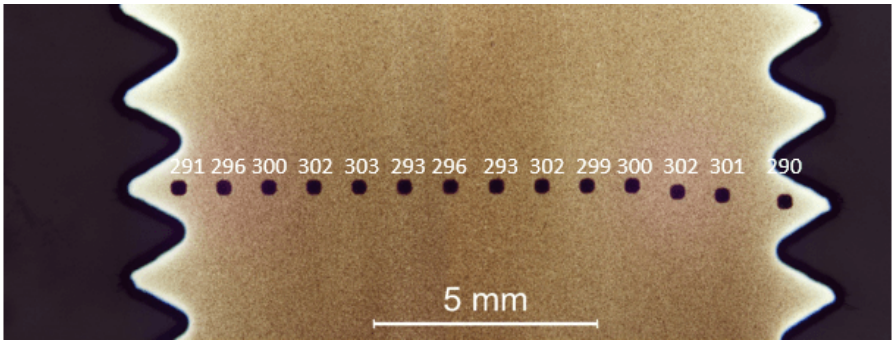

(a) HR-bolt

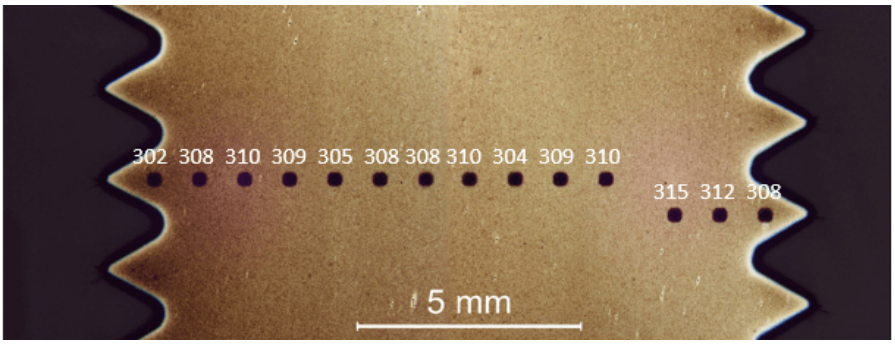

(b) SB-bolt

Figure 4.9: *Vickers hardness* values of bolts

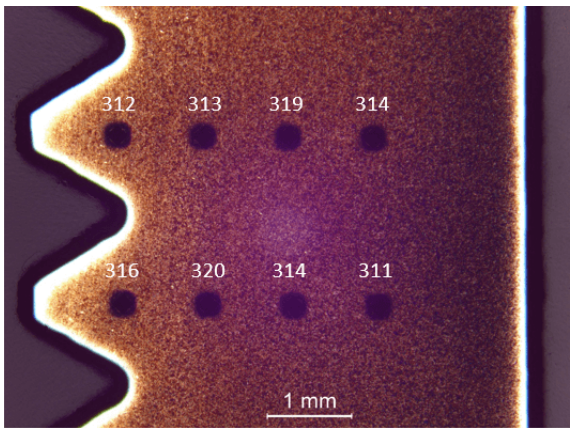

(a) HR-nut

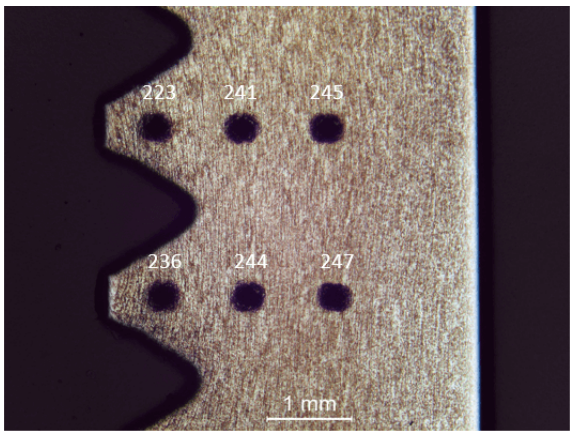

(b) Standard nut (ISO 4032)

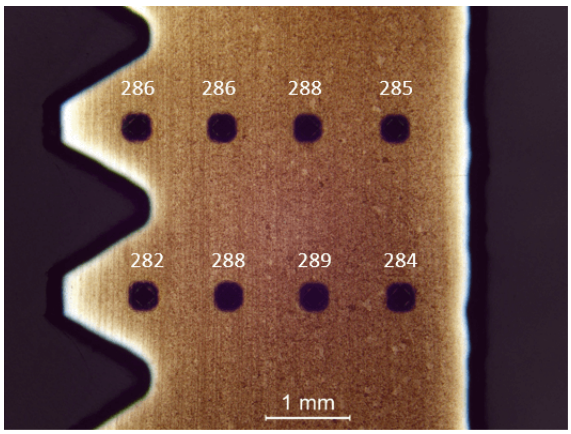

(c) Tall nut (ISO 4033)

Figure 4.10: *Vickers hardness* values of nuts

4.5 Results

This section presents the results from bolt testing and material tests. Some comments to the experimental work follows in the end of this section.

4.5.1 Bolt testing

The results from the bolt tests are presented in Table 4.4, Table 4.5 and Figure 4.11 to Figure 4.24. Note that the plotted deformations were measured by the test machine and includes deformation of the whole test setup; the fastening case and bars, the steel plates and the bolt assembly. This results in slightly larger deformations compared with the bolt assembly itself, around 2 mm. DIC analysis gives the correct deformation, and this deformation was used in comparison with FE models. Further analysis of the fracture surface, except for registration of the fracture mode, was not a part of the experimental work. The only information of interest was whether the bolt failed by thread stripping or bolt fracture. Note that some test series only consists of three tests, because the fracture mode was so evident and no further tests were needed.

From Table 4.4, Table 4.5 and the force-displacement plots in Figure 4.11 - 4.24 the following was observed:

- Fairly good repeatability for the test series, except in the test series: HR-HS-88-87 and HR-NS-88-87. This seemed to be a critical point where the failure mode shifted from thread stripping to bolt fracture.
- All SB-bolts with regular nut (ISO 4032) failed by thread stripping, and all SB-bolts with high nut (ISO 4033) failed by bolt fracture. In addition, the high nut improved both ductility and maximum tensile force.
- For all bolt and nut assemblies, the maximum tensile forces was registered for the shortest grip length. In other words, the maximum force decreased in correlation with longer grip lengths.

Test number	Failure mode	Maximum tensile force [kN]
SB-NS-88-81-1	Thread stripping	135.91
SB-NS-88-81-2	Thread stripping	141.30
SB-NS-88-81-3	Thread stripping	143.19
SB-NS-88-81-4	Thread stripping	141.08
SB-NS-88-81-5	Thread stripping	142.85
SB-NS-88-89-1	Thread stripping	140.71
SB-NS-88-89-2	Thread stripping	139.06
SB-NS-88-89-3	Thread stripping	131.63
SB-NS-88-89-4	Thread stripping	137.29
SB-NS-88-89-5	Thread stripping	140.14
SB-NS-88-101-1	Thread stripping	135.23
SB-NS-88-101-2	Thread stripping	140.20
SB-NS-88-101-3	Thread stripping	137.21
SB-NS-88-101-4	Thread stripping	133.40
SB-NS-88-101-5	Thread stripping	141.13
SB-NS-88-81D-1	Bolt fracture	157.93
SB-NS-88-81D-2	Bolt fracture	159.43
SB-NS-88-81D-3	Bolt fracture	158.82
SB-NS-88-81H-1	Bolt fracture	160.77
SB-NS-88-81H-2	Bolt fracture	161.00
SB-NS-88-81H-3	Bolt fracture	161.04
SB-NS-88-89H-1	Bolt fracture	149.62
SB-NS-88-89H-2	Bolt fracture	151.52
SB-NS-88-89H-3	Bolt fracture	151.04
SB-NS-88-101H-1	Bolt fracture	147.89
SB-NS-88-101H-2	Bolt fracture	147.62
SB-NS-88-101H-3	Bolt fracture	147.68
SB-HS-88-101-1	Thread stripping	139.75
SB-HS-88-101-2	Thread stripping	146.06
SB-HS-88-101-3	Thread stripping	140.53
SB-HS-88-101-4	Thread stripping	145.05
SB-HS-88-101-5	Thread stripping	139.97

Table 4.4: Bolt test results: SB-bolts
SB - Structural Bolt. **NS** - Normal Speed. **88** - Strength class.
E.g. **101H-3** - Grip length 101 mm, high nut and test number 3

Test number	**Failure mode**	**Maximum tensile force [kN]**
HR-NS-88-81-1	Thread stripping	148.92
HR-NS-88-81-2	Thread stripping	145.56
HR-NS-88-81-3	Thread stripping	145.16
HR-NS-88-85-1	Thread stripping	143.16
HR-NS-88-85-2	Thread stripping	142.25
HR-NS-88-85-3	Thread stripping	141.85
HR-NS-88-85-4	Thread stripping	146.97
HR-NS-88-85-5	Thread stripping	143.37
HR-NS-88-87-1	Bolt fracture	145.60
HR-NS-88-87-2	Thread stripping	143.60
HR-NS-88-87-3	Bolt fracture	144.23
HR-NS-88-87-4	Thread stripping	141.24
HR-NS-88-87-5	Thread stripping	146.07
HR-NS-88-89-1	Bolt fracture	140.49
HR-NS-88-89-2	Bolt fracture	145.07
HR-NS-88-89-3	Bolt fracture	143.89
HR-NS-88-89-4	Bolt fracture	144.15
HR-NS-88-89-5	Bolt fracture	143.35
HR-NS-88-101-1	Bolt fracture	139.36
HR-NS-88-101-2	Bolt fracture	138.54
HR-NS-88-101-3	Bolt fracture	140.99
HR-HS-88-87-1	Bolt fracture	143.83
HR-HS-88-87-2	Thread stripping	150.11
HR-HS-88-87-3	Thread stripping	150.05
HR-HS-88-87-4	Bolt fracture	146.21
HR-HS-88-87-5	Bolt fracture	147.85

Table 4.5: Bolt test results: HR-bolts
HR - High strengh bolt. **NS** - Normal Speed. **88** - Strength class.
E.g. **101-3** - Grip length 101 mm and test number 3

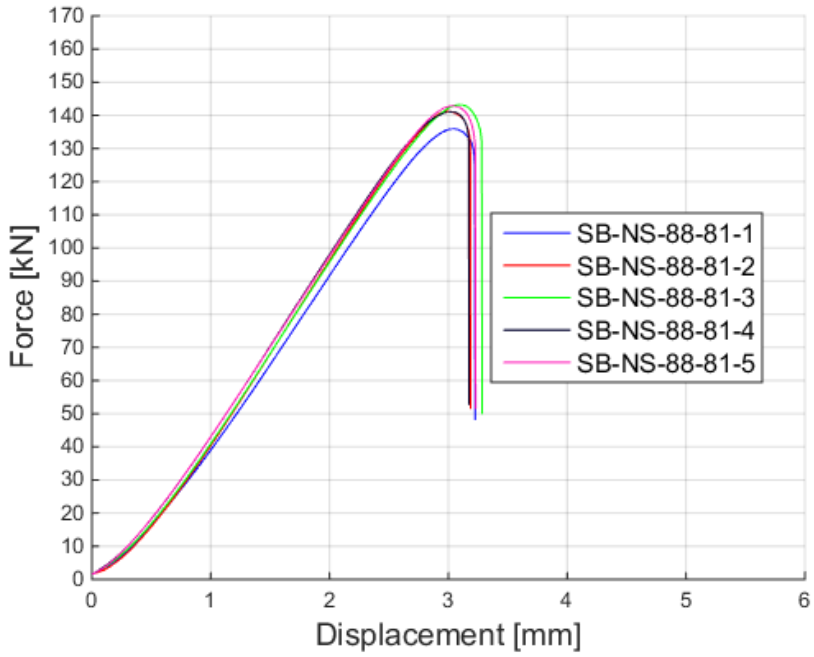

Figure 4.11: Bolt tests: SB-NS-88-81
All failed by thread stripping

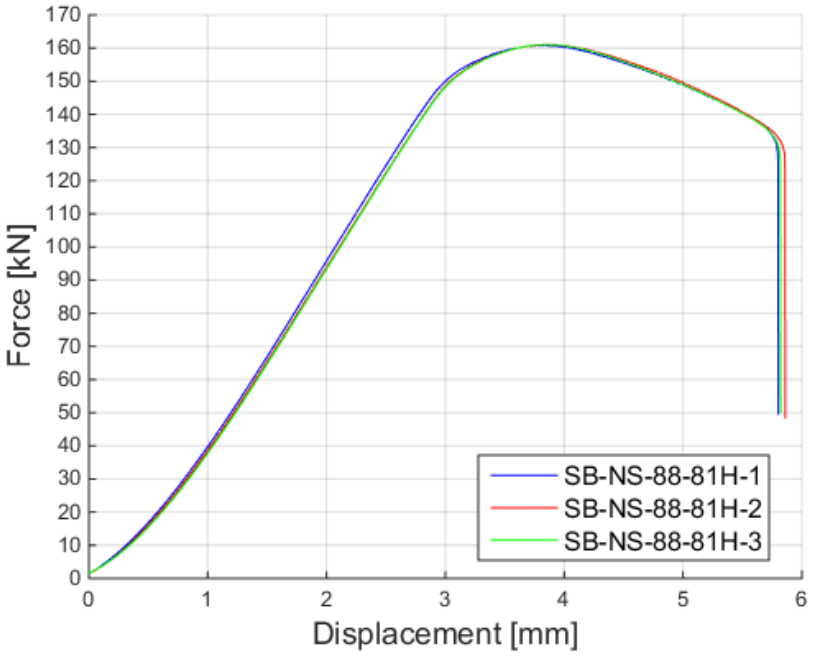

Figure 4.12: Bolt tests: SB-NS-88-81H
All failed by bolt fracture

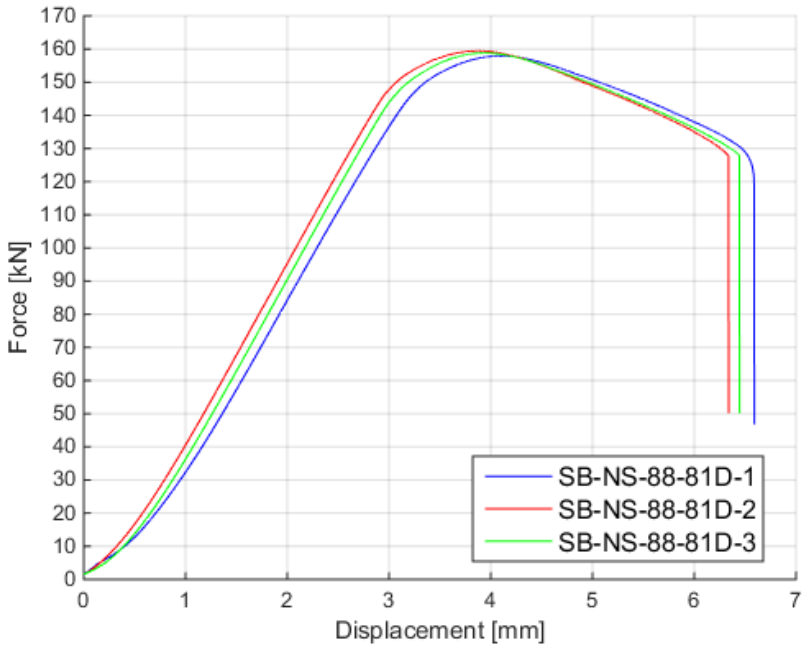

Figure 4.13: Bolt tests: SB-NS-88-81D
All failed by bolt fracture

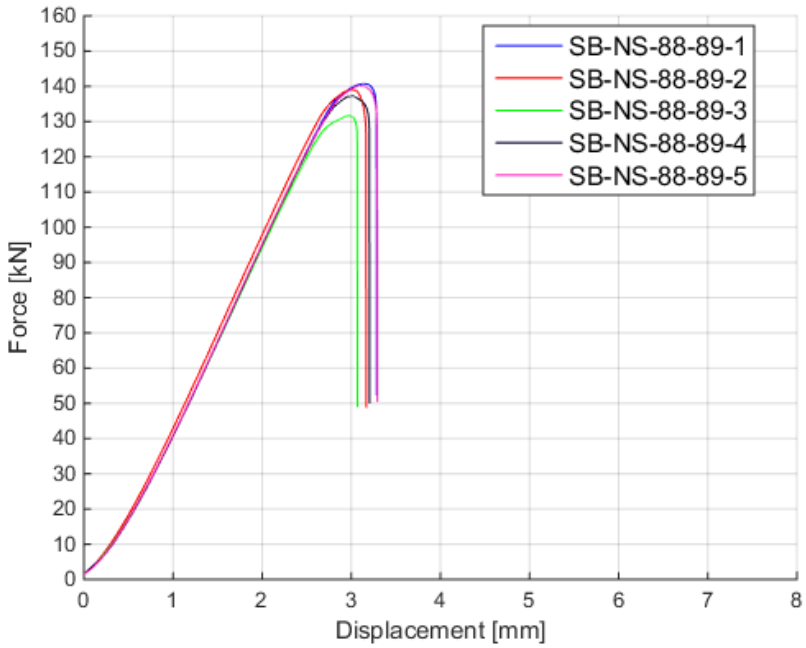

Figure 4.14: Bolt tests: SB-NS-88-89
All failed by thread stripping

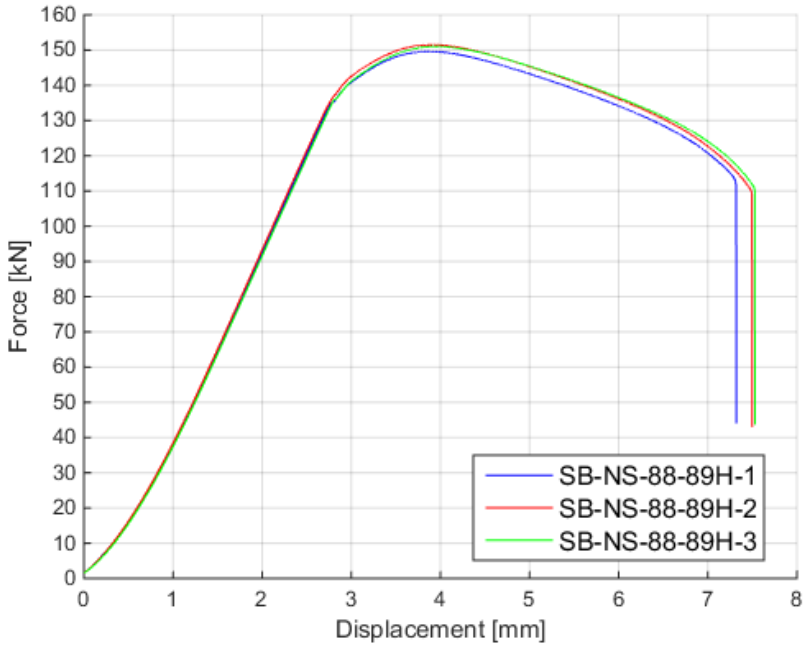

Figure 4.15: Bolt tests: SB-NS-88-89H
All failed by bolt fracture

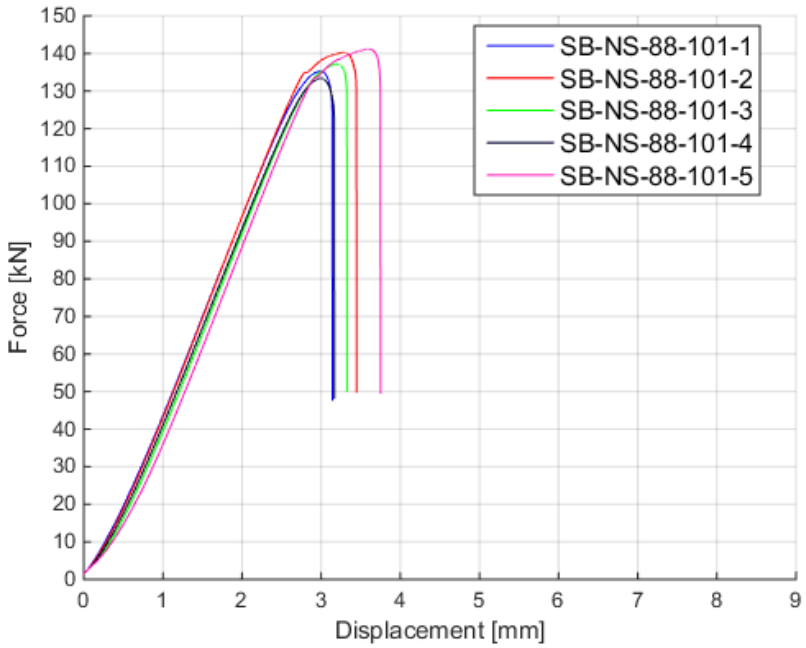

Figure 4.16: Bolt tests: SB-NS-88-101
All failed by thread stripping

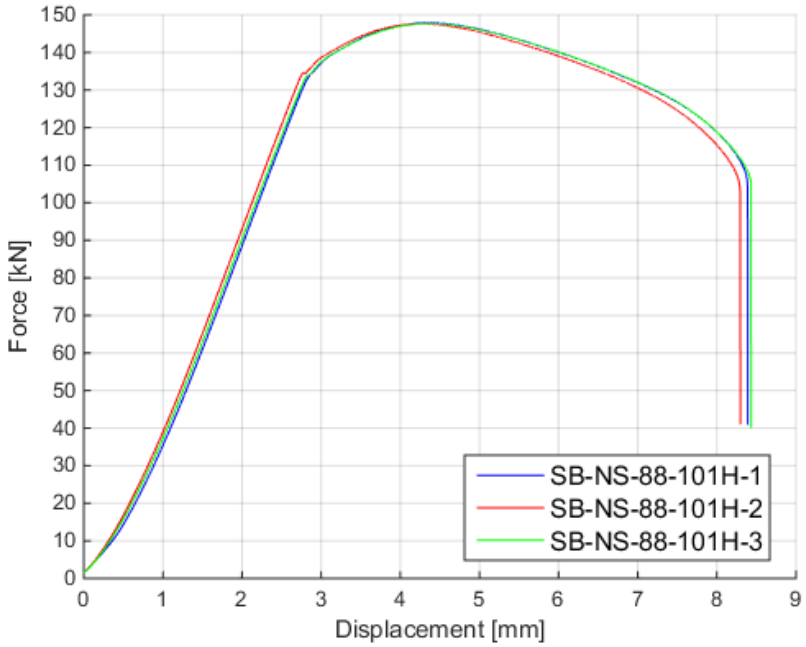

Figure 4.17: Bolt tests: SB-NS-88-101H
All failed by bolt fracture

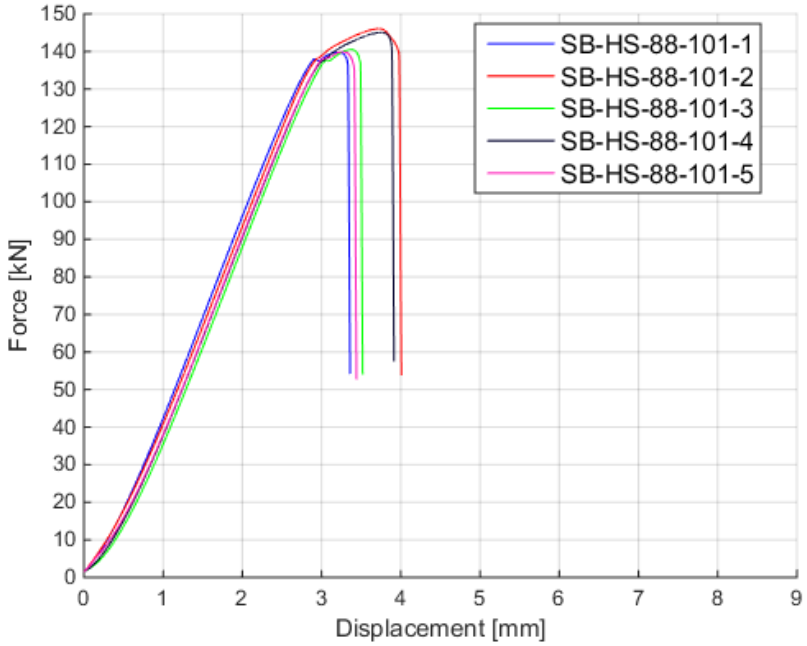

Figure 4.18: Bolt tests: SB-HS-88-101
All failed by thread stripping

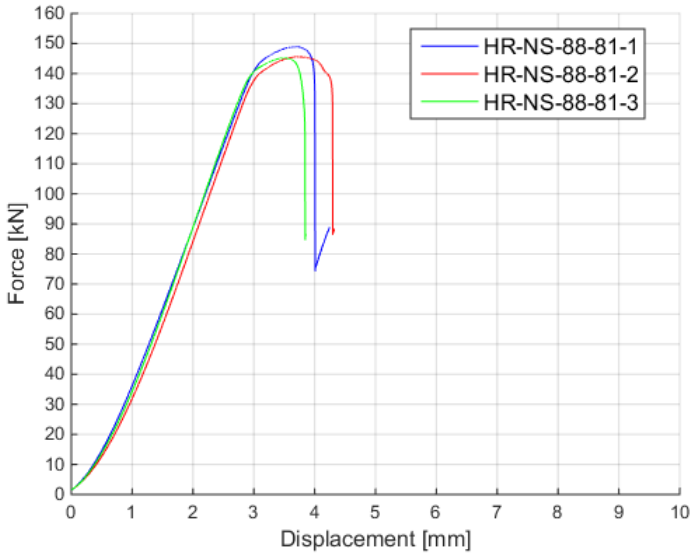

Figure 4.19: Bolt tests: HR-NS-88-81
All failed by thread stripping

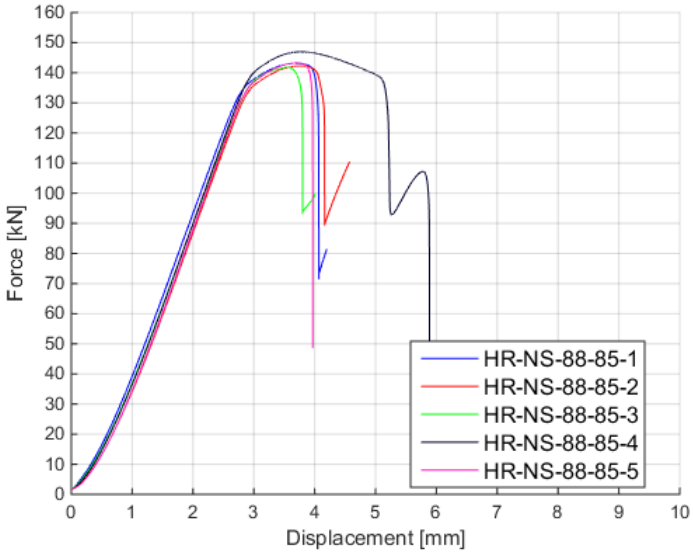

Figure 4.20: Bolt tests: HR-NS-88-85
All failed by thread stripping. Note that test specimen 4 was crookedly loaded

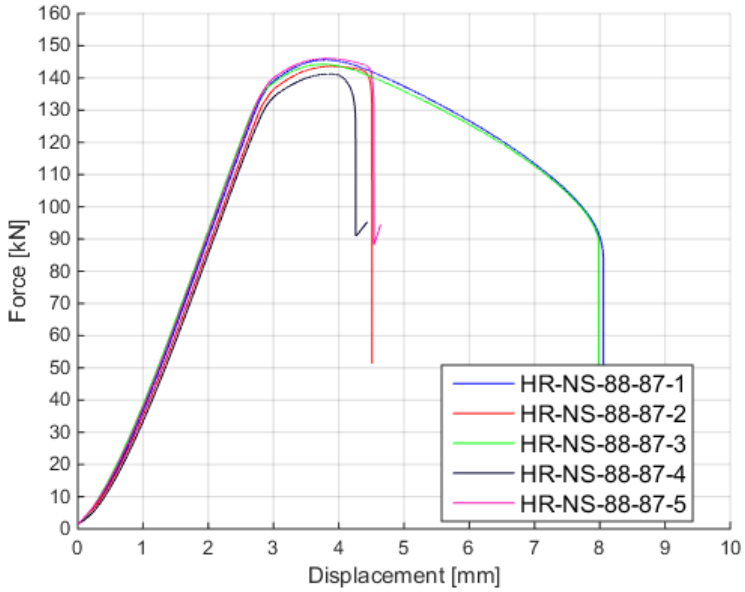

Figure 4.21: Bolt tests: HR-NS-88-87
Test specimen 1 and 3 failed by bolt fracture, the rest failed by thread stripping

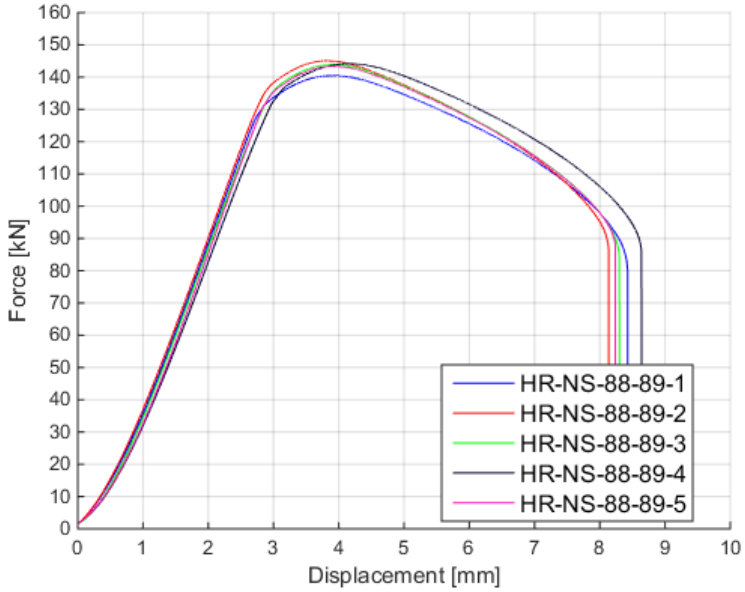

Figure 4.22: Bolt tests: HR-NS-88-89
All failed by bolt fracture

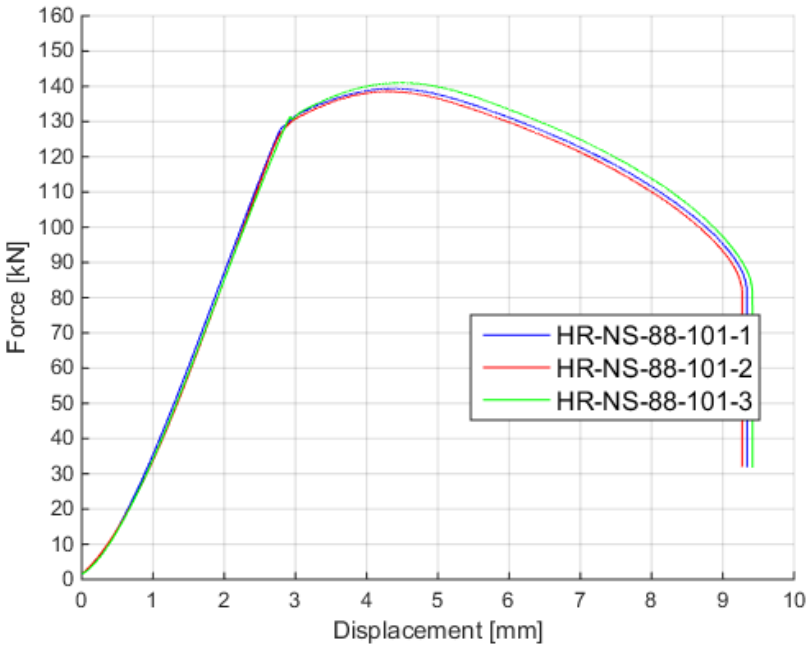

Figure 4.23: Bolt tests: HR-NS-88-101
All failed by bolt fracture

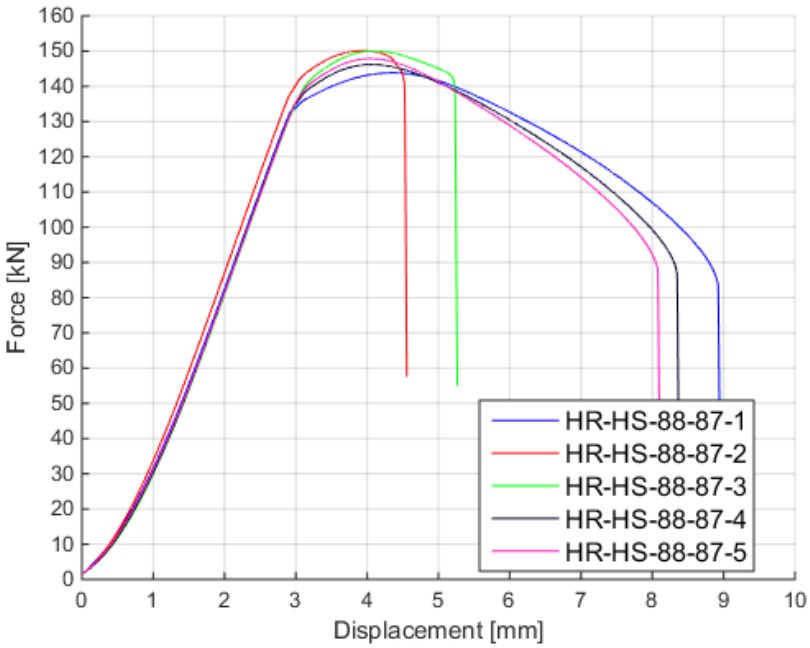

Figure 4.24: Bolt tests: HR-HS-88-87
Test specimen 2 and 3 failed by thread stripping, the rest failed by bolt fracture

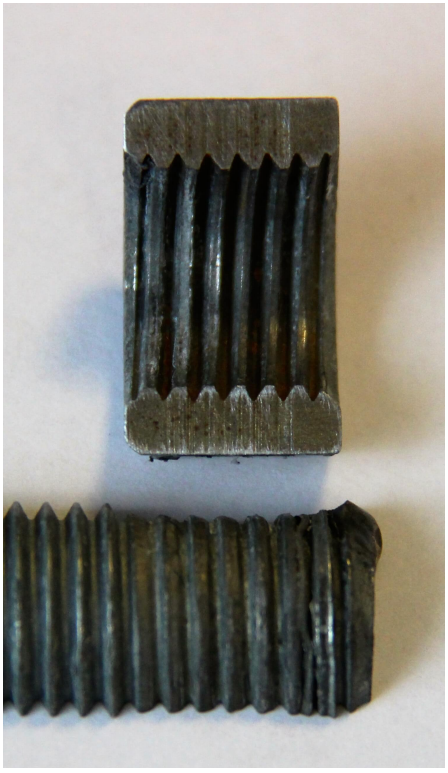

(a) Clearly bent bolt threads

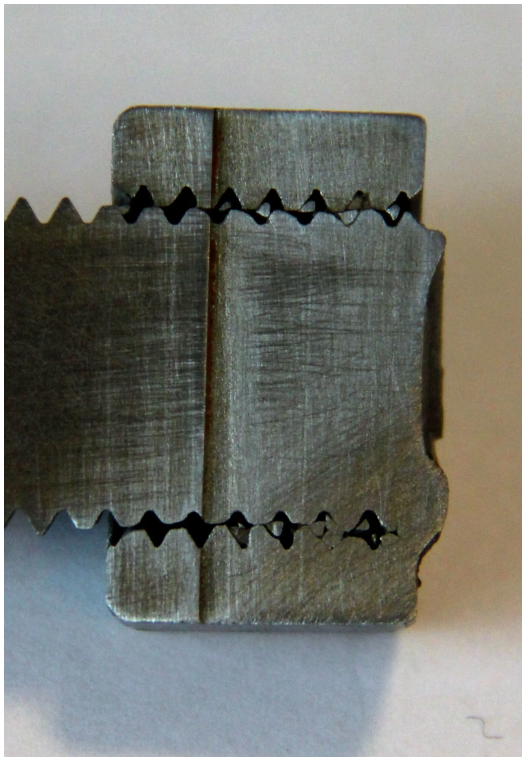

(b) Bending and shear failure in threads. Note that nut was welded to the bolt prior to cutting.

Figure 4.25: Bolt and nut failed by thread stripping (SB-NS-101)

Figure 4.25 shows a sawn bolt and nut that failed by thread stripping. The threads have clearly experienced yielding and are bent. Some of the threads are even sheared off. The nut have dilated in the radial direction due to large compression at the most loaded end, on the left hand side in Figure 4.25b. Threads in test series that failed by bolt fracture were almost unaffected, and figures are omitted.

4.5.2 Material tests

Results from material tests are presented in the current section. Figure 4.27 and Figure 4.28 shows the force and displacement plots taken from the test machine. Therefore, as mentioned in Section 4.5.1, the plotted deformation is slightly too large. As expected, the data showed good repeatability and only two tests were conducted for each bolt type. All specimens failed by the same failure mode as shown in Figure 4.26.

Figure 4.26: Fracture of material test specimen

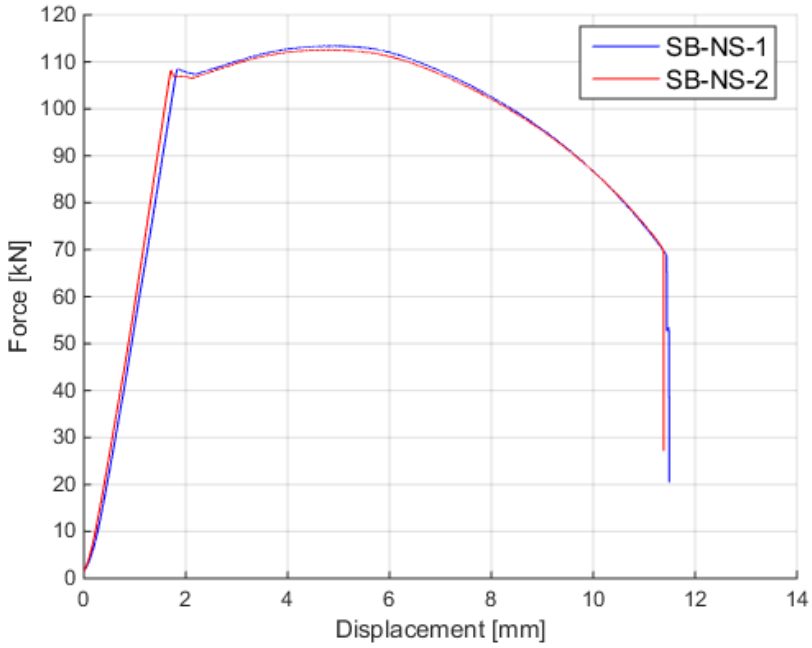

Figure 4.27: Material tests: SB-NS

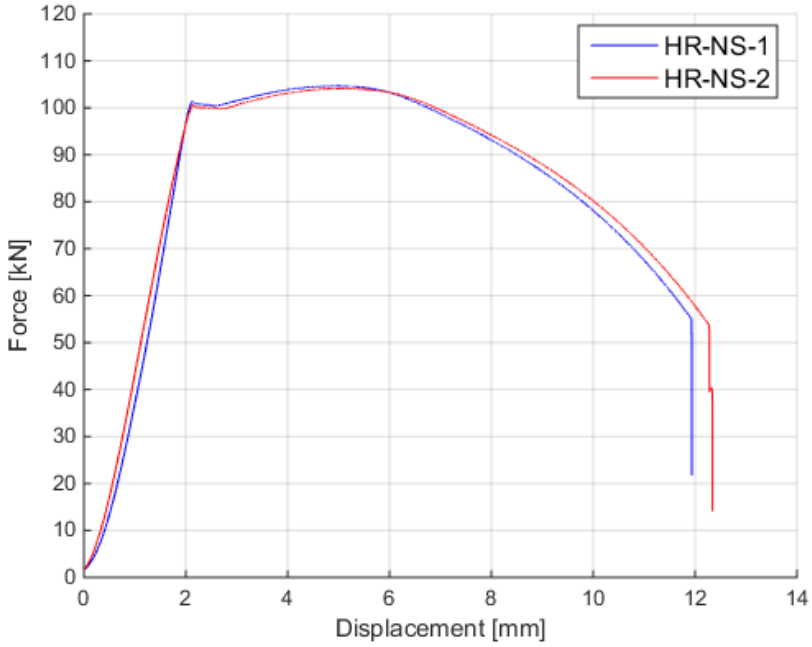

Figure 4.28: Material tests: HR-NS

4.6 Comments to the experimental work

During assembly of the SB-bolt and regular nut, the fit felt less tight compared to the high nut. This can be seen in Figure 4.29, and may be an influencing reason for the repeated thread stripping. The picture was taken when both nuts were moved to one side of the bolt, which gave the maximum gap on the opposite side. Further investigation of this observation is performed in Chapter 6, in relation with tolerance limits from the ISO standard.

As opposed to SB-bolts, the HR-bolts experienced a change of failure mode. The failure mode changed when the grip length was larger than 87 mm, see Table 4.5. More extensive testing at this grip length should have been performed, but it was not possible due limited amount of available test specimens.

There was only performed one test series with higher speed on each bolt type, as can be seen in Table 4.1. The failure mode did not change with higher deformation rate. In addition, the tests with higher speed did not show any remarkable differences in the response. The maximum force deviated with 2 %, and only small differences in stiffness and hardening were observed. Because of these observations, in addition with comparison of theoretical strain-hardening effect in Chapter 5.1, it was decided to not perform further tests with high speed. To obtain noticeable effects the test speed should have been much higher, but it was limited by the maximum camera frequency.

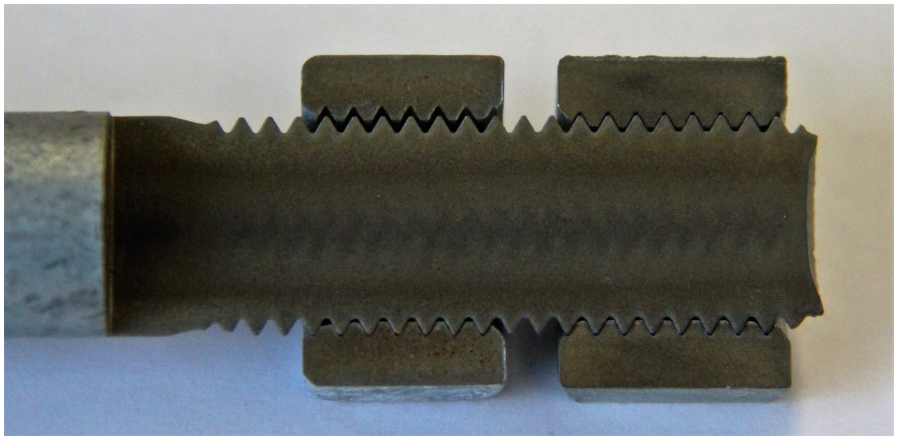

Figure 4.29: Gap between bolt and nut threads
Regular nut to the left, and high nut to the right

5. *Material parameters identification*

Based on test results from material tests in the laboratory, material parameters for FE simulations were determined. Detailed description of the process is presented in this chapter. All illustrations and examples are related to the test case; HR-NS-2. Because of minor differences in material response, only one test was used to determine material parameters for each bolt type. The same procedure as described in this chapter was used for determining material parameters for all bolt and nut types. Test procedure and geometry of test specimens are described in Chapter 4.3. Likewise, the description of the FE models of the material test specimen is covered in Chapter 6.1.

The SB-bolt, regular nut and high nut were assigned the same material properties calibrated for the SB-bolt. The HR-bolt and HR-nut were assigned the same material properties as calibrated for the HR-bolt. This was done because of the limited knowledge of the nut properties. A parameter study, in Chapter 6.3, examine this assumption.

5.1 Material hardening by *Voce law*

After yielding of the test specimen, most of the deformation was localized to the necking zone. It may be advantageous to calibrate the material parameters based on material behaviour in the zone of necking, instead of using the global response. DIC was used to measure local material behaviour, as described in Chapter 3.4. A virtual vector was placed in the transversal direction to trace the diameter reduction, $\frac{d}{d_0}$, in the zone of necking, as seen Figure 5.1. The longitudinal strain was calculated from the change in diameter by using the assumption of plastic volume conservation and Eq. 3.22.

Voce law [26] was used in a curve fitting process, where a stress-strain relationship was fitted and extrapolated based on experimental data. The iterative process of changing the constants in *Voce law*, went on until the graph with force and diameter reduction from FE simulations coincided with the experimental test data. The final constants used in *Voce law* are presented in Table 5.1. One equation was used for each bolt type and corresponding nut, independent of element type and size used in FE modeling. This was done because the element type and size had negligible effect on hardening under quasi-static conditions. Parameters for material hardening was written to a text file and exported to Abaqus.

Based on preliminary experimental tests, the strain rate effect were neglected from the hardening model. Figure 5.2 shows the difference between *Voce law* with, and without strain rate hardening effects. This effect is based on Equation 3.16 with the constants q and $\dot{\varepsilon_0}$ taken from Grimsmo et. al. [23]. The preliminary strain rates test were; 0.8 mm/min and 60 mm/min.

Table 5.1: *Voce law* constants

	σ_y	Q_1	c_1	Q_2	c_2
SB	913.7	-55010	0.01217	106.7	-41.59
HR	890.1	-54000	0.009104	70	-32.83

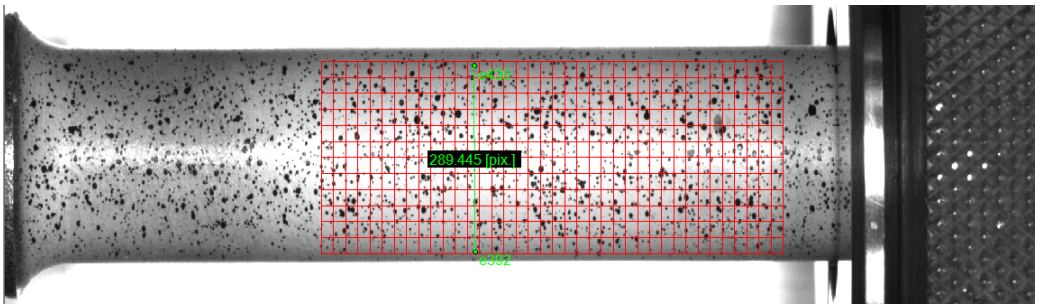

(a) Virtual vector at test start

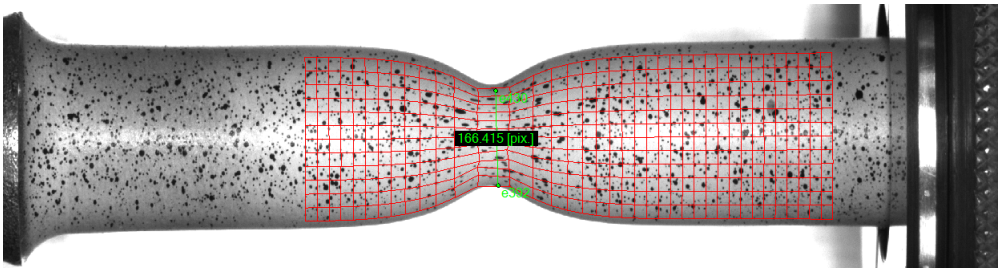

(b) Virtual vector after necking

Figure 5.1: Trace of necking in material test specimen by DIC

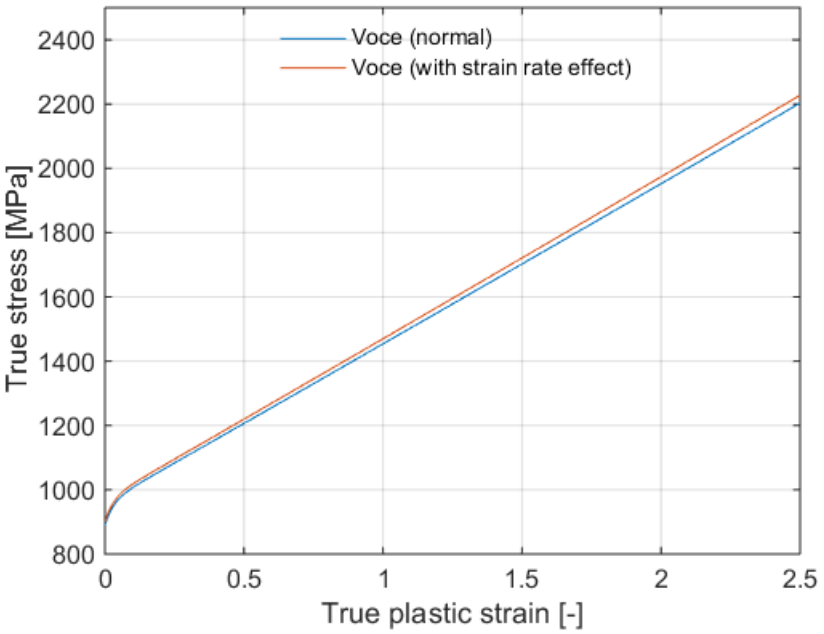

Figure 5.2: Strain rate effect for *Voce law*

5.2 Calibration of W_c - number

When the hardening parameters were determined, a criterion to predict fracture was needed in FE simulations. The *Extended Cockcroft-Latham* fracture criterion, under the assumption of plane stress was employed. This criterion and the calibration process was known from the *Specialization Project - TKT4511 Computational Mechanics*, taken fall 2015, and was used because of its easiness due to calibration and implementation. For calibration of this criterion, the W_c - number is needed. The W_c - number represents the total strain energy per unit volume prior to fracture.

From the graph of force and diameter reduction, the time of fracture was localized to the point where the experimental test data ends. At the same diameter reduction, the same time for fracture, $t_{fracture}$, was found in the data from the FE simulation. As described in Eq. 3.19, the maximum principle stress and equivalent plastic strain was integrated to fracture strain at time $t_{fracture}$ for calculating W_c. This was performed individually for elements over the cross-sectional diameter in the zone of necking, resulting in different W_c-numbers for each element.

Ambiguity arises when choosing a W_c-number. W_c-number from an element at the core would give a fracture that propagates from the core and outwards, resulting in a global fracture too late. Contrary, a W_c-number from an element at the edge would predict fracture too early. Thus, a optimization of the W_c - number was performed. This resulted in fracture for the same diameter reduction as the experimental tests, and thereby representing the global response.

Table 5.2 presents how the W_c-number varies for elements over the cross-sectional diameter, and element numbers are illustrated in Figure 5.3. Element 1 is always located in the core of the specimen. Figure 5.4 illustrates how maximum principle stress and equivalent plastic strain varies for elements over the cross-sectional diameter. Elements located near the core are exposed to more plastic work, which results in a higher W_c-number. The plot from experimental test is located lower since it represents a mean value for the whole cross-section. Data from FE simulations goes beyond the data from experiments, because the fracture criterion was not employed in these FE simulations.

The W_c-number was found highly mesh sensitive. Therefore, calibrations were performed individually for different element types and sizes. Table 5.3 and 5.4 presents the calibrated W_c-numbers.

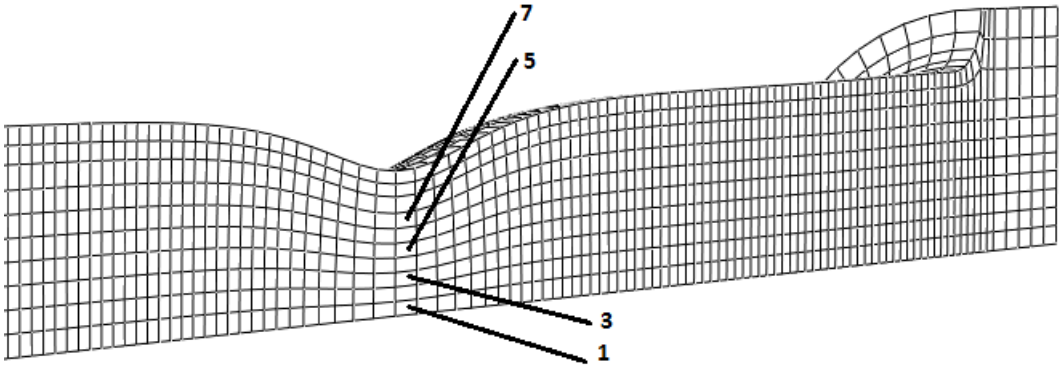

Figure 5.3: Cross-sectional element numbering for calculation of W_c

Table 5.2: Variation of W_c - numbers for cross-sectional elements

Find corresponding element number in Figure 5.3

Element size [mm]	**Element number**	W_c **- number**
0.5	1	2599
	3	2570
	5	2499
	7	2385
	9	2223
	11	1985

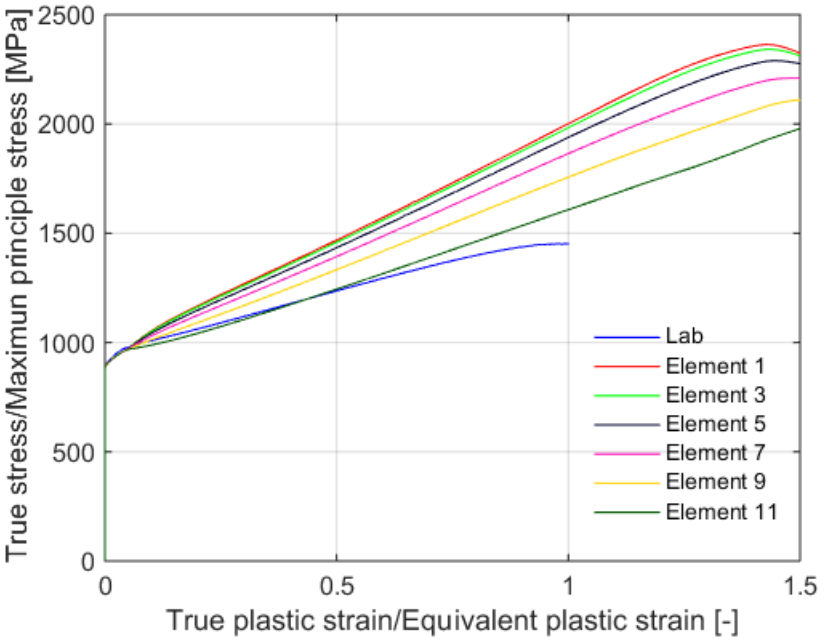

Figure 5.4: Principle stress and equivalent plastic strain for cross-sectional elements (HR-NS-2)

Table 5.3: SB-bolt: W_c - numbers for different element types and sizes

Element type/ Model	**Element size [mm]**	W_c**-number**
Axisymmetric	0.4	2 577
	0.1	2 680
3D Non helix	0.5	2 425
	0.2	2 663
3D Helix	0.4	2 545

Table 5.4: HR-bolt: W_c - numbers for different element types and sizes

Element type/ Model	**Element size [mm]**	W_c**-number**
Axisymmetric	0.4	2 570
	0.1	2 741
3D Non helix	0.5	2 441
	0.2	2 643
3D Helix	0.4	2 632

5.3 Fracture criterion

When the W_c-number was calibrated, the relationship between fracture strain and triaxiality could be determined, as seen in Figure 5.5. Due to the fact that some threads failed in shear (See Figure 4.25), the *Extended Cockcroft-Latham* fracture criterion was used instead of the classical version. Figure 5.5 shows the difference between the two criteria. The extended version gives a lower fracture strain for shear dominated stress states, i.e. triaxiality around zero, as discussed in Chapter 3.2.3.

Figure 5.6 illustrates how different W_c-numbers from Table 5.2 affected the time of fracture for test case HR-NS-2. W_c-numbers from inner elements caused a delay of fracture, while using outer elements caused a premature fracture. The time fracture occurred between element 5 and 7, and the mean of $W_{c,5}$ and $W_{c,7}$ gave an appropriate W_c-number for representation of fracture. Analogous procedure was performed to determine the fracture parameters for all element types and sizes.

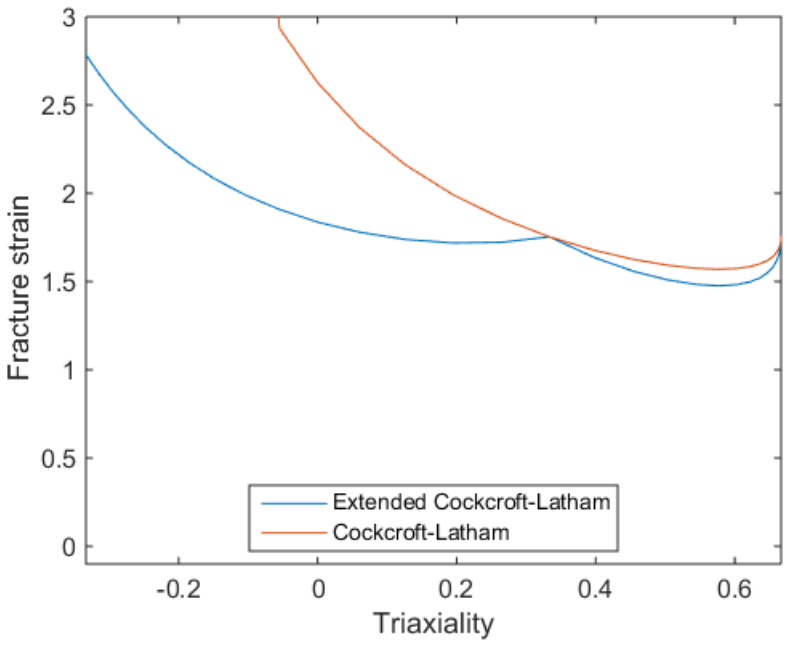

Figure 5.5: Comparison of classical and extended *Cockcroft-Latham fracture criterion*

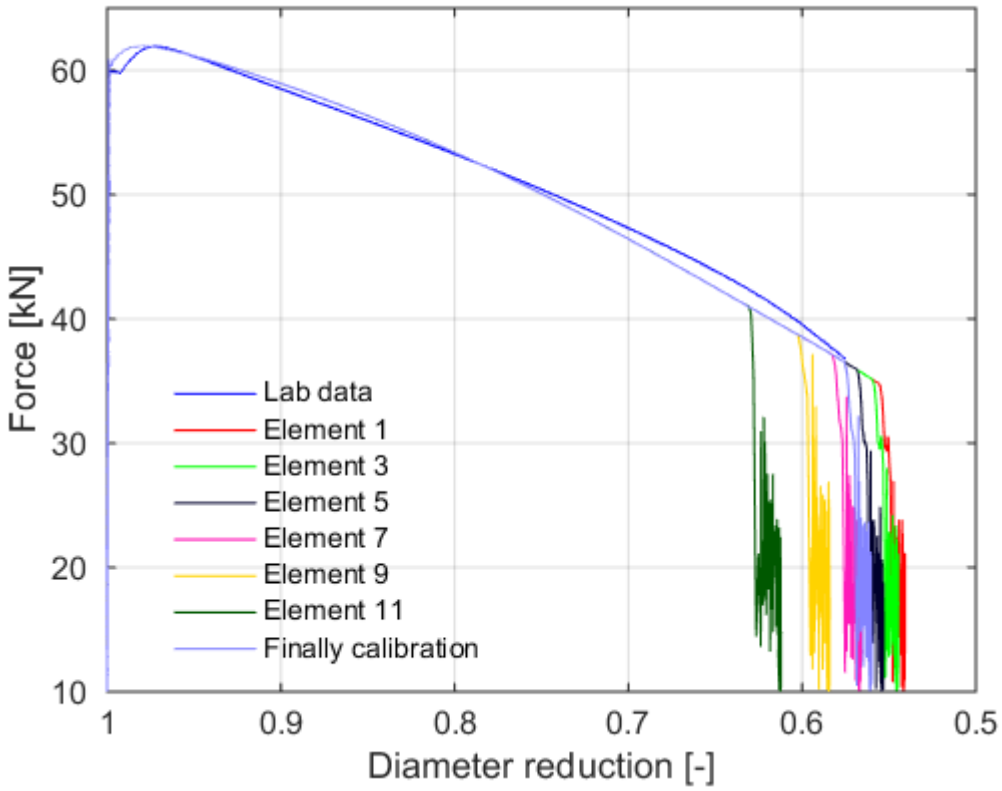

Figure 5.6: Occurance of fracure for cross-sectional elements with different W_c - numbers (HR-NS-2)

6. *Finite element modelling*

Finite element models of tension loaded bolts and material tests were used to study the bolt behaviour in detail. Three different models has been constructed: One axisymmetric model, and two 3D models. One of the 3D models included the helical geometry of the threads, while the other was simplified with circular threads. In addition, one axisymmetric model and one 3D model for the material tests were created to calibrate the material parameters.

Some models had an extremely large number of elements in addition with small critical time steps. Simulations could not be handled by standard laptops because of the computational requirements. A supercomputer named *Vilje* that is shared by NTNU, Norwegian Meteorological Institute and UNINETT Sigma [5], handled the most demanding simulations. Most of the simulations were performed on a cluster named *Snurre* at the Department of Structural Engineering, with a total of 252 cores.

This chapter describes the construction of the different models. It also presents a parameter study and a comparison between the models. All simulations and analysis were performed with the FE program Abaqus/Explicit V6.14, and all the models were constructed using *Python* scripting [6].

6.1 Modelling of material test

The geometry of the test specimens is illustrated in Figure 4.7. The 3D model was constructed as solid revolution, and the axisymmetric model was constructed in a axisymmetric plane. To reduce the number of elements, the treaded part and the bolt head was excluded from the model. Since deformation was localized to the section with reduced diameter, this simplification seemed reasonable. See Figure 6.1 for illustration of the 3D model. The same element types and sizes used for the material tests were used in the bolt assembly models. This ensured the best material response representation in the FE models with similar element type and element size.

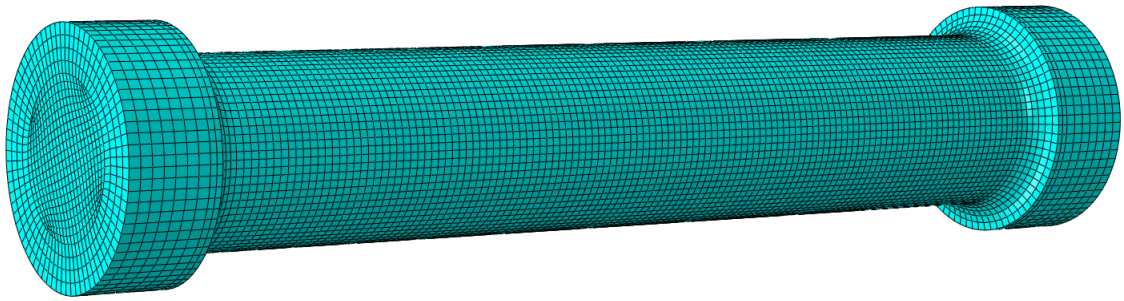

Figure 6.1: 3D FE model of material test specimen (0.5 mm element size)

6.2 Modelling of bolt assembly

Creating the three different models have been a comprehensive part of this thesis. Especially the complex geometry of the 3D helix model required a lot of work. Some simplifications were introduced, without sacrificing important physical properties. This was necessary to make the simulations run. Each of the models were assigned material properties, as determined in Chapter 5, based on the element type and size.

6.2.1 Geometry

The initial models were created utilizing the geometrical sizes from respective ISO-standards [15] [16] [17] [19]. Some general comments valid for all models is presented in the list below:

- The dimensions of the threads are not fully according to ISO 68-1 [20]. Measured dimensions, as seen in Figure 6.2, were employed by the use of a relative pixels to mm technique.
- The small round off geometry of thread valleys and thread tips was omitted. It was difficult to measure the exact curvature because of the small dimensions, and it was assumed to have negligible effect.
- The complete bell mouth shape of the nut in the axisymmetric and 3D non helix model was not taken into account, since this was studied by Skavhaug and Østhus [35]. However, the reduced height of the two outermost threads in both ends of the nut was constructed in relation with the countersinks. This can bee seen in Figure 6.3.
- The bell mouth shape of the nut was included in the 3D helix model, because it was desirable to use as exact geometry as possible. The bell mouth shape can be seen in Figure 6.2 and Figure 6.3a
- The washer in simulations with HR-bolts was omitted. This part was expected to have negligible influence on the results.

The most important geometrical approximations will be presented in the following sections. Further geometrical details are presented in Appendix A.

Axisymmetric model

The major geometrical simplification in this model was that the threads were modelled as circular, without the helical shape. The axisymmetric model was drawn in the x-y plane. Because of this, the hexagonal shape of the nut was also impossible to capture in a axisymmetric model. This may influence the radial dilation of the nut. An average of width across flats and with across corners was used as the diameter of the circular nut. Figure 6.6 illustrates the final geometry of the model.

3D model without helical shape of threads

Similar geometrical simplifications as mentioned for the axisymmetric model were also implemented for the 3D non helix model. The benefits of a 3D model is that it enables to position the nut non centric, in addition to model a hexagonal shape of the nut and bolt

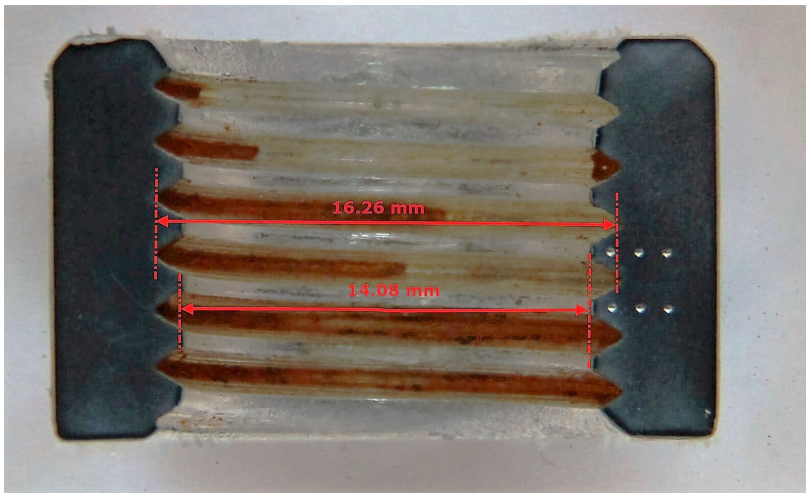

(a) Regular nut

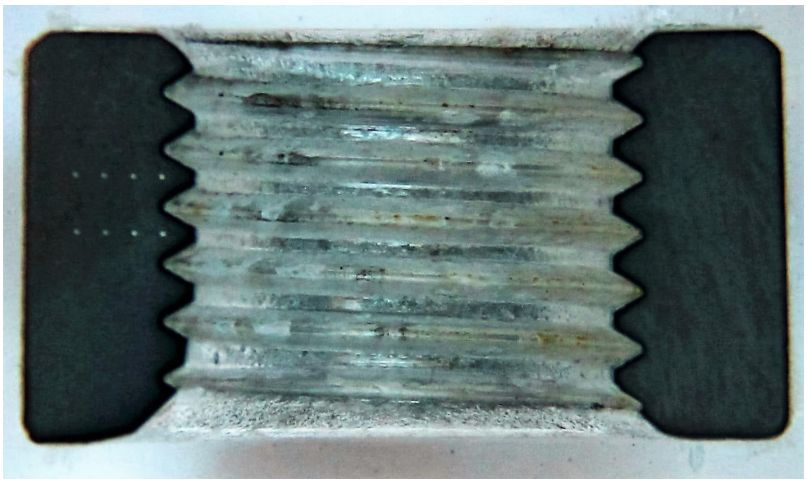

(b) HR-nut

Figure 6.2: Cutted nuts

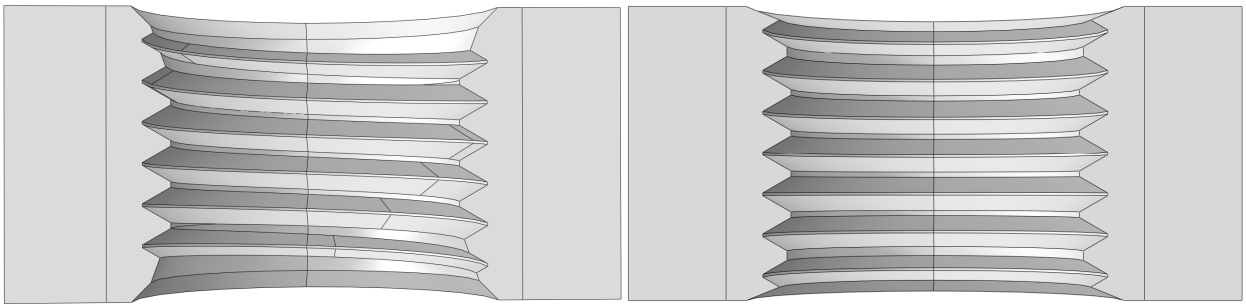

(a) Nut with helix threads (Bell mouth shape)

(b) Nut without helix threads (Reduced thread height in each end of countersink)

Figure 6.3: Cutted nuts from FE models

head. A non centric position of the the nut could alter the load distribution among the threads, which can affect the failure mode.

As seen in Figure 6.6 for the axisymmetric model and Figure 6.7 for the 3D non helix model, the height of the first bolt thread above the shaft was smaller compared to the others. The lowermost thread starts from zero height and increases gradually up to full height as it rotates upward in a helix. Reducing the height of the first bolt thread will somehow ensure the thread runout effect of the bolt.

3D model including helical shape of threads

Modelling a full 3D model with helical threads was challenging. The complexity of the thread structure made it impossible to create a perfect model. Some approximations were introduced to make the model run at all, and a lot of trial and error was necessary.

Threads in the nut were made by cutting out the thread geometry inside a hole in a cylinder. The threads gradually fades out as they near the countersink in both ends of the nut. A numerical infinity problem arose due to this fading, because some elements became distorted. Figure 6.4 illustrates the problem, and how this was circumvented by stopping the fading prematurely. This resulted in a sharp edge, but enabled meshing without to distorted elements. Small amount of forces should have been taken by this omitted area, but the geometrical approximation should have negligible effect on the global response.

The threaded part of the bolt was created in a similar way as the nut; by rotating the thread geometry upward with a pitch height when cutting into a cylinder. Production of bolt threads is often performed by roll-threading, that makes a gradual transition from the shank to the threaded part of the bolt. The threads gradually increase to full height over the first pitch. To reproduce this geometry, a small cut appears in the chamfer area where the cutting starts, as seen in Figure 6.5. ISO 1090-2 [18] requires for non preloaded bolts (SB-bolts) that *at least one full thread (in addition to the thread run out) shall remain clear* from interaction with the nut. For preloaded bolts (HR-bolts), four full threads shall remain free. Because of this requirement, the cut should not affect the global response since the nut will be placed above this section.

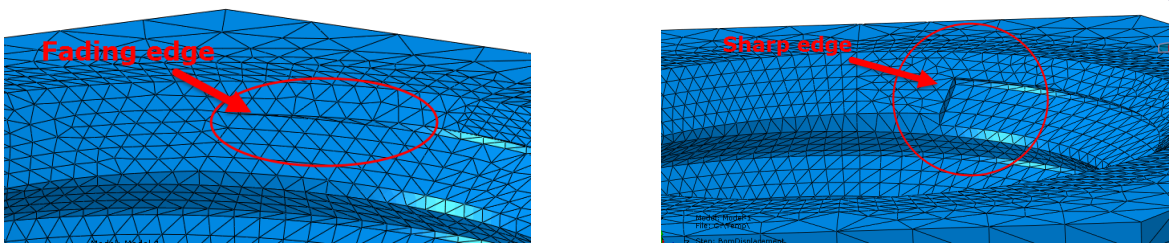

(a) Fading edge in countersink

(b) Simplification

Figure 6.4: Solution of numerical infinite problem due to complex geometry

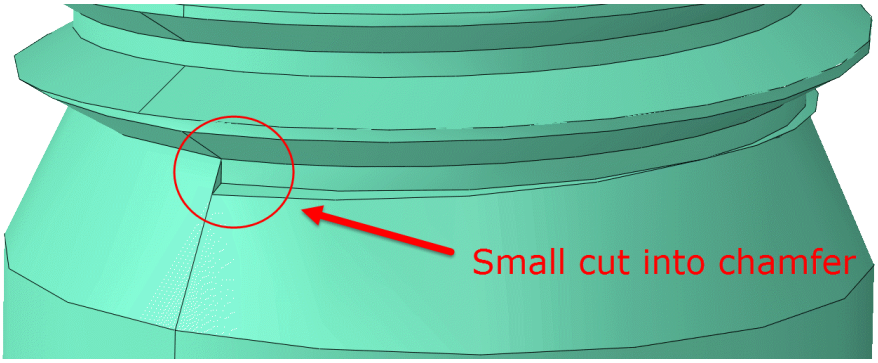

Figure 6.5: Small cut in the chamfer part of the bolt

6.2.2 Element types

All three models had different characteristics and it was therefore advantageous to use different element types.

Axisymmetric model

The whole model employed continuum axisymmetric 4-node reduced integration elements, CAX4R. Reduced integration is preferable because it reduced the computational cost, since each element contains only one integration point. Axisymmetric solid elements are completely defined in a 2D plane, similar as ordinary 2D elements [31]. In addition, these elements account for the circumferential strain in the shape functions, and the strain and stiffness matrix. A 3D model can therefore be described in a 2D plane, which enables a large number of small elements at the same time as the computational cost is reduced.

3D non helix model

A solid linear continuum 8-node brick element with reduced integration, C3D8R, was used as element type. The element was chosen because it gave reasonably structured mesh, and it is computationally more effective with the same result compared to similar higher order elements or tetrahedral elements [3]. That is advantageous because of the large number of small elements needed for being able to correctly describe the stress state in the threads.

Since the C3D8R element is described by linear shape functions, it can not reproduce bending correct because element edges remains straight instead of being curved. This induces unnatural shear forces (shear locking or hourglass modes), and the element acts overly stiff [30] without sufficiently large stress and strain state. To circumvent this problem, the Abaqus user manual suggests to use at least four elements over the thickness [1]. Abaqus provides a built in hourglass control to use for coarser mesh [3].

3D helix model

The complexity of the helix model made it necessary to utilize tetrahedral elements in order to capture all geometrical aspects. Tetrahedral elements are advantageous because of an effective meshing algorithm that allows irregular volumes to be meshed effectively. The element chosen was the C3D10M, a modified 10-node second order tetrahedral element with hourglass control.

With 10 nodes the element is described by quadratic shape functions. Thus, the strain matrix is linear such that bending is reproduced correctly as long as the edges of the element remains straight [30]. Abaqus describes this element as *robust for large deformation problems and contact* [3], exactly what was the case in this study. By using first order tetrahedral, the problem with shear locking arises and very fine mesh is needed for the solution to converge. A fine mesh with tetrahedral elements would result in a extremely large number of elements with further increase of the CPU cost. Using the second order tetrahedral element allowed for bigger element sizes because of correct bending representation, at the same time as Abaqus describes C3D10M as robust. Note that this element is computational demanding, because of four integration points and hourglass control [3].

6.2.3 Mesh

Due to computational efficiency it was desirable to reduce the total number of elements as much as possible. In areas of interests the mesh was refined, and it was kept coarser in areas of less importance. This can be seen from illustrations that follows in this chapter. Areas with different mesh sizes were assigned the respectively calibrated material parameter for that specific element type and size.

The total number of elements in each of the three models is presented in Table 6.1.

Table 6.1: Number of elements in each FE model

Model	**Approximate number of elements**
Axisymmetric (0.1 mm)	9 200
Non helix (0.2 mm/0.5 mm)	2 320 000/ 206 000
Helix (0.4 mm)	1 258 000

Axisymmetric model

Figure 6.6 illustrates the meshed model assembly. As seen, the threads in contact with the nut had the smallest elements. This section was separated by partition, and assigned 0.1 mm element size. It seemed to give a sufficient number of elements over the thread height, such that thread stripping could be predicted. Remaining parts of the threaded area had 0.4 mm element size, such that bolt fracture could be detected.

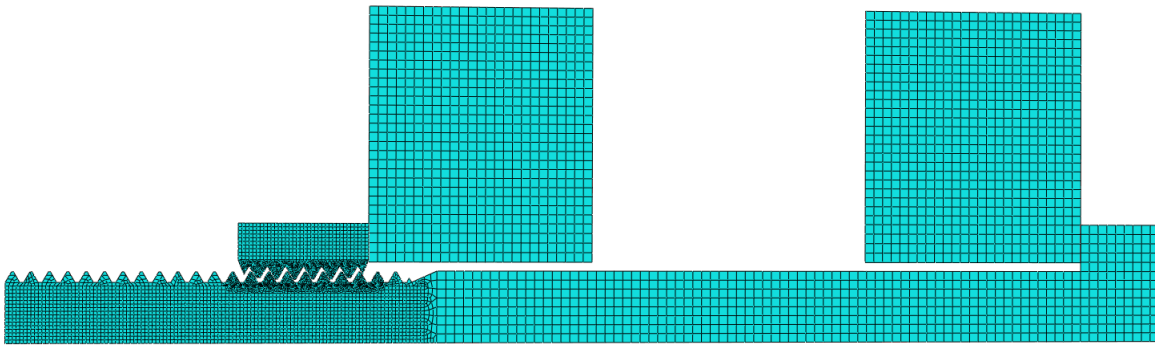

(a) Global mesh

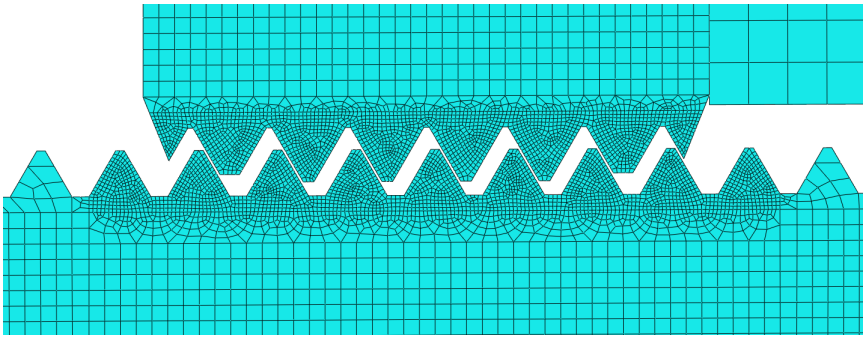

(b) Mesh in threads

Figure 6.6: Mesh and geometry of the axisymmetric model

3D non helix model

The bolt was separated into three different parts (bolt head, shank and the threaded part) to ease and improve meshing. By doing this, the total number of elements was reduced because the shank and bolt head was assigned a coarser mesh. It was also easier to improve the structure of the mesh in each part, because of no mesh transition. Since the threaded part of the bolt and nut was of interest, these parts were assigned a finer mesh. In the threaded sections, the element size was 0.2 mm which seemed to give a sufficient number of elements over the thread height (based on discussions in Section 6.2.2). Figure 6.7 and 6.8 illustrates the result. Note that some of the simulations had element size 0.5 mm in the threaded sections, giving four elements over the height, because that reduced the simulation time with at least 20 hours.

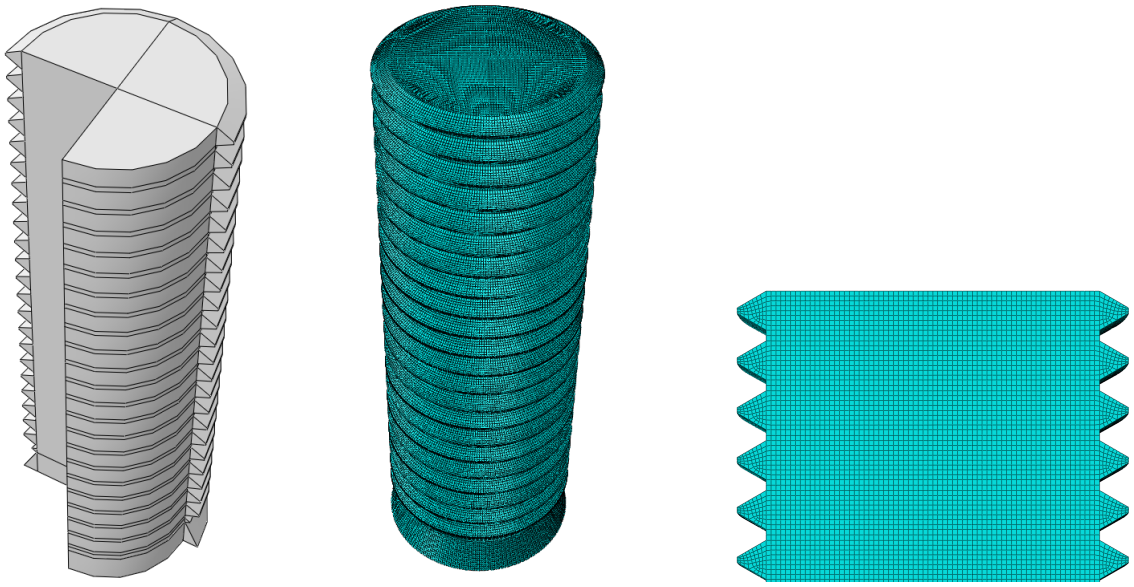

(a) Illustration of partition

(b) Entire mesh of the threaded part

(c) Detailed view of mesh through the cross-section

Figure 6.7: Threaded part from 3D non helix model

A circular partition to separate the threads from the bolt core was constructed, in addition to vertical partitions into four equal parts. Figure 6.7a illustrates these partitions. This gave a better mesh structure, and made it possible to use a meshing technique called sweep with medial axis as meshing algorithm. Similar circular and vertical partitions were made for the nut with sweep as meshing algorithm. Figure 6.8a illustrates the same partitions for the nut.

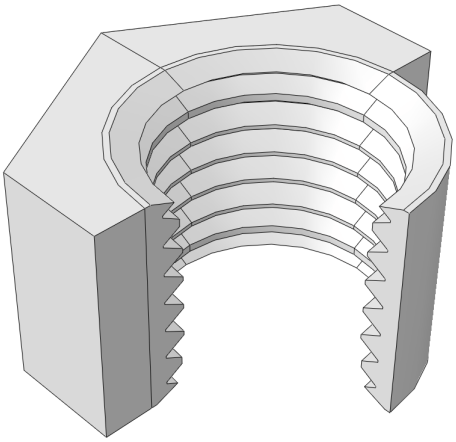

(a) Illustration of partition

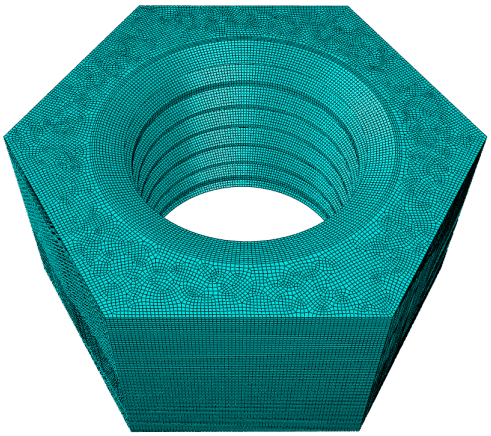

(b) Global mesh

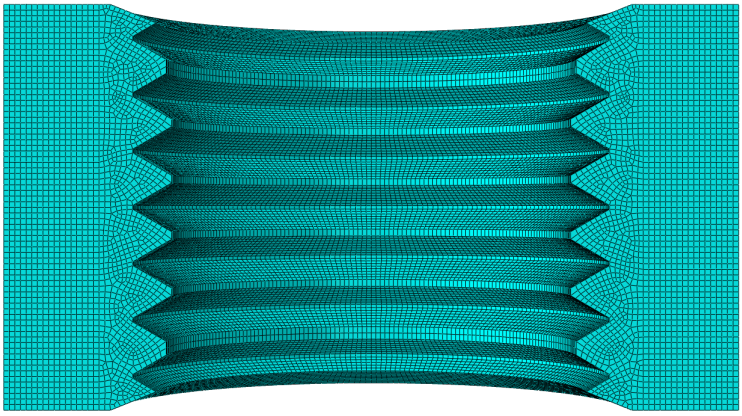

(c) Detailed view of mesh through cut

Figure 6.8: Nut from 3D non helix model

In Figure 6.9 the total assembly is presented, and the relative mesh sizes are illustrated. The steel plates are omitted in Figure 6.9b to clarify the mesh of the bolt and nut.

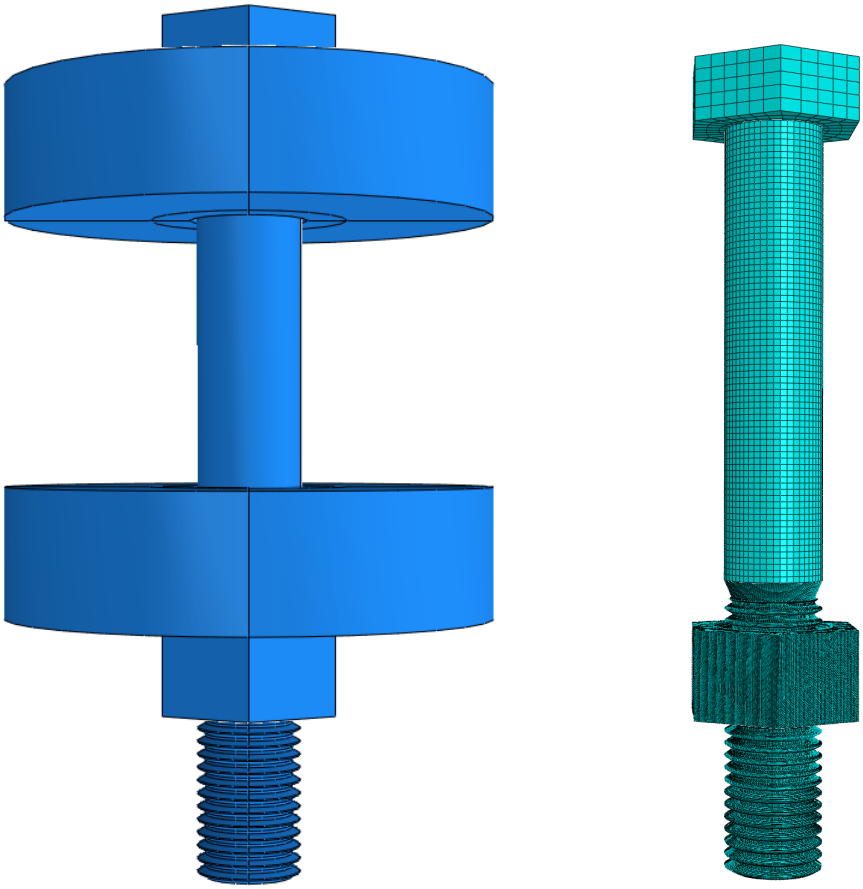

(a) Total assembly without mesh

(b) Mesh of bolt and nut assembly

Figure 6.9: Assembly of 3D non helix model

3D helix model

In the 3D helix model, the bolt was also separated into; bolt head, shank and the threads as separate parts. This simplified meshing and reduced the computational cost. In addition, it allowed to use different element types and sizes in each part. Because of the geometry, the threaded part was forced to contain tetrahedral elements. This resulted in a large number of elements compared to the use of brick elements that was employed in the shank. The element size was increased in the shank and head, since these regions were of less importance.

The threaded part was assigned a mesh size of 0.4 mm. This gave a reasonably number of elements over the thread height, at the same time as it gave a manageable number of elements considering computational cost. As discussed in section 6.2.2, using quadratic C3D10M elements allowed for bigger element sizes without losing important information.

10 mm of the unthreaded shank was included in the threaded part. The reason for this is further described in Section 6.2.5. A circular partition was made straight through the threaded part, because that made a reasonably structured mesh by the use of the free meshing technique. Figure 6.10 illustrates the result.

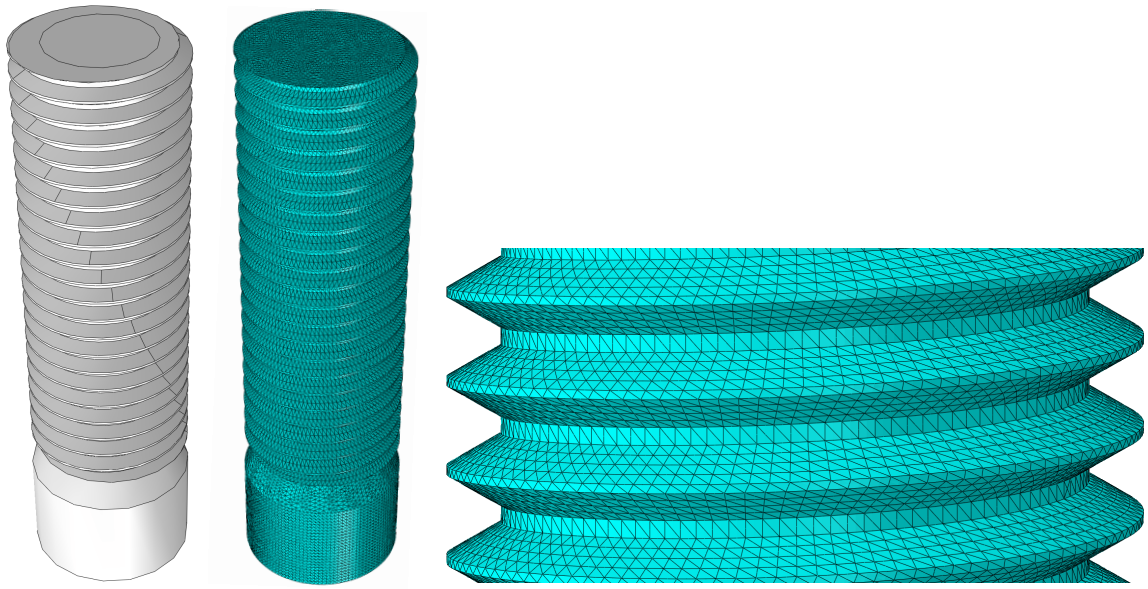

(a) Circular partition (b) Global mesh (c) Detailed mesh from outside

Figure 6.10: Threaded part from 3D helix model

Tetrahedral elements were also used in the nut. Since the threads were most interesting, the outer parts of the nut were assigned larger elements. It was preferable to keep the total number of elements as low as possible since tetrahedral elements were used instead of brick elements. This explains the partition of the nut; a circular partition was used to separate the threads from the outer part, which allowed for different element sizes. The outer part was assigned 0.6 mm element size, while the threads were assigned 0.4 mm element size. In addition, vertical partitions were used to structure the mesh. See Figure 6.11 for the result. The total assembly is illustrated in Figure 6.12.

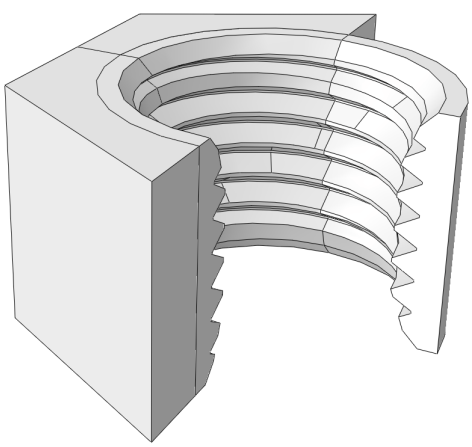

(a) Illustration of partition

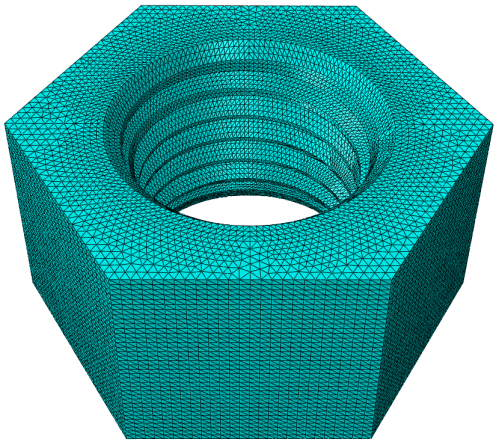

(b) Global mesh

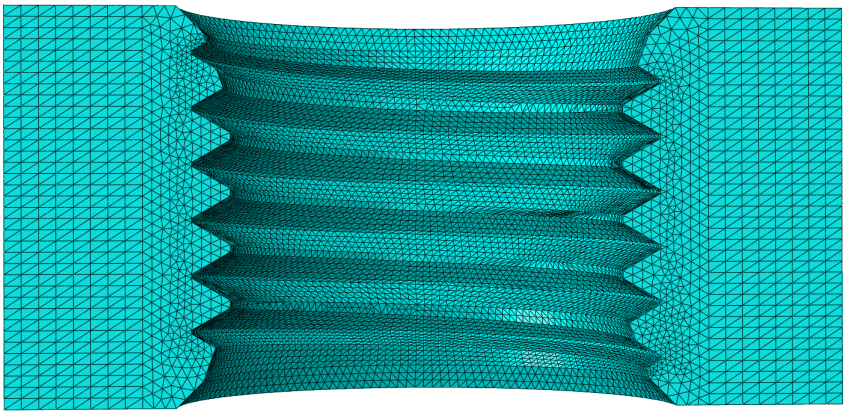

(c) Detailed mesh through cut

Figure 6.11: Nut from 3D helix model

A full analysis of the 3D helix model on a supercomputer with around 50 CPU's needed approximately 30-70 hours to complete. Therefore, only a limited number of analysis were performed with the 3D helix model.

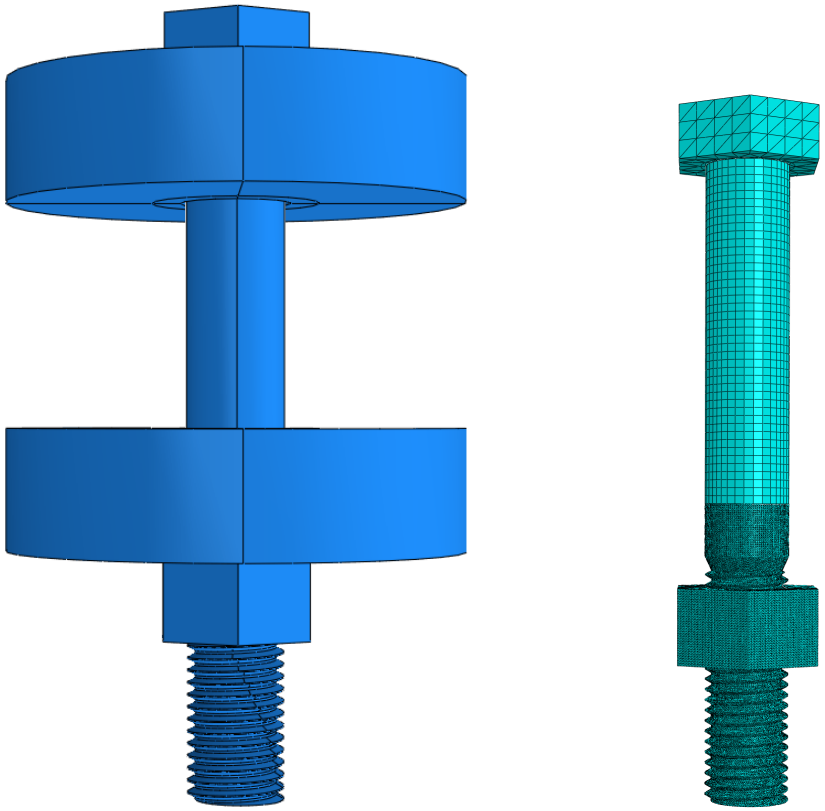

(a) Total assembly without mesh

(b) Mesh of bolt and nut assembly

Figure 6.12: Assembly of 3D helix model

6.2.4 Boundary conditions

As described in Chapter 4.2, the lower steel plate was restricted in the longitudinal direction. The steel plate at the bolt head were given a velocity of $v = 0.01333\,\mathrm{m/s}$, i.e. $0.8\,\mathrm{mm/min}$, in the longitudinal direction. These conditions were implemented in all FE models.

6.2.5 Interaction

NS-EN 1090-2 state that the friction coefficient for rolled steel surfaces is $\mu = 0.2$ [18], and this value was employed in all three FE models. Preliminary studies of the importance of friction were conducted and it was discovered that the choice of friction coefficient had limited influence. This observation was in accordance with Chen and Shih [9]. Thus, the value from NS-EN 1090-2 was employed in all models.

Axisymmetric model

Surface to surface contact algorithm, with kinematic compliance, was employed between appropriate surface pairs; upper steel plate against bolt head, lower steel plate against nut, and thread contact between bolt and nut. This algorithm results in a very precise solution, as it does not allow the surfaces to penetrate each other.

All surface pairs had approximately the same mesh size, but the master surface was chosen to have coarser mesh. The master surface cannot penetrate nodes on the slave surface, and by that it is advantageous to keep the slave mesh as small as possible. Hard contact was chosen in the normal direction, and tangential behaviour was employed with finite sliding and default settings. This allows for large relative displacement between surfaces, which can happen as the mating threads begins to slip.

Kinematic compliance is generally more computational demanding than the full penalty algorithm, but a simulation time of 4-6 hours was found acceptable.

3D models

A general contact algorithm with penalty formulation was employed because of its robustness. Abaqus user manual recommends this algorithm for models with complex geometry and multiple contact surfaces [2]. This was the case for the contact between threads. Abaqus also states that the algorithm is usually faster than defining contact pairs in complex 3D models. It was also easier to use because of less manual control, and initially overclosure (as in both ends of nut threads in 3D helix model) was automatically resolved. The contact properties were the same as for the axisymmetric model. Hard contact in the normal direction and finite sliding in the tangential direction were also employed.

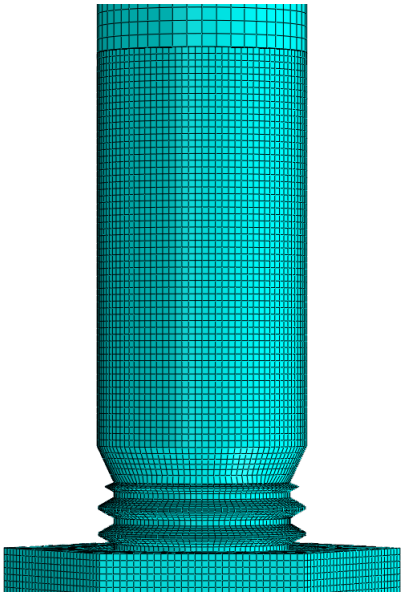

Figure 6.13: 3D non helix model: Tie constraint moved 30 mm upward the bolt shaft

Both 3D models had separated the bolt into three parts; bolt head, shank and the threaded part. They were all linked together using a tie constraint algorithm. This algorithm ensures equal deformation between different parts, but can impose some numerical noise in the transition between the parts. In the 3D helix model, 10 mm of the shaft was included in the threaded part. This prevented numerical noise from the tie constraint, originating from incompatibly of the different elements types in the shank and the threaded part. When the tie constraint was placed close to threaded part, strange forces appeared in the tied connection. Figure 6.13 illustrates when the tie constraint was localized 30 mm upwards the shaft during testing with the 3D non helix model. The problem was smaller for the 3D non helix model because the same element type was used in the threaded and unthreaded part of the bolt.

6.2.6 Computational efficiency

Some of the implementations for improving the computational efficiency is already mentioned as reducing the number of elements. In order to perform an efficient quasi-static analysis, it is essential to either scale the time or the mass, as discussed in Chapter 3.5. Semi-automatic mass scaling was used in this thesis, and the critical target time step was set between $t_{cr} = 0.01s$ and $t_{cr} = 0.0001s$ depending on the type of analysis. It was desirable to use the bigger value, but carefulness had to be exerted so that no dynamic effects influenced the response. This was controlled in every analysis by performing a energy check, and no remarkable dynamic effects were observed.

When using the semi-automatic mass scaling, elements are scaled with different factors such that all elements reaches t_{cr}. The smallest elements, located in the threaded part of the bolt and nut, will then be scaled by the highest factor and hence get the largest mass. Figure 6.14 illustrates the highlighted elements with $t_{cr} < 10^{-6}$s and $t_{cr} < 10^{-7}$s. Since the bolt head moved upwards, the heaviest elements were located in parts almost without movement. This was advantageous for reducing the oscillations and inertia forces.

Note that the critical time step in every models was predetermined by the geometry, and especially the dimension of the thread tip. This size was so small ($\approx$ pitch/8 = $\frac{2\text{mm}}{8}$ = 0.25mm) that even with quite large elements the critical time step was in between 10^{-8} to 10^{-10}. As mentioned in Section 6.2.1 for the 3D helix model, the thread fading was stopped earlier to prevent the time step to further decrease.

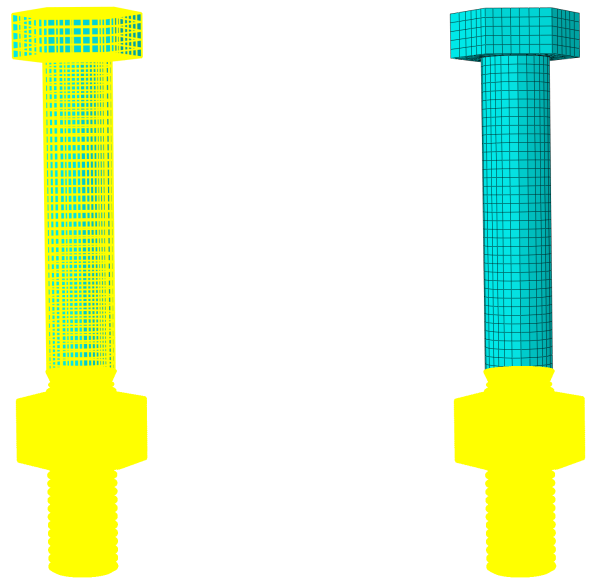

(a) $t_{cr} < 10^{-6}$ s

(b) $t_{cr} < 10^{-7}$ s

Figure 6.14: Highlighted elements with critical time step

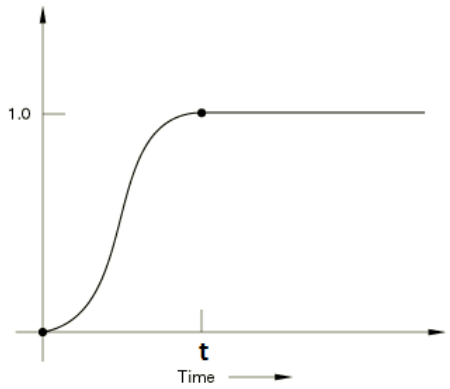

Figure 6.15: Smooth step function

When displacement is instantaneously applied, numerical problems could arise due to stress wave propagation [4]. To circumvent this, the built in smooth step amplitude function in Abaqus was applied. This function is illustrated in Figure 6.15. Full amplitude was reached after $t = 20s$. The total simulation time was in between 250 s an 1200 s, depending on the failure mode.

6.3 Parameter studies

All the three different models presented previously could be used to describe the behaviour of bolted assemblies. A comparison of the three models is discussed in Chapter 6.4. The axisymmetric model gave reasonable results with only a fraction of the computational time. Therefore, only the axisymmetric model was used through this parameter study with except for the study of nut offset. Note that further discussions concerning results presented in this section is found in Chapter 7. The parameter study includes the following:

- Mesh sensitivity
- Change in yield strength of nut based on hardness tests
- Tolerance requirements of geometry
- Effect of high nut and the number of nut threads
- Nut offset

6.3.1 Mesh sensitivity

In the study of mesh sensitivity, the material and geometry of the HR-bolts was used because these experimental tests resulted in both fracture modes. The objective was to see if different mesh size altered the fracture mode in FE simulations. The grip lengths tested was 81 mm, 87 mm and 101 mm. Figure 6.17 presents force-displacement plots from axisymmetric simulations compared to the experimental tests. The displacement from experiments was measured using DIC as illustrated in Figure 4.5 and described in Chapter 4.2.3. Displacements of corresponding nodes defining a vector from the nut to the head were measured analogous in the FE models.

As can be seen in Figure 6.17 the maximum force was less influenced by the mesh size. All grip length configurations predict approximately the same maximum force. The overestimated deviation from the experimental tests was less than 5 %.

The predicted displacement to failure was about 50% longer than in the experiments. Possible explanations to the overly large deformations will be discussed in Chapter 7.

Figure 6.17b and 6.17c shows grip length 87 mm because this configuration resulted both thread stripping and bolt fracture. FE simulations resulted in bolt fracture for grip length 87 mm, regardless of mesh size. This explains the large overestimation of the displacement in Figure 6.17c. For grip length 81 mm and 101 mm both element sizes were able to predict the correct failure mode; thread stripping for 81 mm and bolt fracture for 101 mm. However, the finest mesh produced a smoother equilibrium path and was able to detect fracture earlier, in better accordance with experimental tests. Some oscillations were seen in the plots as small fractures occurred. This was assumed not to influence the results.

Total analysis time with the finest mesh was 3 to 6 hours, compared to 2 hours for coarser mesh. This argument, in addition with the previous observations, are reasons for why the finest mesh was used throughout further analysis.

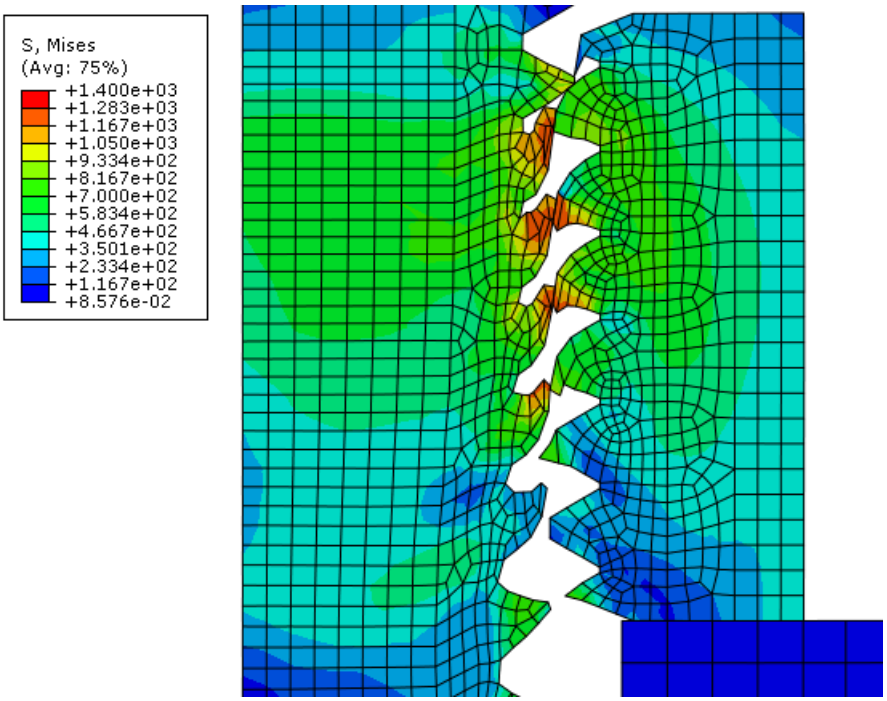

(a) 0.4 mm element size

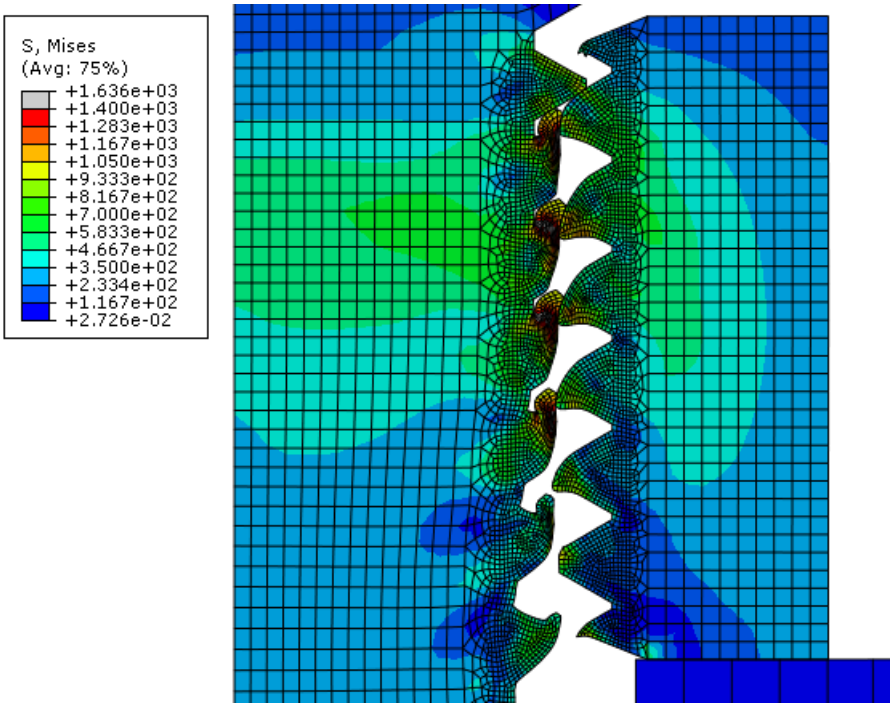

(b) 0.1 mm element size

Figure 6.16: Illustration of mesh sensitivity for SB-bolts
The finer mesh gives a smother deformation compared to the coarser mesh

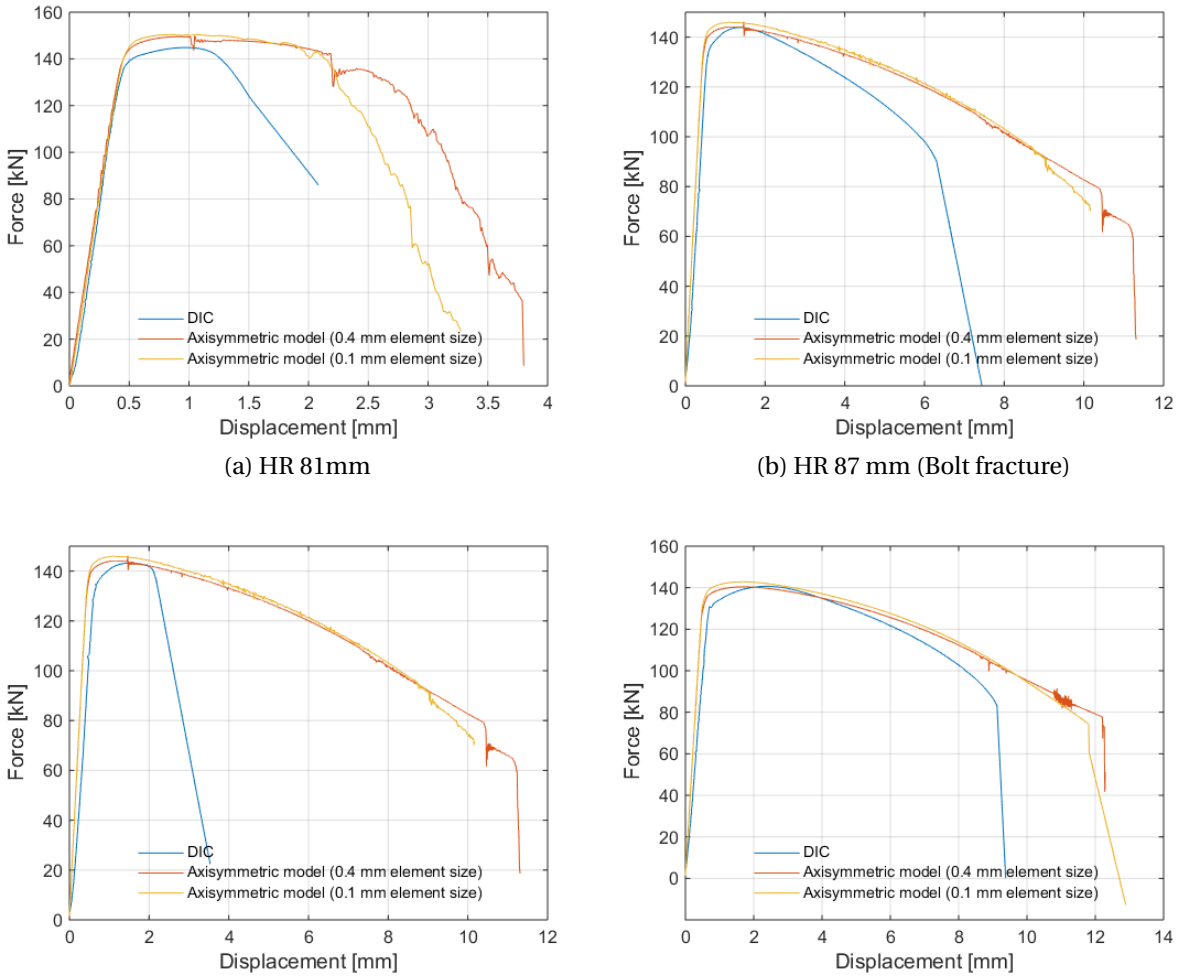

(a) HR 81mm

(b) HR 87 mm (Bolt fracture)

(c) HR 87 mm (Thread stripping)

(d) HR 101 mm

Figure 6.17: Parameter study: Mesh sensitivity

6.3.2 Hardness of material

As opposed to Skavhaug and Østhus, all SB-bolt with regular nut fail by thread stripping regardless of grip length. The initial model had the same yield strength in the nut and bolt. *Vickers hardness* test revealed large differences especially between the SB-bolt and the regular nut. The nut had an average of approximately 78 % of the average bolt hardness, and 70 % in the threads. However, because of only one hardness test it is hard to state if this observation is valid in general.

According to Alexander [7], a reduction in the nut strength can provoke thread stripping. It was therefore conducted a parameter study where the nut strength was reduced. The yield strength was scaled as a factor of the hardness difference, based on the fact that yield strength can be approximated as: $\sigma_y \simeq 3\times$ HV. In other words, the yield strength was assumed proportional to the hardness.

The study was carried for a SB bolt with a regular nut strength of 90 %, 80 %, 78 %, and 70 % compared to the initial strength. This was carried out for grip length 81 mm, 87 mm and 101 mm. Force-displacement plots are presented in Figure 6.18.

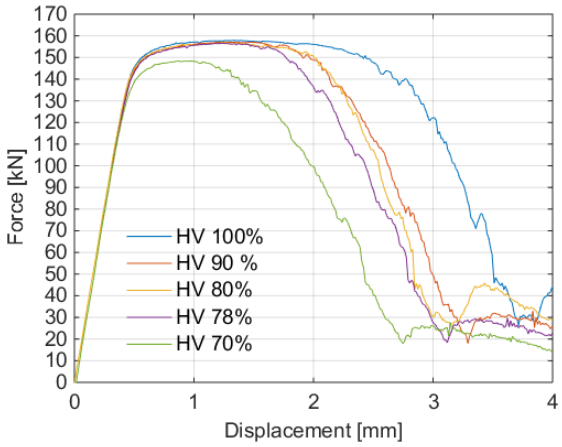

(a) SB 81mm

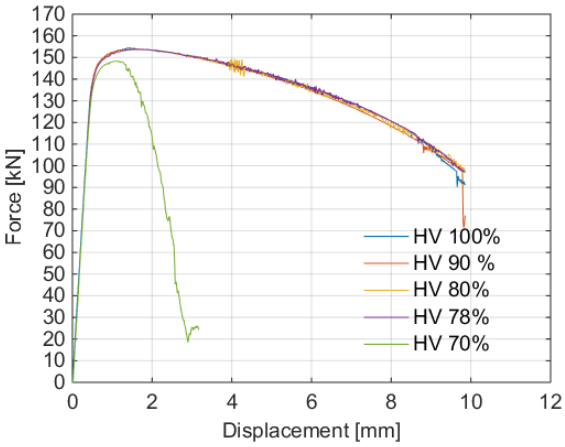

(b) SB 87 mm

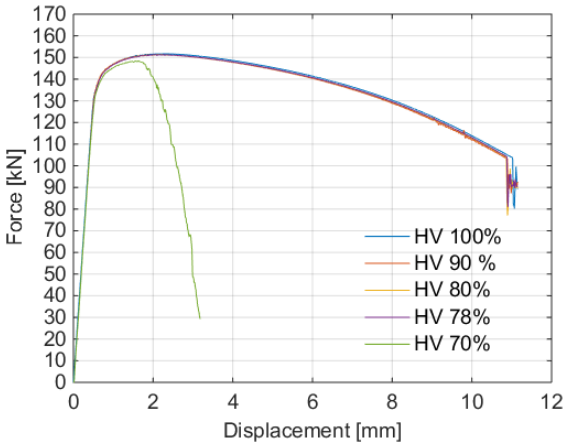

(c) SB 101 mm

Figure 6.18: Parameter study: Hardness of material

As predicted, a reduction of the nut strength effected both failure mode and ductility. The deformation to failure decreased in correlation with reduced nut yield strength for simulations with grip length 81 mm. A noticeable reduction of the maximum force was only registered for the simulation with a nut strength of 70 %.

For simulations with larger grip length (87 mm and 101 mm), all nut strength except for HV 70 % resulted in bolt fracture, whereas HV 70 % resulted in thread stripping. The change of failure mode reduced both displacement and maximum force, as can be seen in Figure 6.18b and 6.18c. This observation was in accordance with the experimental tests. It should be noted that the two lowest hardness measurements in Figure 4.10b were observed in the nut threads, with a relative hardness of 70 %. This was the same value that resulted in thread stripping for all grip lengths in the FE models.

Test simulations were performed with a HR-bolt which only had a difference of 5 % in relative hardness. The test simulations gave no change of response, indicating that the difference in hardness was not large enough to provoke thread stripping.

6.3.3 Geometry tolerance

As mentioned in Chapter 4.6, the regular nut felt less tight compared to the high nut. Further examination revealed this suspicion, as seen in Figure 4.29. The regular nut to the left, showed a gap between the threads. The high nut to the right, was much tighter. Based on this observation it was decided to investigate if geometrical tolerance requirements affected the type of failure mode. It was chosen to study SB-bolts with grip length 85 mm and 87 mm. These grip lengths were chosen because this domain seemed to be a critical point of failure mode for the HR-bolt. This domain coincided with the results of both Grimsmo et al. [23] and Skavhaug and Østhus [35]. The parameter study was carried out with the maximum and minimum geometrical tolerances of the bolt and nut threads from ISO 965 [21]. Note that the geometry measurements of the nuts in Figure 4.29 are within these requirements, however in the lower domain.

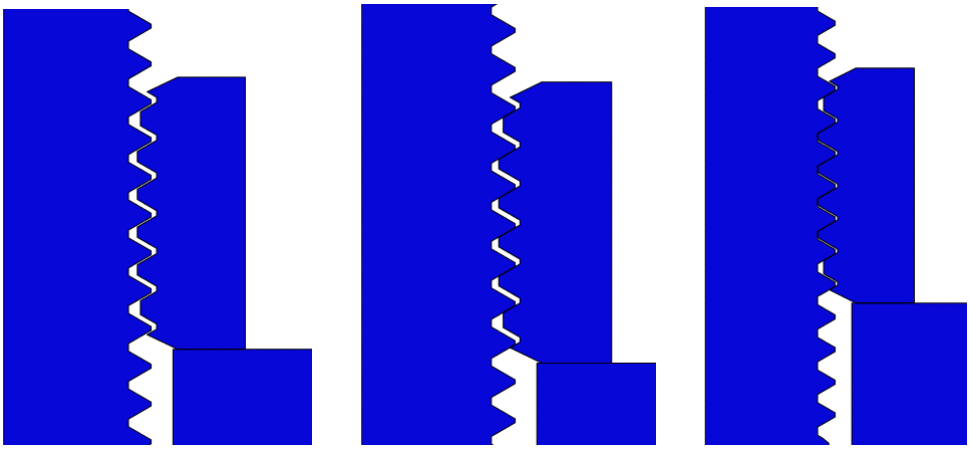

(a) Minimum (b) Actual (c) Maximum

Figure 6.19: Illustration of geometry tolerances

Figure 6.20 shows the force-displacement plots for the simulations with grip length 85 mm and 87 mm. It is clear that the simulations with maximum tolerances give an increased maximum force. This must be caused by an increased bolt thickness and greater overlap of the mating threads. A larger cross-section should give a higher capacity with the same material properties.

As seen in Figure 6.20a, it is clear that the minimum tolerance changed the failure mode from bolt fracture to thread stripping. The displacement to failure was also reduced. Change of failure mode may be explained by the fact that the minimum tolerance resulted in little overlap of the mating threads. This further lead to thread stripping. Failure modes with grip length 87 mm seemed unaffected of the tolerance requirements and all simulations ended with bolt fracture. Further comments to these observations can be found in Chapter 7.

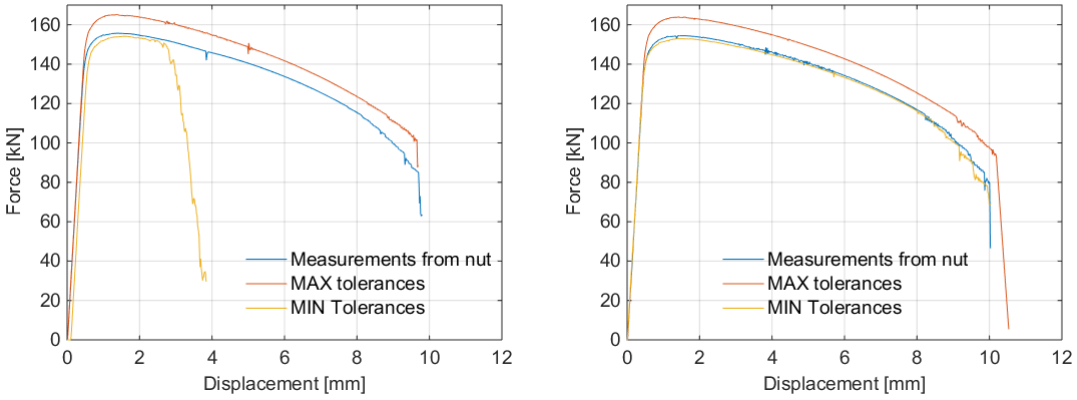

(a) SB 85mm

(b) SB 87 mm

Figure 6.20: Parameter study: Geometry tolerance

6.3.4 Effect of high nut and number of nut threads

High nut

An alternative to the regular nut is to use a high nut. A high nut is approximately 2 mm higher, and this allows for one more thread over the height.

Simulations were performed with grip length 81 mm since this configuration was most likely to result in thread stripping, both for SB-bolts and HR-bolts. As opposed to simulations with a regular nut, the simulation with a high nut predicted bolt fracture in accordance with experimental results. The force-displacement plot in Figure 6.21 show that the displacement to failure was too large for both simulations. Simulations with high nut and regular nut overestimated the displacement to failure with approximately 300 %. In addition, the maximum force for the regular nut was about 9 % higher compared to the experimental test and almost equal with the high nut. Further discussions concerning these large deformations and maximum force levels, is presented in Chapter 7.

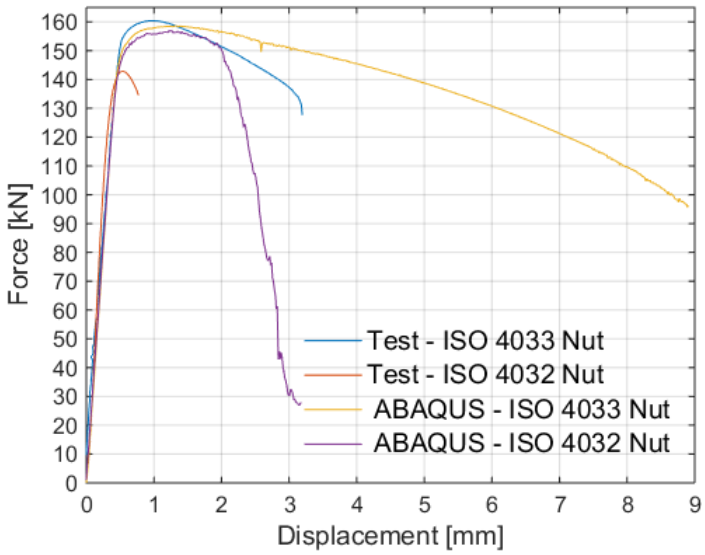

Figure 6.21: Parameter study: Effect of high nut (ISO 4033)

Number of threads

As can be seen in Figure 6.2, the number of full threads in each of the nuts is quite ambiguous because of the helix shape and the thread runout in both ends. It is difficult to state the exact number of threads that should be used, because of the geometrical limitations using a axisymmetric FE model. In general, all simulations were performed with six full threads for the regular nut, and seven full threads for the high nut. To investigate the effect number of threads, simulations were performed with one regular nut of five full threads. The simulations had 87 mm and 101 mm grip length and HR-bolt material

properties, since these configurations exclusively resulted in bolt fracture by the use of six full threads. It was not performed a simulation with grip length 81 mm, because six full threads predicted thread stripping.

The result from the simulations is presented in Figure 6.22. As predicted, the failure mode in the simulation with grip length 101 mm did not change. In order for a change of failure mode the localization of necking has to be close enough to the nut. The bolted assembly with a grip length of 101 mm was to far away from the necking zone and was unaffected. Thereby, the number of threads was of less importance.

On the other hand, the simulation with grip length 87 mm and five threads resulted in thread stripping. The change of failure mode could imply that the number of nut threads is of importance when the nut is positioned close to zone of necking.

Generally, this could indicate that it is not clear which geometrical simplification one should use for a axisymmetric model. The simplifications in geometry with circular threads introduces uncertainties, as it deviates from the exact shape. These observations and their influence will be further discussed in Chapter 7.

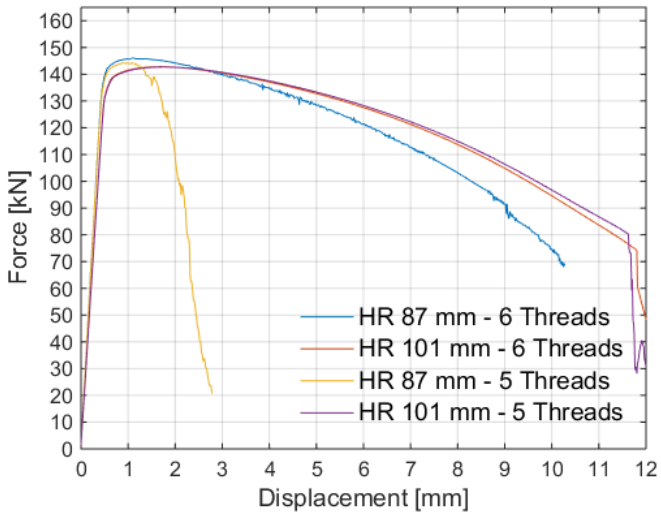

Figure 6.22: Parameter study: Number of nut threads

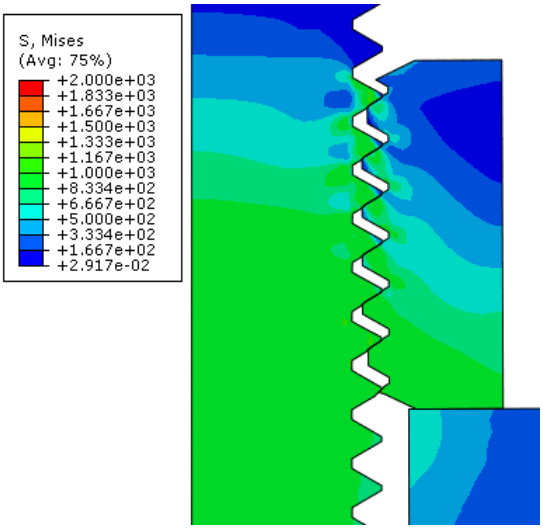

(a) Displacement 0.55 mm

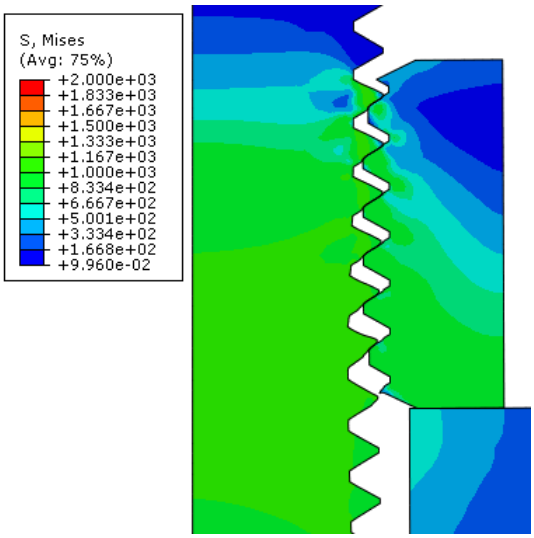

(b) Displacement 1.29 mm. Maximum force

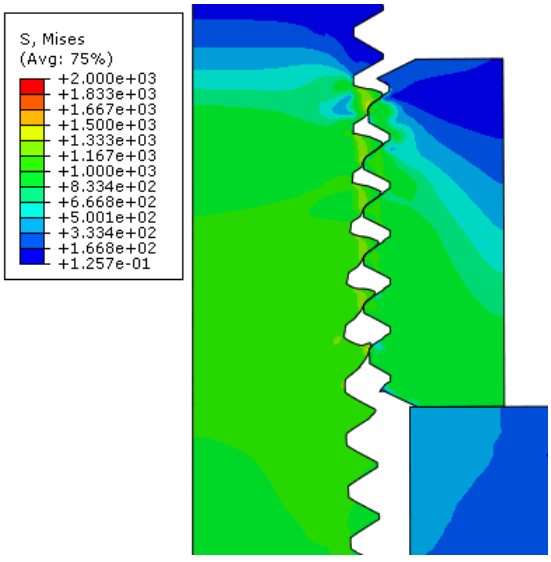

(c) Displacement 2.01 mm

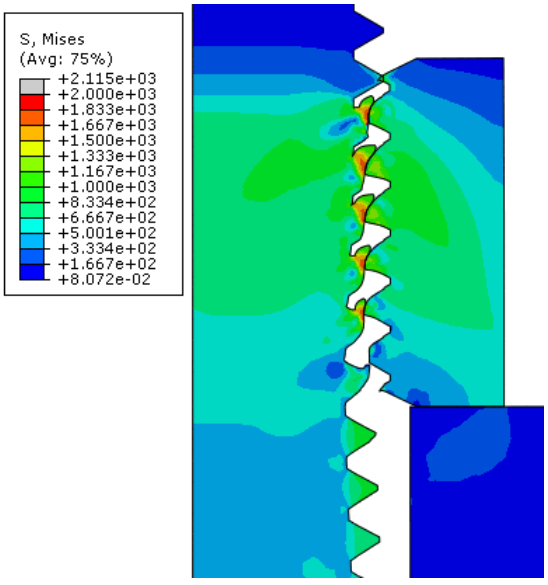

(d) Displacement 2.77 mm. After thread failure

Figure 6.23: Deformation progress for SB-bolt and regular nut with grip length 81 mm

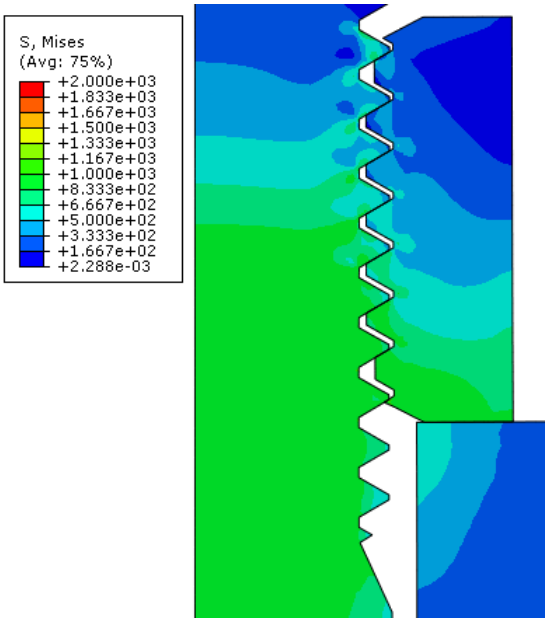

(a) Displacement 0.55 mm

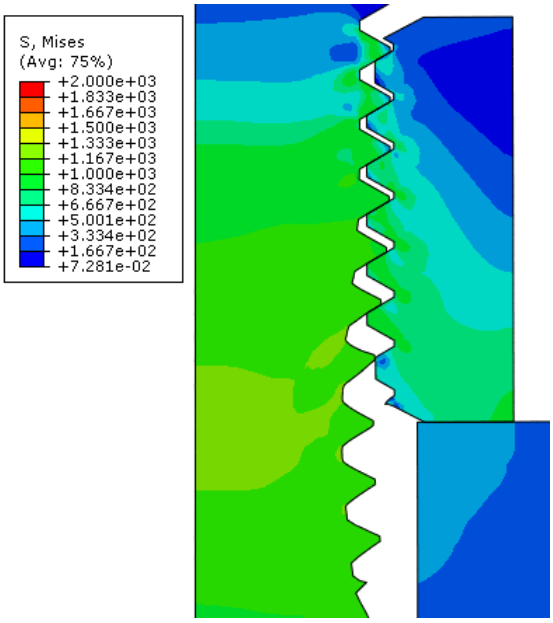

(b) Displacement 2.75 mm. Note that the first and second threads are slipping

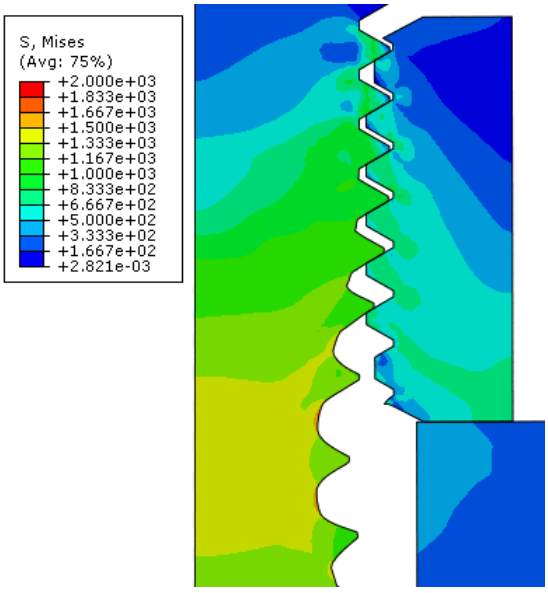

(c) Displacement 5.68 mm. Necking of the bolt

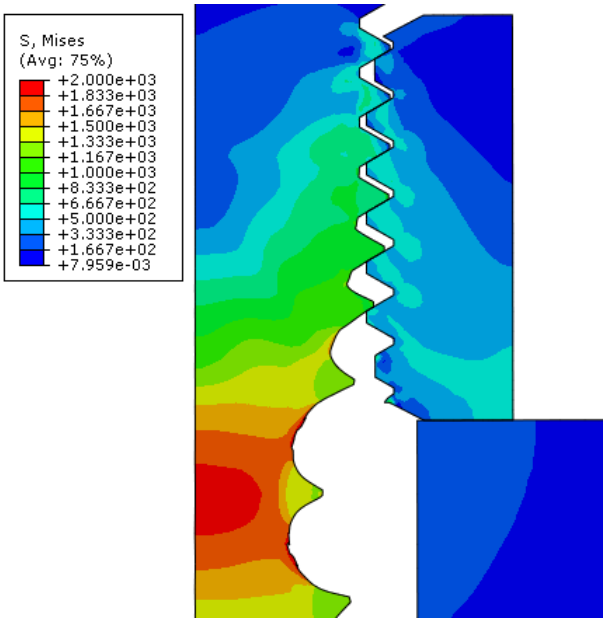

(d) Displacement 8.60 mm. Immediately before bolt fracture

Figure 6.24: Deformation progress for SB-bolt and high nut with grip length 81 mm

6.3.5 Nut offset

A horizontal offset of the nut was studied by the use of the 3D non helix model with 0.5 mm element size. HR-bolt material and five full nut threads was used with grip length 81 mm and 101 mm. The nut was positioned to one side of the bolt threads, resulting in a gap on the opposite side. Figure 6.25 presents the results from the simulations with grip length 81 mm and 101 mm. The displacement to failure was larger for both simulations with nut offset, and the maximum force appeared later in time but with the same value. As can be seen from the deformation pattern in Figure 6.26 and 6.27, the nut moved back into a centric position before the normal deformation progress initiated. This explains the delay in response, and was common for both grip lengths. The deformation progress was almost identical as for simulations without the initial nut offset, only small variations in the stress state could be observed. Simulations with nut offset and 87 mm grip length were also tested and ended with bolt fracture, as before.

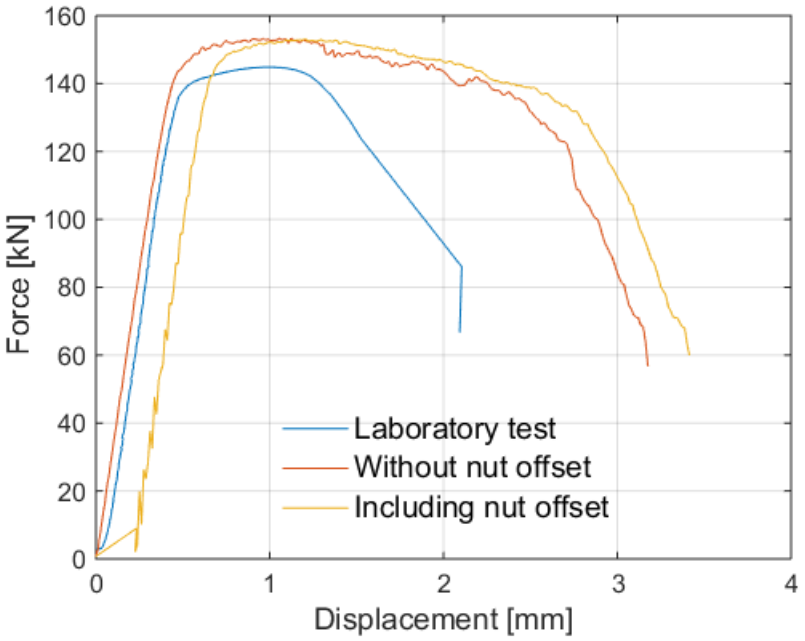

(a) Grip length 81 mm

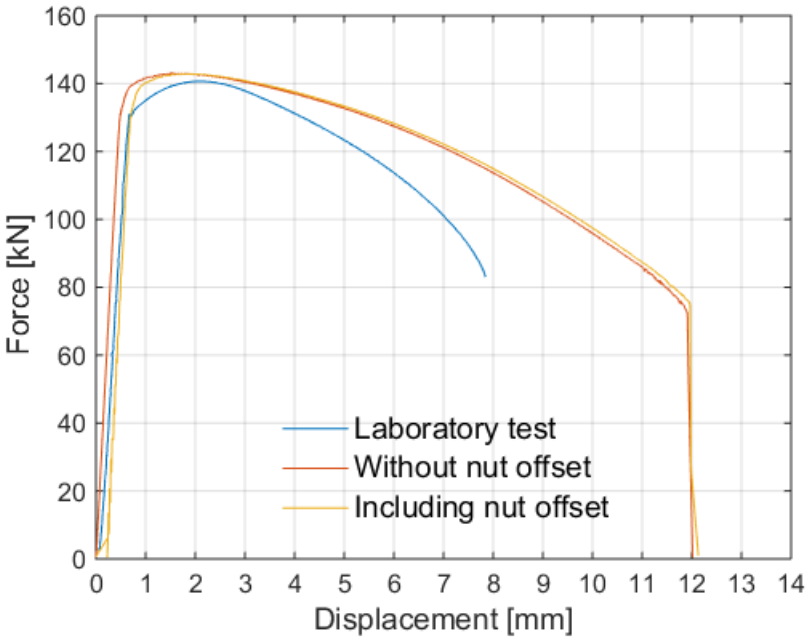

(b) Grip length 101 mm

Figure 6.25: Parameter study: Nut offset
3D non helix model with HR-bolt and five nut threads

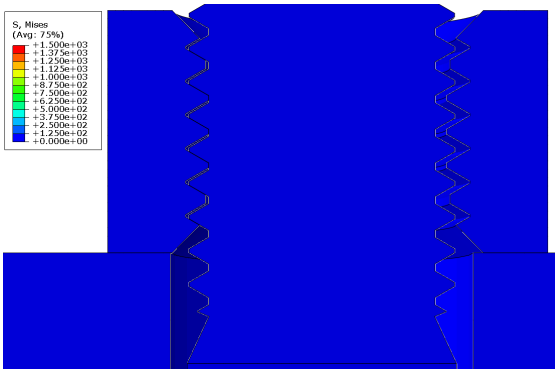

(a) Displacement 0.0 mm. Initial nut offset

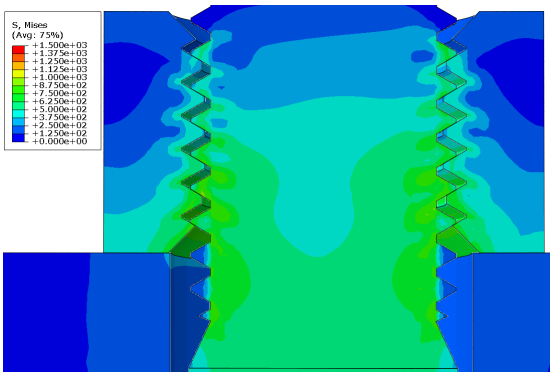

(b) Displacement 0.5 mm. Repositioning of nut into center before normal deformation progress

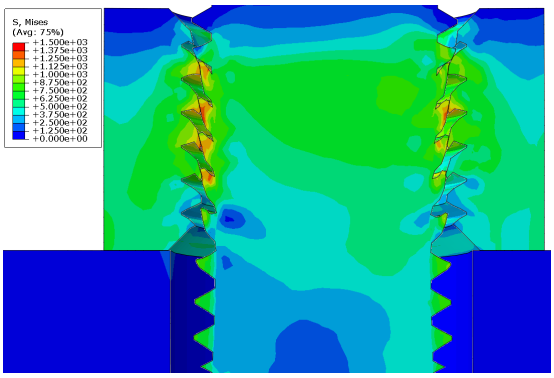

(c) Displacement 3.7 mm. Loss of capacity and thread stripping

Figure 6.26: Deformation progress for axisymmetric model of HR-bolt with nut offset and 81 mm grip length

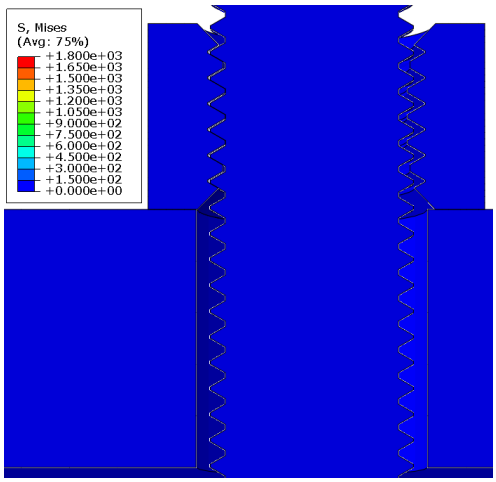

(a) Displacement 0.0 mm. Initial nut offset

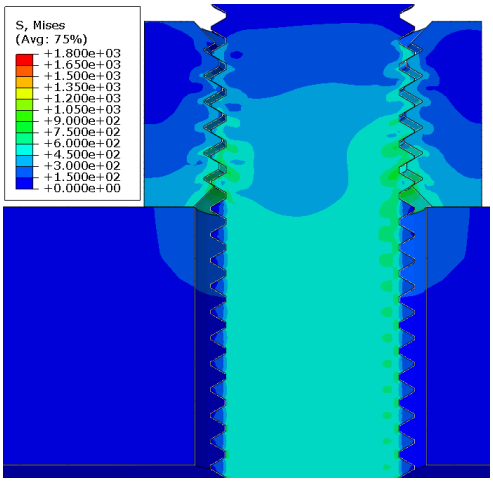

(b) Displacement 0.5 mm. Repositioning of nut into center before normal deformation progress

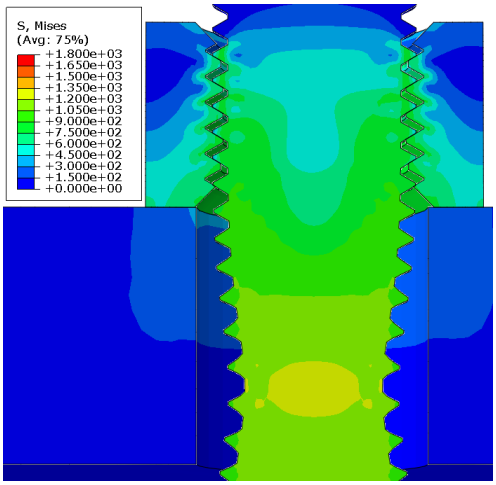

(c) Displacement 6.1 mm

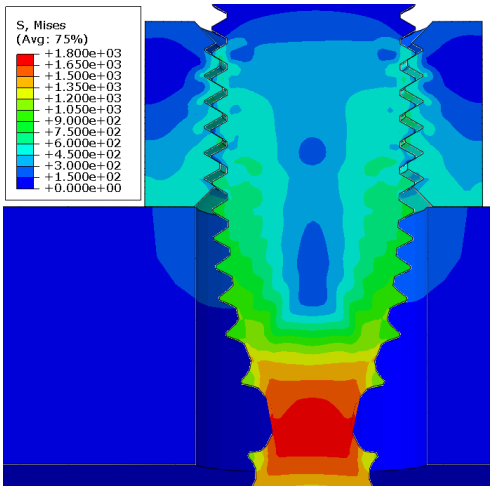

(d) Displacement 11.7 mm. Immediately before bolt fracture

Figure 6.27: Deformation progress for axisymmetric model of HR-bolt with nut offset and 101 mm grip length

6.4 Comparison of models

Results from simulations with the 3D models is presented in the following. Both models, non helix and helix, is compared with results from the axisymmetric simulations and the experimental tests. Quality of the results and computational cost will be considered. Some of the parameters tested in the parameter studies for the axisymmetric model, were also implemented in the 3D models. The objective was to see if the 3D models gave a better representation of the experimental tests, and whether it is necessary to use such models instead of a simpler axisymmetric model. Further discussions regarding results and observations presented in the following can be found in Chapter 7.

6.4.1 3D non helix model

The initial 3D non helix model had 0.5 mm element size. Some modifications were later introduced, enabling the model to reproduce the correct failure modes as observed in the laboratory.

HR-bolt

Since the objective with this study was to compare the 3D non helix model with the axisymmetric model and the experimental tests, material parameters for HR-bolts were used. A FE model should be able to predict thread stripping and bolt fracture with the same model, exactly what happened with the HR-bolts. Observations from the simulations is presented in what follows:

- Figure 6.28a presents the results for simulations with grip length 81 mm and mesh size 0.5 mm and 0.2 mm. The difference between the two mesh sizes is minimal, and none of the models were able to predict thread stripping like the axisymmetric model. It was therefore decided to use 0.5 mm element size for further comparison of models, although the finest mesh resulted in fracture earlier. With 0.5 mm element size, four elements covered the thread height. This should be enough elements according to what Abaqus indicates, as discussed in Section 6.2.3. Also, the simulation time was reduced from around 30 hours to six hours by use of 0.5 mm instead of 0.2 mm element size. This was preferable when running a lot of simulations. It should be noted that some of the stress concentrations may fail to appear with such large elements, and that the finest mesh is probably better suited for detailed research.

- Results from each of the modifications with grip length 81 mm is presented and compared in Figure 6.28b. Moving the tie constraint, as described in Section 6.2.5, had no influence compared with the initial model.

- By using incompatible elements, the response was slightly softened and the total displacement to failure was reduced with half a millimeter. The maximum force was still 5 % too high, and thread stripping was not predicted. Note that the response curve with incompatible elements was almost the same compared to the use of 0.2 mm element size in Figure 6.28a. Although incompatible elements gave slightly better prediction of the response, the computational effort increased.

- The only modification that predicted thread stripping was by reducing the number of nut threads. By using five full threads instead of six, the response was almost the same as with the axisymmetric model. Displacement to failure and maximum force was anyhow to large compared with experimental tests. Figure 6.30 illustrates the deformation progress with the initial model including six nut threads, compared to the use of five nut threads in Figure 6.31.

- Since five nut threads produced the correct failure mode for grip length 81 mm, five threads was also tested and validated for grip length 101 mm. Similar to the experimental tests, this resulted in bolt fracture and five nut threads seemed appropriate for the HR-bolt. See Figure 6.29 for force-displacement plots. The deformation to failure was still too large compared with experimental tests.

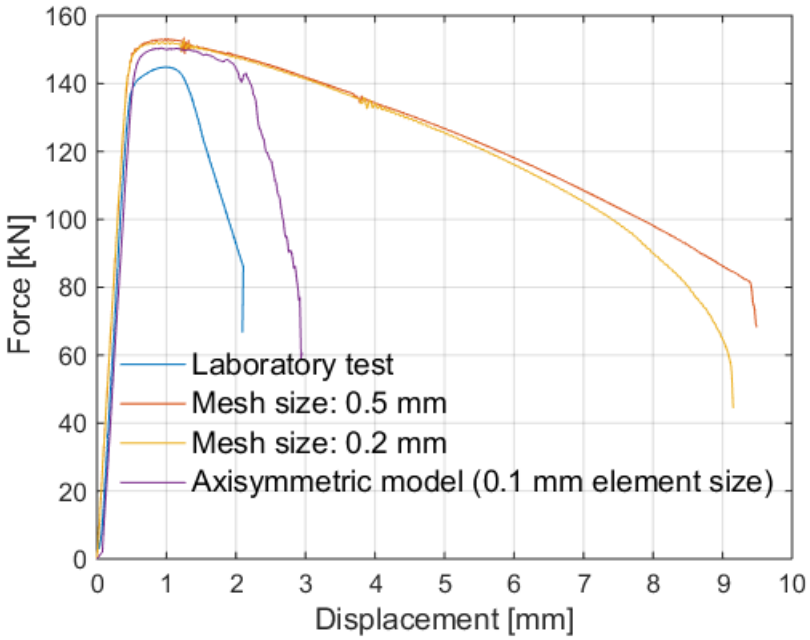

(a) Importance of mesh size. Grip length 81 mm

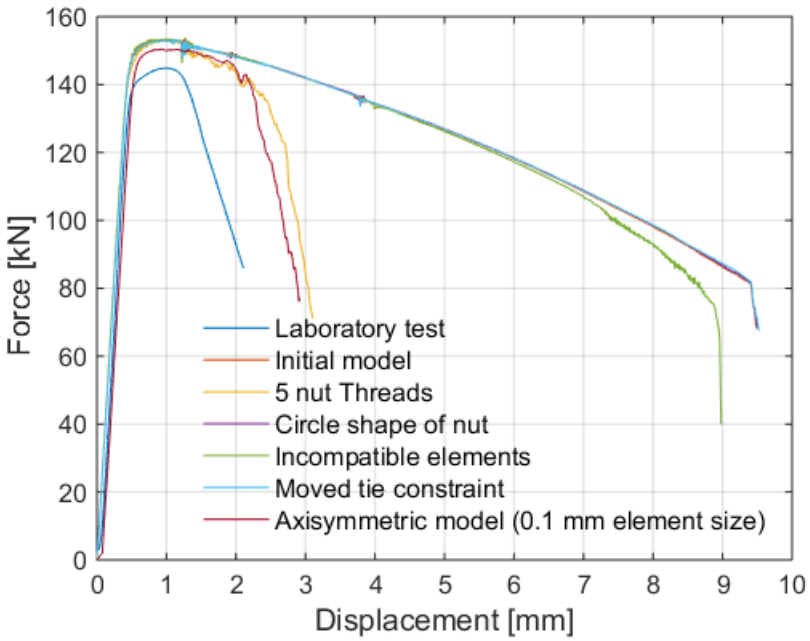

(b) Effect of different modifications. Grip length 81 mm

Figure 6.28: Comparison of models: 3D non helix model with HR-bolt.

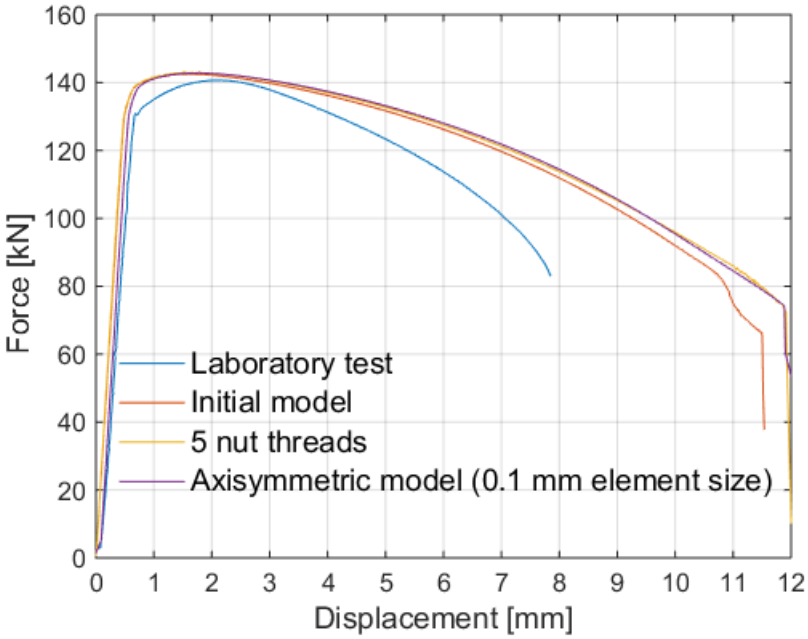

Figure 6.29: Comparison of models: Five nut threads
3D non helix model with HR-bolt and grip length 101 mm

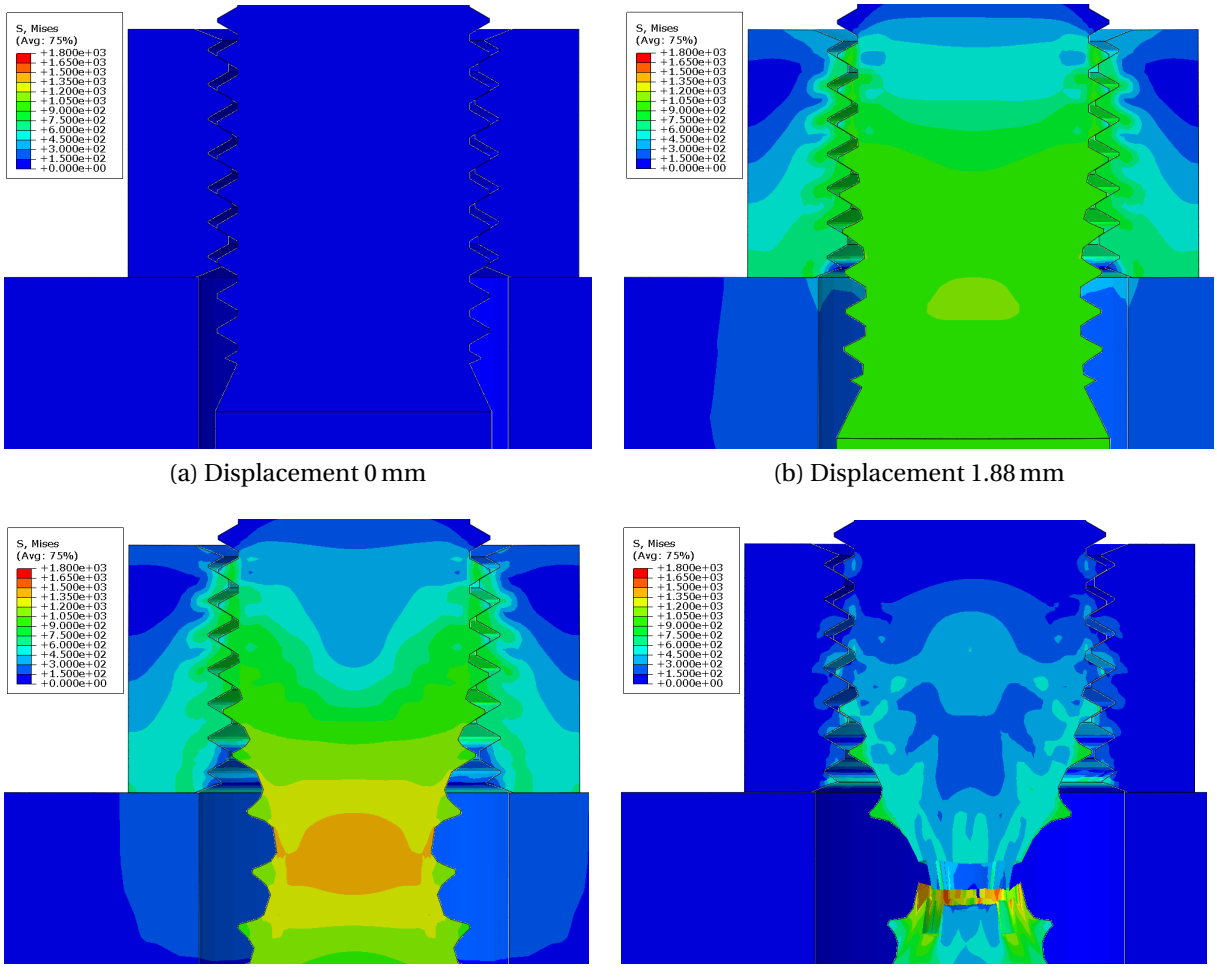

(a) Displacement 0 mm

(b) Displacement 1.88 mm

(c) Displacement 6.28 mm. Clearly necking

(d) Displacement 10.03 mm. After fracture

Figure 6.30: Deformation progress for 3D non helix model of HR-bolt with 81 mm grip length

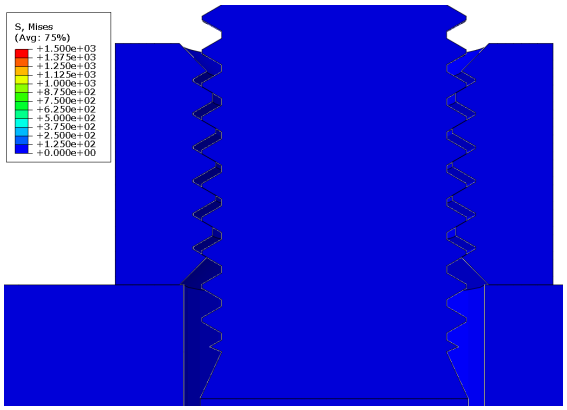

(a) Displacement 0 mm

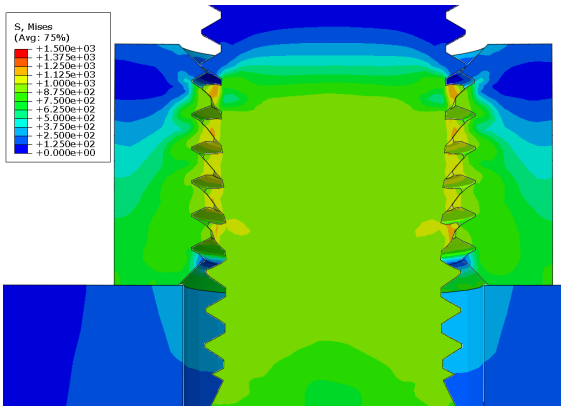

(b) Displacement 2.09 mm. Maximum force reached

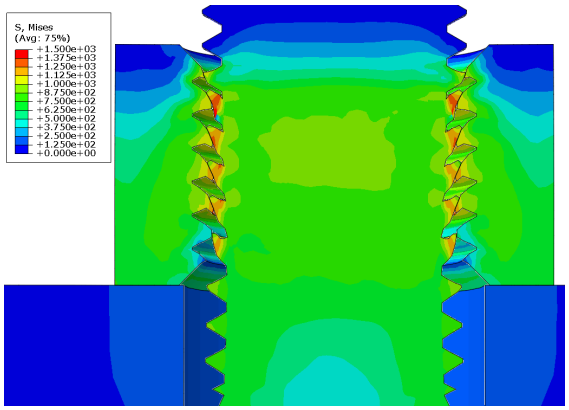

(c) Displacement 2.90 mm

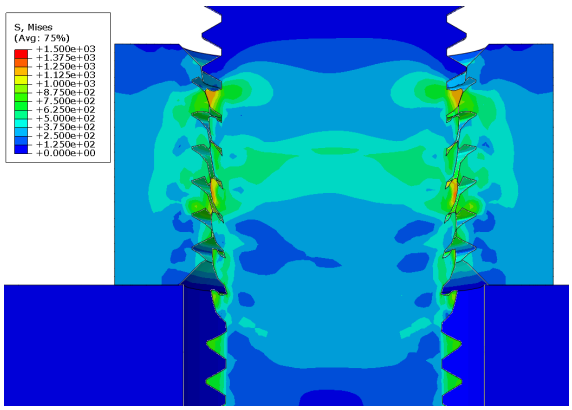

(d) Displacement 6.11 mm. Way after fracture, continious thread stripping

Figure 6.31: Deformation progress for 3D non helix model of HR-bolt with five nut threads and 81 mm grip length

SB-bolt

A few analysis were also performed with the SB-bolt, to validate if the 3D non helix model were able to predict thread stripping for all grip length with the regular nut. Observations is presented in the following:

- For grip length 81 mm, a regular nut with reduced yield strength of 78 % was necessary to predict thread stripping. See Figure 6.33a for force-displacement plot. The axisymmetric model were able to predict thread stripping without any modifications of nut.
- It was possible to predict thread stripping with the 3D non helix model for grip length 101 mm, by using five nut threads in addition with a nut yield strength of 70 %. See Figure 6.33b for plots, and Figure 6.32 for illustration of thread stripping. Note that the nut has dilated in the radial direction.

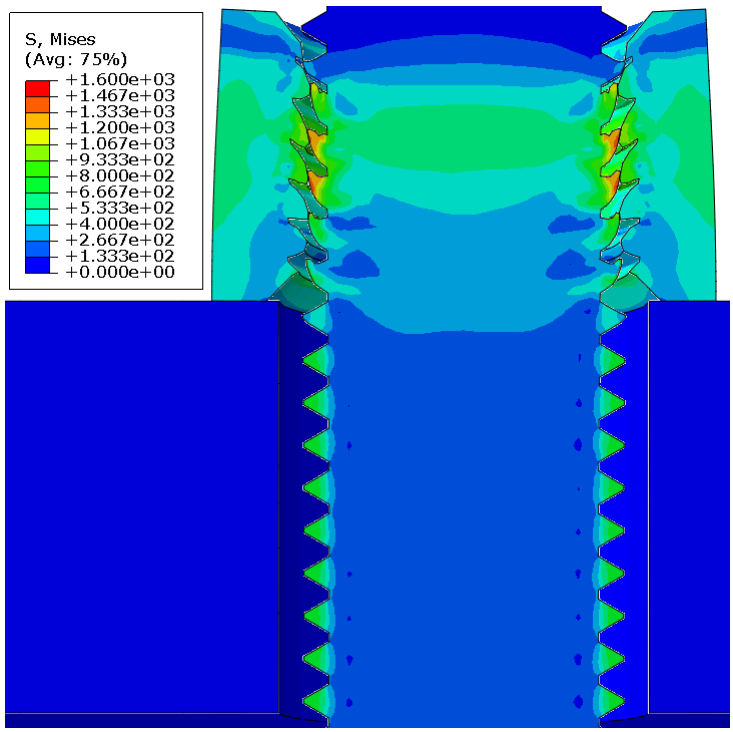

Figure 6.32: Thread stripping for 3D non helix mode with five nut threads and 101 mm grip length. Reduced nut yield strength of 70 %.

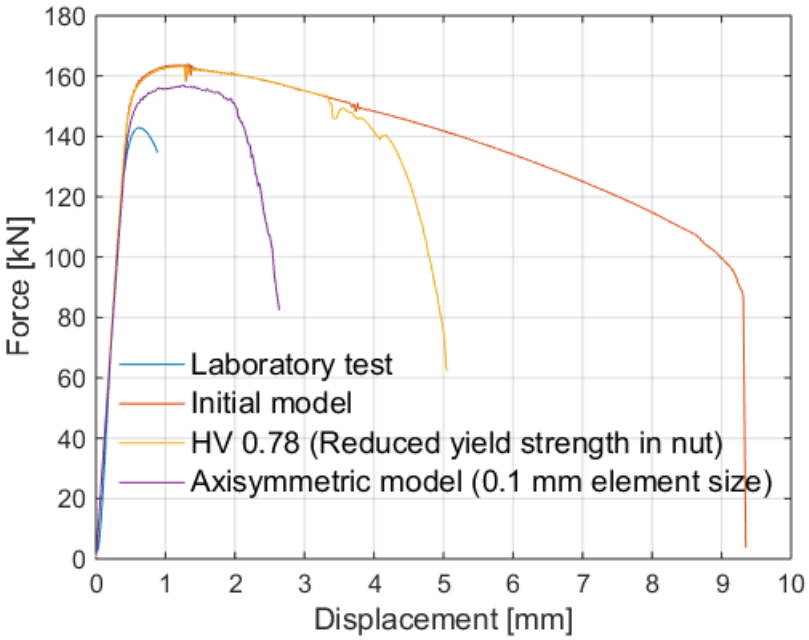

(a) Grip length 81 mm

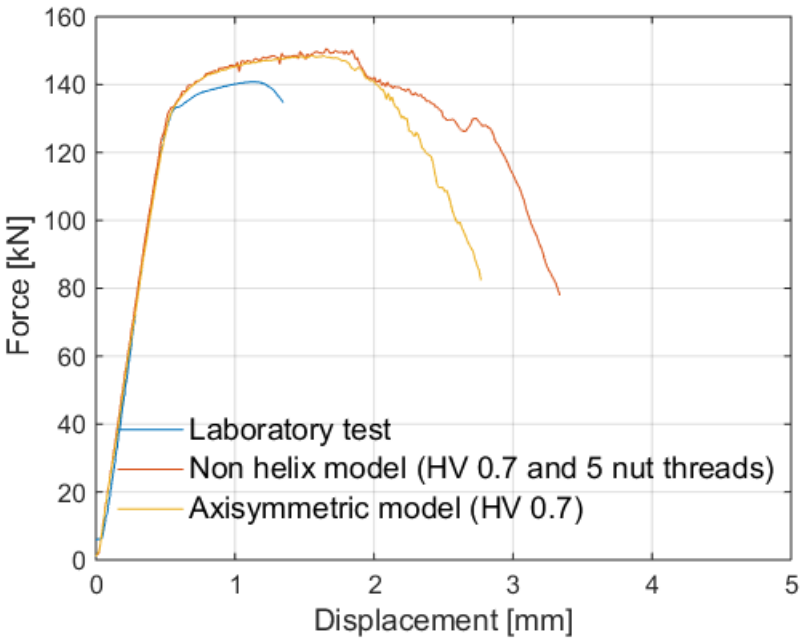

(b) Grip length 101 mm

Figure 6.33: Comparsion of models 3D non helix: SB grip length 81 mm and 101 mm

6.4.2 3D helix model

Simulations with the 3D helix model were performed with 0.4 mm element size. The total simulation time between 30 to 70 hours on supercomputers. Simulations with smaller elements seemed unpractical and was not performed.

The objective was to study how the helical shape of the threads influence the FE results. Therefore, simulations with material and geometrical parameters for HR-bolts were primarily used for this purpose. Simulations with a HR-bolt should be able to predict both thread stripping and bolt fracture with the same model.

A few simulations were also performed with material and geometrical parameters for SB-bolts, just to verify if the model was able to predict thread stripping for a regular nut. Note that only a few analysis were performed in total, because of long simulation time.

HR-bolt

Figure 6.35 presents force-displacement plots for grip lengths 85 mm and 89 mm. Results from the 3D helix model are presented together with results from experimental tests and axisymmetric simulations. Figures from Abaqus of the deformation progress, with respective grips lengths, are illustrated in Figure 6.36 and Figure 6.37.

Note that one simulation for grip length 85 mm was performed with a nut that had a slightly larger chamfer. This was done because of uncertainties of the chamfer size.

Observations based on the results is presented in the following:

- The 3D helix model was able to predict the correct failure modes, i.e. thread stripping for grip length 85 mm and bolt fracture for grip length 89 mm. No modifications from the parameter studies were implemented for this initial model. No simulations were performed for grip lengths 81 mm and 101 mm. Grip lengths larger than 89 mm would result in bolt fracture, and grip lengths shorter than 85 mm would result in thread stripping.

- The shape of the curve from the 3D helix model in Figure 6.35b was more like the response observed in the experimental tests, especially at the end of the curve prior to bolt fracture. It was observed that the hardening was too large, especially after maximum force compared to the experimental test. Figure 6.34 illustrates that the realistic fracture surface was inclined, and that the 3D helix model was able to predict this inclined surface as opposed to the axisymmetric model (and the 3D non helix model) which predicted a plane fracture surface.

- Deformations to failure were in general too large with the 3D helix model, compared to experimental tests. Reasons for this difference is discussed in Chapter 7. Anyhow, the maximum force was predicted fairly well, with a deviation of only 3 % for both grip lengths.

- Figure 6.36 shows that the nut with the largest chamfer predicted a smaller displacement to failure, closer to the experimental test data. The largest chamfer reduced the thread shear area such that the necking of the bolt had less influence of displacement. For the smallest chamfer, displacement to failure was affected by the fact that the bolt almost failed by bolt fracture.

- Note that the stress level during deformation in Figure 6.36 and 6.37 exceeded 2000 MPa. This seemed unrealistic and may be caused by distorted elements. It was only a few elements located at the tip of some threads that exceeded this stress level, and it was assumed to have negligible effect on the global response.

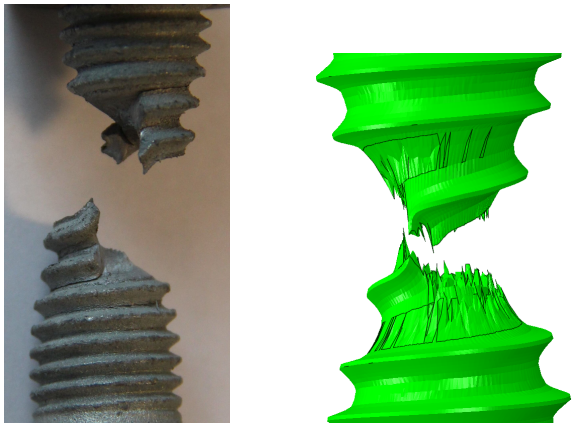

(a) Realistic fracture surface

(b) Fracture surface with 3D helix model

Figure 6.34: Fracture surface at bolt fracture
The fracture is inclined and seems to be affected by the helical threads

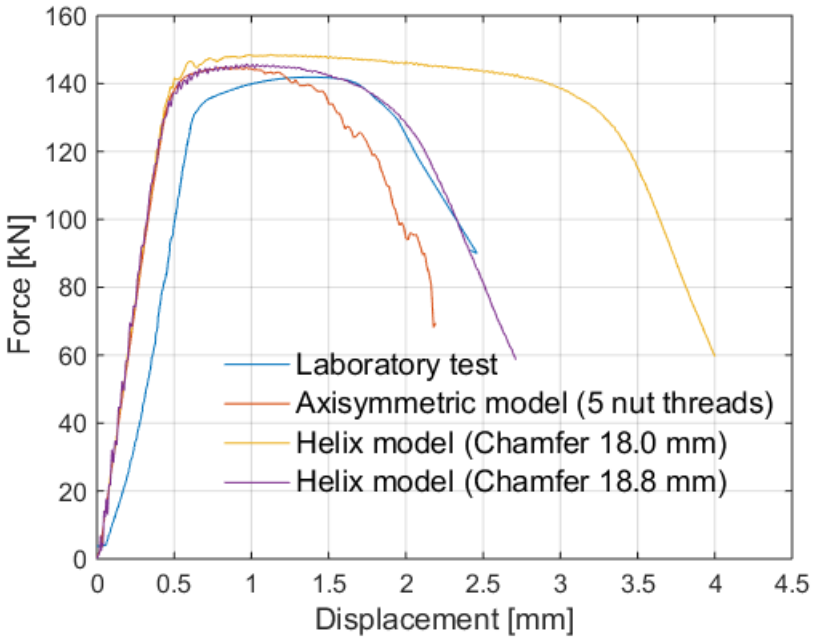

(a) Comparsion of models 3D helix: HR grip length 85 mm

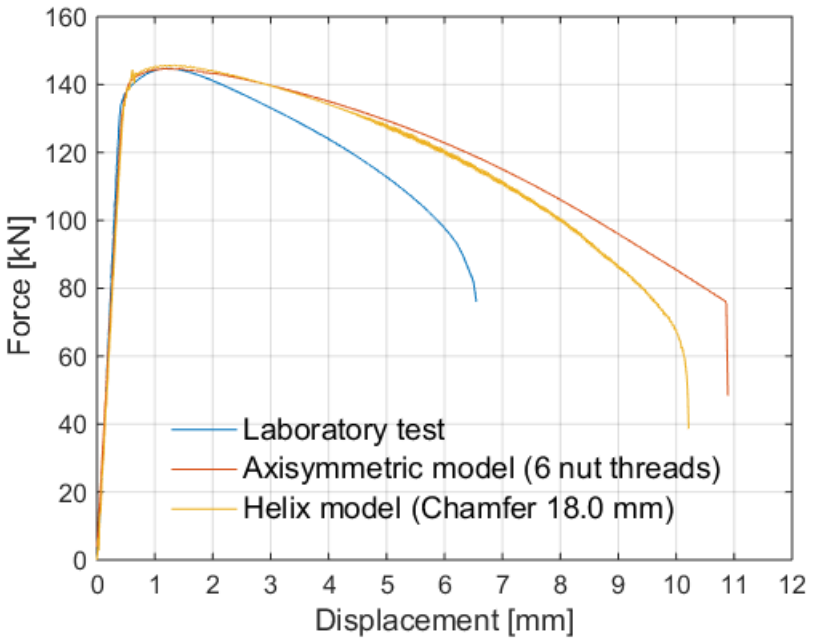

(b) Comparsion of models 3D helix: HR grip length 89 mm

Figure 6.35: Comparsion of models 3D helix: HR grip length 85 mm and 89 mm

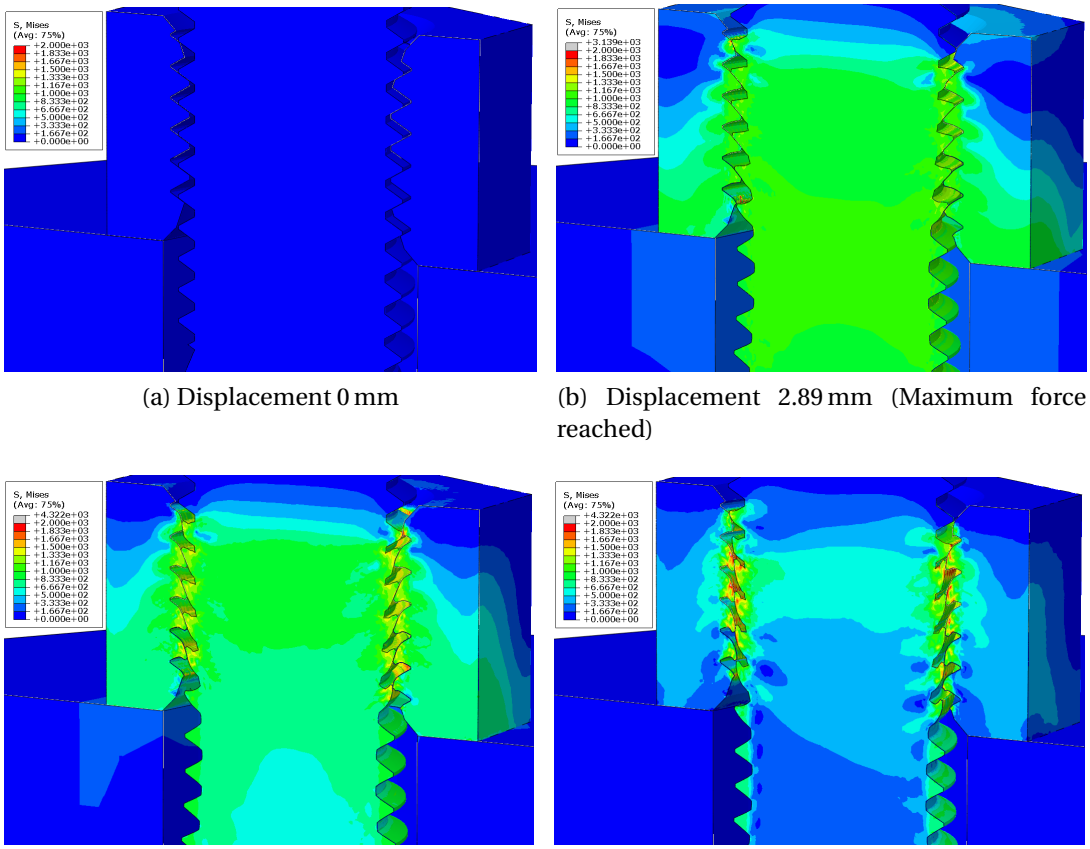

(a) Displacement 0 mm

(b) Displacement 2.89 mm (Maximum force reached)

(c) Displacement 3.7 mm (Deformation of threads)

(d) Displacement 4.5 mm (Capacity lost)

Figure 6.36: Deformation progress for 3D helix model of HR-bolt and 85 mm grip length

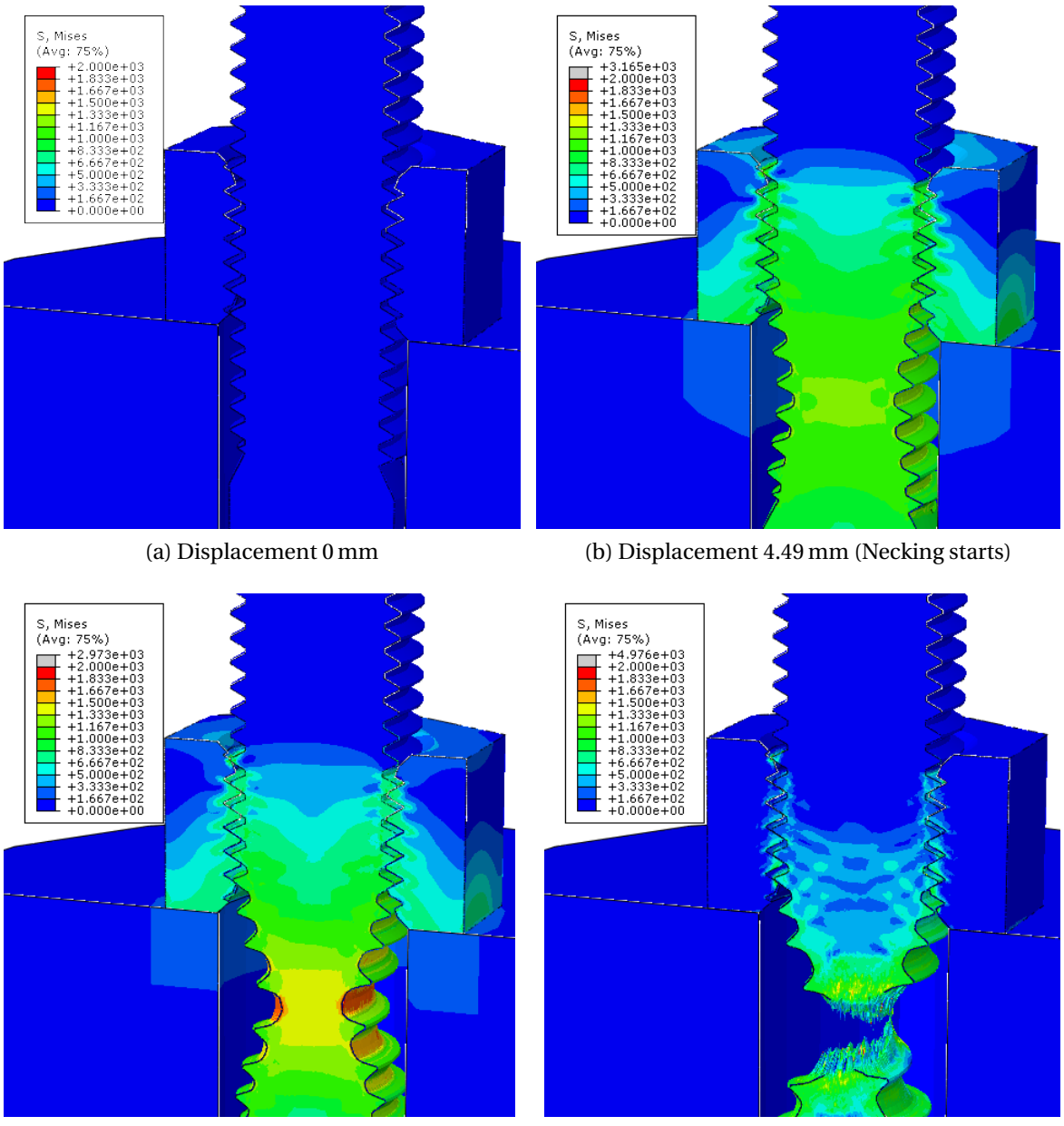

(a) Displacement 0 mm

(b) Displacement 4.49 mm (Necking starts)

(c) Displacement 7.69 mm (Before fracture)

(d) Displacement 10.24 mm (After fracture)

Figure 6.37: Deformation progress for 3D helix model of HR-bolt and 89 mm grip length

SB-bolt

Two simulations, with grip length 81 mm and 101 mm, were performed with material and geometrical properties for a SB-bolt and regular nut with reduced yield stress of 70 %. Figure 6.38 presents force-displacement plots from simulations, in addition to data from experiments and axisymmetric simulations. Observations is presented below:

- Simulation with grip length 81 mm resulted in thread stripping, as observed in experimental tests. The 3D helix model predicted nearly 12 % too large maximum force, and 250 % larger displacement to failure compared to the experimental test. Reasons for this is discussed in Chapter 7.
- Bolt fracture was registered for the simulation with grip length 101 mm, and thereby not predicting the correct failure mode. Some thread bending was registered, but necking in the threaded part of the bolt dominated such that bolt fracture was a fact. In other words, thread stripping was almost predicted. The maximum force was almost 5 % larger compared with experimental data.

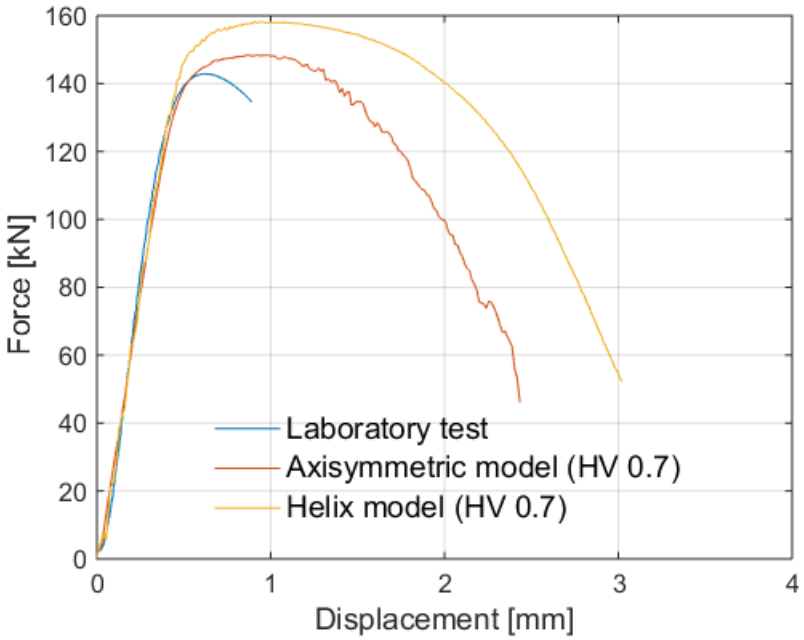

(a) Comparsion of models 3D helix: SB grip length 81 mm

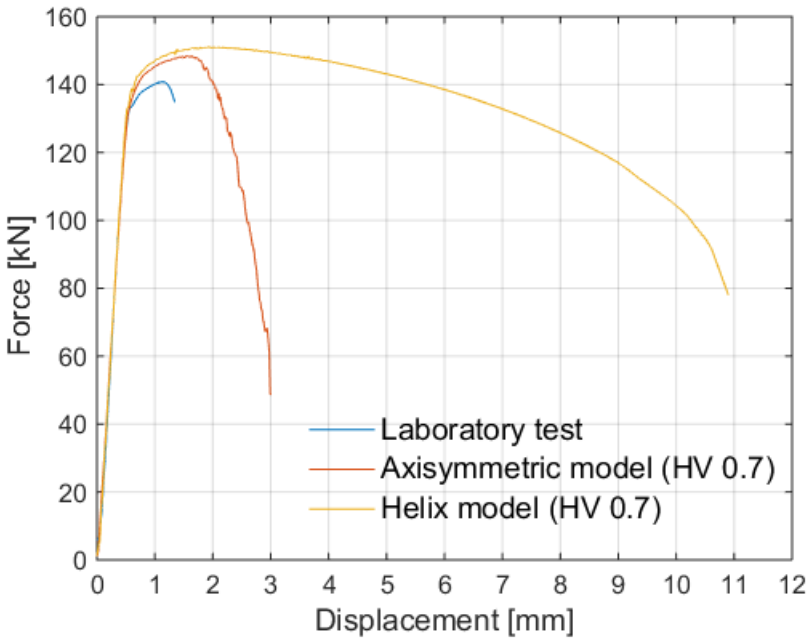

(b) Comparsion of models 3D helix: SB grip length 101 mm

Figure 6.38: Comparsion of models 3D helix: SB grip length 81 mm and 101 mm

7. *Discussion*

This chapter contains discussions and comments of observations and results from experimental tests and FE simulations. Some of the topics from Chapter 6.3 are more extensively discussed here.

7.1 Force and displacement in FE models

The majority of all FE simulations presented in Chapter 6 predicted too large displacement and maximum force. Several suggestions for this observation are discussed below:

- Thread stripping in FE simulations was more like thread bending, as opposed to shear cutting that was observed in the experimental tests. Shear cutting of threads is depicted in Figure 4.25b. A difference in local fracture modes could explain the the large displacement and maximum force; shear fracture is typically considered as more brittle compared to the ductile behavior in bending. Furthermore, this could imply that the *Extended Cockcroft-Latham* fracture criterion does not fully capture the nature of thread stripping. A remedy could be to use a fracture criterion with better representation of shear fracture. On the other hand, it can be difficult to calibrate such a criterion due to difficulties in performing sensible material tests of the threads alone.

- The employed fracture criterion is based on the assumption of plane stress. This assumption may not be correct for the stress state in the threads, as it may be more complex. Figure 7.2 illustrates the deformation of bolt threads affected by thread stripping. This can be a contributing reason for the prediction of too late fracture and overly large forces. It is also observed that the maximum force deviates more in cases of thread stripping compared to bolt fracture. The stress state in bolt fracture have more similarities with plane stress, compared with the more complex stress state in thread stripping. In addition, the fracture criterion was calibrated based on cross-sectional fracture of the FE material model. This may be a reason for why bolt fracture is better predicted than thread stripping. No further investigation regarding the stress state of the bolted assembly was conducted.

- Due to difficulties in performing material tests on the nut, the same material parameters were used in the bolt and nut. First, hardening and fracture strain may not be equal in the bolt and nut. Secondly, the assumption of plane stress may not be valid for the nut as well.

- An axisymmetric simplification was not able to predict the correct shape of the fracture surface. The fracture surface experienced in axisymmetric simulations was plane, as opposed to the fracture surface experienced in testing as depicted in Figure 7.1b. This could lead to differences in displacement, but it is hard to quantify.
- The realistic helical shape of the threads will make the cross-section vary. The axisymmetric cross-section will either consist of the inner diameter alone, or the inner diameter plus two thread heights. A larger cross section in the fracture zone of the bolt, as seen in Figure 7.1a, can lead to overly large deformations. In addition, the thread run-out geometry of the bolt is not fully captured. When necking occurs in this section, the geometrical simplifications may influence the response.

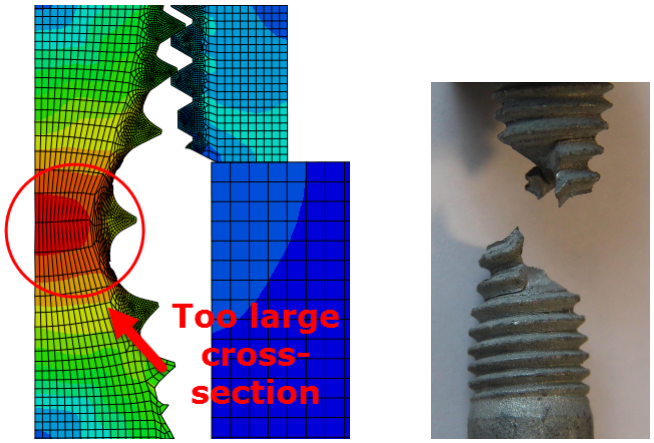

(a) Localization of neck in axisymmetric model

(b) Realistic fracture surface

Figure 7.1: Cross-sectional material in bolt fracture

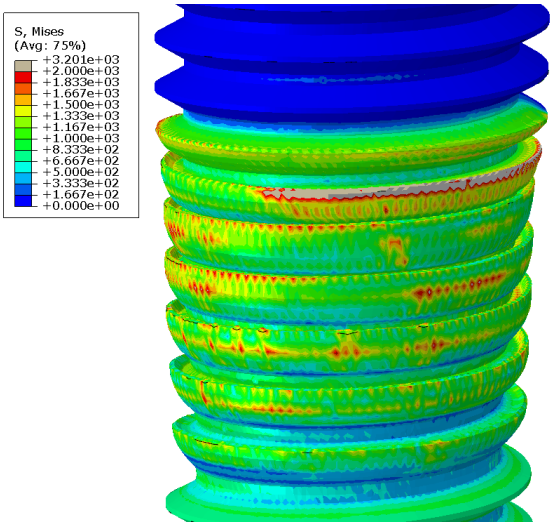

Figure 7.2: Bending of bolt threads in 3D helix model

7.2 Mesh sensitivity

Observations from the parameter study indicated that the computational time was most determinative for the choice of element size. Reduction of the element size had no influence on the fracture mode in none of the FE models. Using the largest elements resulted in at least four elements over one thread height, a number that should be enough to capture the global response. All models were able to predict the correct failure modes by use of the largest element size, but the smallest elements produced a smoother deformation progress and better stress distributions. If a detailed study of the threads is needed, smaller elements may be advantageous.

In axisymmetric simulations, the smallest element size (0.1 mm) was used since these analysis only lasted for a maximum of six hours. The advantageous effects of reducing the element size in the 3D non helix model, was small compared to the increase of computational cost. With 0.5 mm elements the simulations lasted for a maximum of 7 hours, as opposed to at least 30 hours for 0.2 mm elements.

Simulations with the 3D helix model lasted for approximately 30-80 hours on supercomputers, even with quite large elements (0.4 mm element size). Therefore only a limited amount of simulations were performed with this model. It was decided to not increase the element size beyond 0.4 mm, to ensure that important physical behaviour would be captured. Smaller elements would be unpractical due to computational cost.

7.3 Hardness of material

Reduction of the nut yield strength seemed to have significant influence on the FE models ability to predict the correct failure modes. Especially for large grip lengths. The parameter study was primarily performed with the axisymmetric model, but the same similar modification was also necessary in the 3D non helix model to predicts thread stripping for SB-bolts.

Reducing the yield strength of the SB-nut provoked thread stripping for all grip lengths in the axisymmetric model. The strength needed to be reduced to the lowest observations of hardness, i.e. to 70 %. Several factors could influence the observed difference in hardness; chemical composition, fabrication of the threaded part, rolling or cutting out the threads or temperature during processing. The *Vickers hardness* test was only performed for one nut of each type, and it is therefore difficult to state that the observation was valid in general. A sample of five nuts of each type could have been tested to validate this observation.

It should be reasonable to reduce the nut yield strength based on difference in hardness because of the known relationship: $\sigma_y \simeq 3 \cdot \mathrm{HV}$. The low nut hardness may be a contributing reason for why all experimental tests with SB-bolt and regular nut failed by thread stripping. If so, hardness tests seems to be an important part of determining ma-

terial parameters for FE analysis of bolted assemblies.

Note that the reduction of hardness was only applicable for the SB-nut, since both the HR-nut and high nut had minor deviations in hardness compared to their respective bolts. The small deviation of hardness for the HR-bolt and nut was tested in a simulation, without any change of the failure mode.

7.4 Geometry tolerances

It was observed that the failure mode for some grip lengths seemed to be sensitive for small geometrical variations within tolerance requirements given by ISO 965 [21]. Simulations were performed with grip length 85 mm and 87 mm for a SB-bolt and regular nut with full strength. The minimum requirements resulted in thread stripping, but the actual measurements and maximum tolerances resulted in bolt fracture. The minimum requirements reduced the overlap of the mating threads, such that thread stripping occurred.

This observation may indicate a weakness in the standard, but it is probably difficult and uneconomical to tighten the tolerance requirements with respect to the manufacturer. If the goal is to avoid thread failure, it might be more reasonable to use a high nut or two regular nuts. Another alternative is to use fully threaded bolts as Grimsmo et.al [23] and Skavhaug and Østhus [35] found out.

7.5 Effect of high nut and number of threads

The effect of using a high nut and the number of threads is presented together because of their interconnection. Simulations performed in the parameter study indicated that the number of nut threads had significant influence on the failure mode.

High nut

Experimental tests performed with SB-bolt and high nut resulted in bolt fracture for all grip lengths. Exactly the same results was observed in FE simulations with the axisymmetric model, since the simulation with grip length 81 mm predicted bolt fracture. These observations indicates that the use of a high nut is favorable if bolt fracture is desirable.

Number of threads

Ambiguity arises when deciding how many nut threads that should be used in the axisymmetric and 3D non helix model. Based on the parameter study in Section 6.3.4, the correct number of threads seemed to be somewhere in between five and six.

For short grip lengths the nut is influenced by necking of the bolt, and the number of threads seemed to be of importance. Necking of the bolt force some threads to disengage, and the number of remaining threads determined the failure mode. For larger grip lengths, the nut was unaffected by necking and the number of nut threads seemed to have less influence.

Wrong failure mode in FE simulations could be caused by the incorrect geometry of the threads. The missing helical shape in the axisymmetric and 3D non helix model gives wrong thread shear area. An axisymmetric simplification forces the threads to be discrete circles, as opposed to one single continuous thread as the helical shape. A comparison of the total shear area for one discrete circle against one continuous helix over a 2 mm pitch follows:

The total length and shear area for one discrete circle over one pitch is:

$$l_{circle} = \pi \cdot d_{shear} \qquad A_{circle} = l_{circle} \cdot h_{thread} \tag{7.1}$$

where l_{circle} is the length of one circle, d_{shear} is the diameter for the shear surface, h_{thread} is the thread height in the shear surface and A_{circle} is the shear area.

For a continuous helix, the helical length is the same as the hypotenuse in a Pythagorean triangle, with the two cathetus equal to the pitch height and the shear surface circumference:

$$l_{helix} = \sqrt{p^2 + \pi^2 \cdot d_{shear}^2} \qquad A_{helix} = l_{helix} \cdot h_{thread} \tag{7.2}$$

where l_{helix} is the helical length and p is the pitch height. It is not clear which d_{shear} and h_{thread} that should be used, probably somewhere in between the outer and inner

Table 7.1: Difference in shear area between circular and helical threads (d_{shear} for HR-bolts was used)

d_{shear}	h_{thread}	A_{circle} $[mm^2]$	A_{helix} $[mm^2]$
Inner diameter	$p/4$	21.11	21.14
Outer diameter	$p/8$	12.39	12.40
Diameter in between	Middle height	17.21	17.23

diameter of the threads. This depends on the overlap of the mating threads. Table 7.1 presents the shear area for different values.

Table 7.1 shows that the shear area for one circular thread is slightly smaller compared with the helical shape over one pitch. On the other hand, it is not clear how many circular threads that should be used over the full nut height. For a nut height of 14,4 mm (with 2 mm pitch and 1.8 mm chamfer height in each end of the nut) the number of threads should be:

$$n = \frac{14.4 - 2 \cdot 1.8}{2} = 5.4 \text{ circular threads} \tag{7.3}$$

This could explain why there was such difference in fracture mode by using five instead of six full nut threads for critical grip lengths.

7.6 Comparison of models

In this section a comparison of the different models considering both accuracy of results and computational effort is presented.

3D non helix model

Results from simulations with the 3D non helix model did not show any remarkable improvements compared with results from the axisymmetric model. For the 3D non helix model it was necessary with five full nut threads to predict thread stripping, as opposed to six full threads in the axisymmetric model.

Both the axisymmetric and 3D non helix models were able to predict the same failure modes, but the maximum force and displacement to failure were in general higher in the 3D model. The difference in maximum force seems strange, because these two models should be quite identical regarding modeling and element formulation. The reason of these differences was not uncovered, even with a lot of troubleshooting.

It was preferable to use the axisymmetric model with respect to computational time, as discussed in Section 7.2. By using the smallest element size in the axisymmetric model, the analysis time was equal as with the largest element size in the 3D non helix model. Since the results was slightly better, the axisymmetric model can be used except for studies of unsymmetrical effects.

3D helix model

As presented in Section 6.4.2, the 3D helix HR-bolt model predicted the correct failure modes for all grip lengths without any modifications. The helical shape of the threads, in addition with the overall nut geometry, seemed to be accurate enough and a fairly good representation of the realistic geometry. Even with the small simplifications due to the thread runout of the bolt (Figure 6.5), and the fading problem in each end of the countersink area of the nut (Figure 6.4).

SB-bolt simulations with reduced nut yield strength of 70 % were able to predict thread stripping for grip length 81 mm, but not for grip length 101 mm. It was challenging to predict thread stripping for large grip lengths with SB-bolts, because it differed from the expected behavior of bolted assemblies. Generally, large grip lengths should result in bolt fracture. But the SB-bolts tested in this thesis differed from expectations and results of Grimsmo et.al [23]. Therefore, it was difficult to capture the behavior of the tested SB-bolt and regular nut.

The total analysis time with the 3D helix model was too large, such that using this model for an engineering purpose is unpractical and unrealistic due to computational cost. Therefore, an axisymmetric model could be used without any large disadvantages. But the 3D helix model seemed more reliable because of more realistic behavior.

7.7 Calculations of tension capacity

Table 7.2 presents a comparison of the tension capacity from FE simulations compared with analytical calculations. All capacities is presented independent of failure mode, only the lowest value of maximum force was registered. Overall, the FE simulations seems to capture the physical behaviour with reasonable accuracy. Since the lowest force levels was achieved with the axisymmetric models, results from these simulations is presented here. Analytical calculations in Table 7.2 is performed according to Alexanders formulas [7], see Appendix C, and the code NS-EN 1993-1-8 [14].

The nominal capacity given in the code NS-EN 1993-1-8 [14] utilize the nominal ultimate fracture stress for 8.8 bolts, given as 800 MPa. Note that the capacity is calculated using safety factors, which explains the low value of tensile capacity. In the adapted capacity, the nominal ultimate fracture stress from the material tests performed in this thesis was used without any saftey factors. The nominal ultimate fracture stress, σ_u, was set as 928 MPa for the HR-bolt, and 1001 MPa for the SB-bolt.

Table 7.2: Comparison of tension capacity

	SB-bolt	HR-bolt
Experiments	131.6 kN	139.5 kN
Simulation	147.3 kN	140.3 kN
$EC3_{nominal}$	90.4 kN	90.4 kN
$EC3_{adapted}$	141.5 kN	131.2 kN
Alexander	138.4 kN	136.3 kN

SB-bolt

The lowest force from experiments was registered for test case: SB-NS-88-89-3. This value was noticeably lower compared with the other tests from the similar test series, which had an average capacity slightly under 140 kN. FE simulations predicted the lowest force when the yield strength of the nut was reduced to 70 %. Similar to the experiment, this FE simulation with grip length 101 mm failed by thread stripping. Figure 6.18c illustrates the result from the FE simulation representing the lowest force.

Calculation according to Alexander predicted thread stripping in the nut. This is in accordance with the fact that the nut yield strength needed to be reduced in FE simulations for predicting thread stripping.

Generally, some scatter of the force was registered for SB-bolts . Especially the FE simulation predicted about 12 % higher force compared with experiments. Disregarding the nominal calculation, all capacity for the SB-bolt assembly satisfies the requirement of a minimum tensile capacity of 130 kN given in ISO 4014 [15].

HR-bolt

Experimental tests with HR-bolts showed the lowest force for test case: HR-NS-88-101-1. The lowest force predicted by FE simulations was with grip length 101 mm and failed by bolt fracture, the same as in the experiments. Figure 6.17d illustrates the result from this FE simulation with the lowest force.

Calculations according to Alexander also predicted bolt fracture. Generally, it is good accordance of the tensile capacity for the HR-bolts. The FE-simulations seemed to be able to capture the nature of the HR-bolt fairly well. Disregarding the nominal calculation, all capacity for the HR-assembly satisfies the requirement of a minimum tensile capacity of 130 kN given in ISO 4014 [15].

7.8 Comments according to the standards

The probability of thread failure can in many cases be avoided by choosing the correct nut and bolt. The code NS-EN 1090-2 states that non-preloaded bolts shall have at least one full free thread between the thread runout and the shaft, and that preloaded bolt shall have at least four full free threads. These requirements are set to ensure some safety margin due to installation. The idea of the free threads is to prevent the nut from being screwed onto the shank. This can further lead to fracture of the threads or inadequate pretensioning.

According to results in this thesis the probability of thread failure depends on both the nut position and material factors. From an engineering perspective it is more desirable that a bolted assembly fails by bolt fracture instead of thread stripping. Bolt fracture gives a much more ductile behaviour, which is advantageous in structural connections. In case of accidents, the bolt load may exceed the tension capacity requirements of ISO 4014 [15] of 130 kN. The connection should then be able to deform with visible deformations, such that an overloading is visible upon inspections.

It may therefore be common practice to choose bolt and nut types that ensures bolt fracture. If the existing requirements in the standard is to be followed, there may be a note that bolt fracture is preferred.

8. *Concluding remarks*

A summary of the findings and discussions in this master thesis is presented in this chapter along with concluding remarks. Subsequently, suggestions for further work is presented.

Results from the experimental tests revealed that HR-bolts behaved as expected. For short grip lengths the failure mode was thread stripping, and for large grip lengths the failure mode was bolt fracture. This observation is in accordance with Grimsmo et al. [23] and Skavhaug and Østhus [35]. The tipping point seemed to be for grip length 87 mm, with a total of five free threads. All tests with SB-bolts resulted in thread stripping for all grip lengths by use of a regular nut. This deviates with the assumption that large grip lengths gives bolt fracture in general. With use of two nuts or a high nut, the fracture mode changed as expected to bolt fracture. Increasing the deformation rate from 0.8 mm/min to 60 mm/min had no effect on the failure mode. Results from *Vickers hardness* tests pointed out a reduction of hardness in the regular nut compared with the SB-bolt. The nut thread hardness was 70 % of the bolt hardness. No remarkable deviation in hardness was observed for the other bolt and nut assemblies.

All FE models were able to predict the correct failure modes observed in the laboratory with reasonable accuracy. Different modifications were tested out, and some of them were necessary to predict the correct failure mode. The number of full nut threads and reduction of nut yield stress based on values of hardness, seemed to have significant influence in FE simulations with the axisymmetric and 3D non helix model. Results from simulations with the 3D helix model seemed to be more realistic, but the computational cost was very high. No modifications were needed in this model to predict the correct failure modes for HR-bolts. For the SB-bolt and regular nut with reduced yield stress, thread stripping was only predicted for grip length 81 mm. Simulation with grip length 101 mm resulted in bolt fracture. This differ from the experimental tests.

Generally, the maximum force and displacement to failure was higher in FE models compared with results from experimental tests.

Conclusions

The following concluding remarks can be extracted from the work in this thesis:

- Experimental tests for HR-bolts with short grip lengths resulted in thread stripping, and large grip lengths resulted in bolt fracture. The critical grip length was pointed out as 87 mm, i.e. five free full threads between the unthreaded part of the bolt and the underside of the nut. Bolt fracture was ensured with a total of six free full threads.

- All experimental tests with SB-bolts and regular nuts ended with thread stripping for all grip lengths. This contradicts with the assumption of Skavhaug and Østhus [35]; that thread stripping should occur for short grip lengths. A reason for the observed deviation may be related to the reduced value of nut hardness. Only one *Vickers hardness* test was performed so it is hard to state if this is valid in general. Using a high nut or two regular nuts ensures bolt fracture for SB-bolts regardless of the grip length.

- Geometrical approximations of the threads in the axisymmetric and 3D non helix model influence the ability to predict the correct failure mode. Using five or six full circular threads resulted in different failure modes with similar grip lengths, independent of the bolt type. The correct number of circular threads is somewhere in between five and six. The 3D helix model gave a better representation of the realistic thread geometry. In addition, the fracture surface was more realistic. Therefore, the 3D helix model seemed to predict credible failure modes and realistic physical behavior.

- The axisymmetric model seemed to predict the behaviour of the bolted assemblies with reasonable accuracy at a small computational cost, given the correct number of threads. Benefits of using the 3D helix model (and 3D non helix model) are small considering the computational cost. Therefore, an axisymmetric model could be used for an engineering purpose without any large disadvantages.

- Differences in response between FE analysis and experimental tests, may be related to inaccurate assumptions in the material description and geometrical approximations. Further, observations indicate that *Vickers harndess* tests may be an important part of determining material parameters for use in FE simulations.
- A comprehensive amount of time and work has been devoted to construct the 3D helix model. Lots of trial and error was necessary to make the model run because of the complex geometry. The final model seems to be robust and able to predict the physical behaviour of bolted assemblies. Limiting amount of time prevented fine-tuning of the model and further analysis. The scripted model is included after the appendices, and could be used by others to study bolted assemblies.

Suggestions for further work

The following list presents suggestions for further work, based on this study of bolt and nut assemblies subjected to tension load:

- Bolts and nuts with different geometrical sizes, strength classes and standards should be tested to investigate if thread stripping occurs for short grip lengths in general. It is hard to state if this is valid in general with the limited amount of bolted assemblies tested in this thesis. More *Vickers hardness* tests should be conducted.
- The stress state of critical regions should be studied closer. Another fracture criterion, or other fracture modelling techniques could also be employed such that thread shearing might be predicted.
- Try another software to model and mesh the helical geometry in a FE-model. In addition, it would be interesting to study the effect of larger and smaller elements.

References

[1] Abaqus documentation v6.14. `http://abaqus.software.polimi.it/v6.14/index.html`. Accessed: 2016-03-10.

[2] Abaqus inc contact modeling. `http://imechanica.org/files/l4-contact.pdf`. Accessed: 2016-04-28.

[3] Abaqus inc elements. `http://imechanica.org/files/l2-elements.pdf`. Accessed: 2016-04-28.

[4] Abaqus inc quasi static analysis. `http://imechanica.org/files/l5-quasi-static.pdf`. Accessed: 2016-04-28.

[5] About vilje. https://www.hpc.ntnu.no/display/hpc/About+Vilje.

[6] Python website. `https://www.python.org/`. Accessed: 2016-01-20.

[7] E.M. Alexander. Analysis and design of threaded assemblies. Technical report, SAE Technical Paper, 1977.

[8] John Bickford. *An introduction to the design and behavior of bolted joints, Revised and expanded*, volume 97. CRC press, 1995.

[9] Jien-Jong Chen and Yan-Shin Shih. A study of the helical effect on the thread connection by three dimensional finite element analysis. *Nuclear engineering and design*, 191(2):109–116, 1999.

[10] Anil K. Chopra. *Dynamics of structures*, volume 3. Prentice Hall New Jersey, 1995.

[11] Robert D. et.al. Cook. *Concepts and applications of finite element analysis*. John Wiley & Sons, 2007.

[12] Eduardo A de Souza Neto, Djordje Peric, and David Roger Jones Owen. *Computational methods for plasticity: theory and applications*. John Wiley & Sons, 2011.

[13] Egil Fagerholt. *Field measurements in mechanical testing using close-range photogrammetry and digital image analysis, 2012: 95*. PhD thesis, PhD thesis, Norwegian University of Science and Technology, 2012.

[14] European Committee for Standardization (CEN). *Eurocode 3: Design of steel structures, Part 1-8: Design of joints*. Norwegian Standard, 2005.

[15] European Committee for Standardization (CEN). *Hexagon head bolts - Product grades A and B (ISO 4014:2011)*. Norwegian Standard, 2011.

[16] European Committee for Standardization (CEN). *Hexagon high nuts (style 2) - Product grades A and B (ISO 4033:2012)*. Norwegian Standard, 2012.

[17] European Committee for Standardization (CEN). *Hexagon regular nuts (style 1) - Product grades A and B (ISO 4032:2012)*. Norwegian Standard, 2012.

[18] European Committee for Standardization (CEN). *Utførelse av stålkonstruksjoner og aluminiumkonstruksjoner Del 2: Tekniske krav til stålkonstruksjoner*. Norwegian Standard, 2012.

[19] European Committee for Standardization (CEN). *High-strength structural bolting assemblies for preloading - Part 3: System HR - Hexagon bolt and nut assemblies*. Norwegian Standard, 2015.

[20] International Organization for Standardization (ISO). *ISO general purpose screw threads- Basic profile (ISO 68-1)*. Norwegian Standard, 1998.

[21] International Organization for Standardization (ISO). *ISO general purpose metric screw threads – Tolerances*. Norwegian Standard, 2013.

[22] Herman Frich. Beam-column connections subjected to static and dynamic loading. 2014.

[23] Erik L. Grimsmo, Langseth Magnus Aalberg, Arne, and Arild H. Clausen. Failure modes of bolt and nut assemblies under tensile loading. *Submitted for publication*, 2016.

[24] Gaute Gruben, Odd S. Hopperstad, and Tore Børvik. Evaluation of uncoupled ductile fracture criteria for the dual-phase steel docol 600dl. *International Journal of Mechanical Sciences*, 62(1):133–146, 2012.

[25] Masaya Hagiwara and Hiroaki Sakai. Verification of the design concept on nuts in bolt/nut assembly for the revision of iso 898-2 and iso 898-6. *Journal of Advanced Mechanical Design, Systems, and Manufacturing*, 1(5):755–762, 2007.

[26] Odd Sture Hopperstad and Tore Børvik. Lecture notes, tkt 4135 mechanichs of materials. *Department of Structural Engineering, NTNU*, 2012.

[27] Bendik M. Kolberg and Eirik T. Willand. Behaviour and modelling of bolted connectors in road safety barriers. 2014.

[28] Per K. Larsen. *Dimensjonering av stålkonstruksjoner*. Tapir, 2010.

[29] Mohsen Manutchehr-Danai. *Dictionary of gems and gemology*. Springer Science & Business Media, 2013.

[30] Kjell M. Mathisen. *TKT4192 Finite Element Methods In Strength Analysis: Lecture 15 - Finite Element Formulations for Solid Problems*. Norwegian University of Science and Technology (NTNU), 2014.

[31] Kjell M. Mathisen. *TKT4192 Finite Element Methods In Strength Analysis: Lecture 16 - Axisymmetric Solids*. Norwegian University of Science and Technology (NTNU), 2014.

[32] Kjell M. Mathisen. *TKT4197 Nonlinear Finite Element Analysis: Lecture 7 - Solution of the Dynamic Equilibrium Equations by Explicit Direct Integration*. Norwegian University of Science and Technology (NTNU), 2015.

[33] Kjell M. Mathisen. *TKT4197 Nonlinear Finite Element Analysis: Lecture 9 - Solution of the Nonlinear Dynamic Equilibrium Equations*. Norwegian University of Science and Technology (NTNU), 2015.

[34] Joshua Pelleg. *Mechanical properties of materials*, volume 190. Springer Science & Business Media, 2012.

[35] Elin S. Skavhaug and Svanhild I. Østhus. Tension-loaded bolted connections in steel structures. 2015.

[36] Yu Juan Sun and Ri Dong Liao. The effect of helix on the nonlinear analysis of threaded connection. In *Advanced Materials Research*, volume 148, pages 1741–1744. Trans Tech Publ, 2010.

Appendices

A. *Geometry of bolt*

This appendix presented illustrations and geometrical measurements of bolt and nut according to their respective standards and codes. All the dimensions refer to Figure A.1 and is based on averaged measurements prior to experiments.

External threaded denotes the bolt. Internal threaded denotes the nut.

SB-bolt

The the geometry of the SB-bolt follows the requirements in ISO 4014 - *Hexagon head bolts – Product grades A and B* [15]. Average measurements from experiments can be seen in Table A.1

Table A.1: Geometry of SB-bolt

Bolt				
Height of head	:	k	=	9.92 mm
Length of unthreaded part	:	l_g	=	73.84
Length of threaded part	:	b	=	43.96 mm
Diameter of unthreaded part	:	d_s	=	15.88
Diameter of threaded part	:	d	=	15.77 mm
Width across flats	:	s	=	23.70 mm
Width across corners	:	e	=	26.95
Length	:	l	=	119.87 mm
Regular nut (ISO 4032)				
Width across flats	:	s	=	23.88 mm
Width across corners	:	e	=	27.28 mm
Height of nut	:	m	=	14.59 mm
Tall nut (ISO 4033)				
Width across flats	:	s	=	24.05 mm
Width across corners	:	e	=	27.43 mm
Height of nut	:	m	=	16.19 mm

HR-bolt

The HR-bolt follows the requirements of NS-EN 14399-3 [19]. There are minor differences between a HR-bolt and a SB-bolt. The basic geometrical measurements and shape are identical with a SB-bolt, as can be seen in Figure . For exact details see NS-EN 14399-3. Average measurements from experiments can be seen in Table A.2

Table A.2: Geometry of HR-bolt

Bolt				
Height of head	:	k	=	10.32 mm
Length of unthreaded part	:	l_g	=	73.43 mm
Length of threaded part	:	b	=	44.60 mm
Diameter of unthreaded part	:	d_s	=	15.97
Diameter of threaded part	:	d	=	15.78
Width across flats	:	s	=	25.98 mm
Width across corners	:	e	=	30.07 mm
Length	:	l	=	120
Nut				
Width across flats	:	s	=	26.59 mm
Width across corners	:	e	=	30.20 mm
Height of nut	:	m	=	14.64 mm

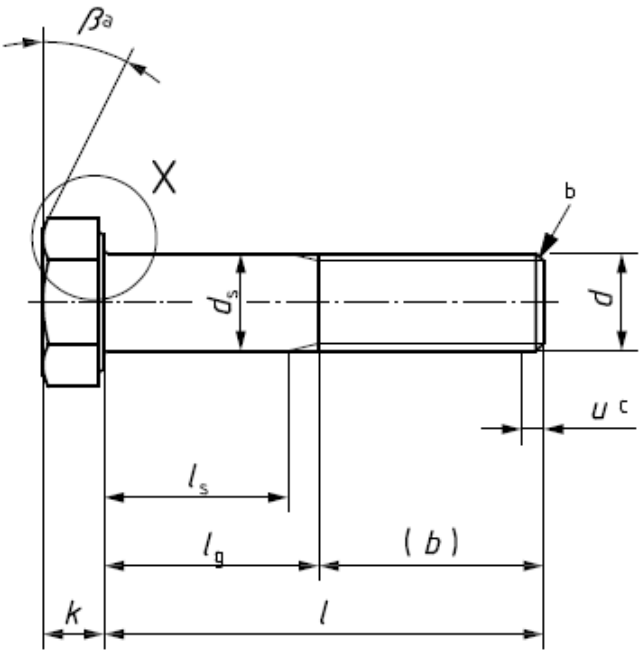

(a) Geometry of threaded bolt

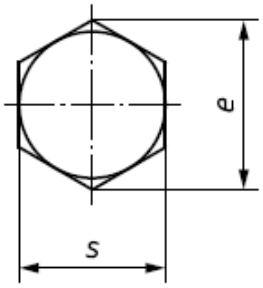

(b) Geometry of bolt head

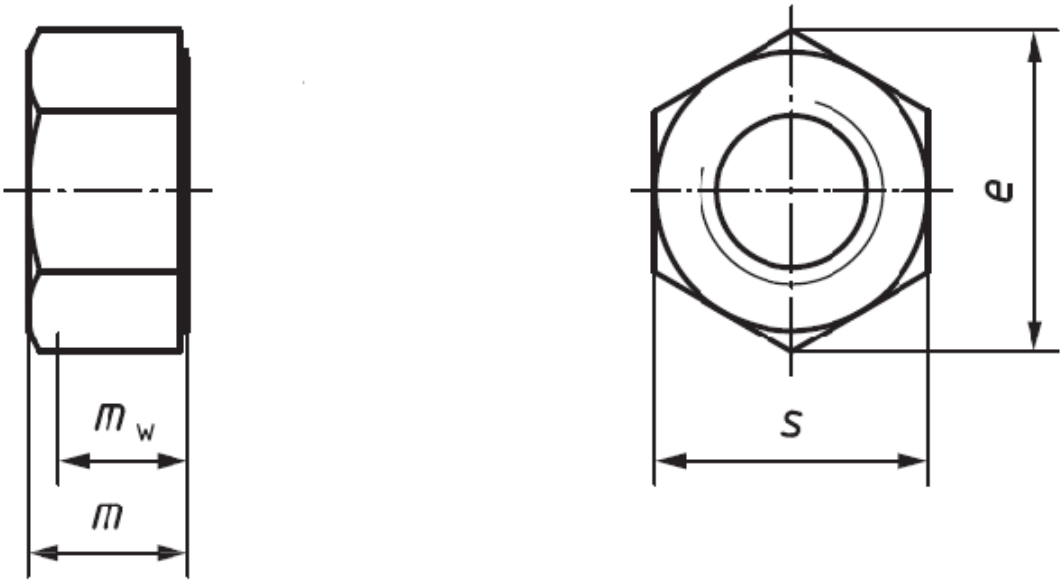

(c) Geometry of nut

Figure A.1: Bolt and nut geometry according to ISO 4014 [15] and ISO 4032 [17]

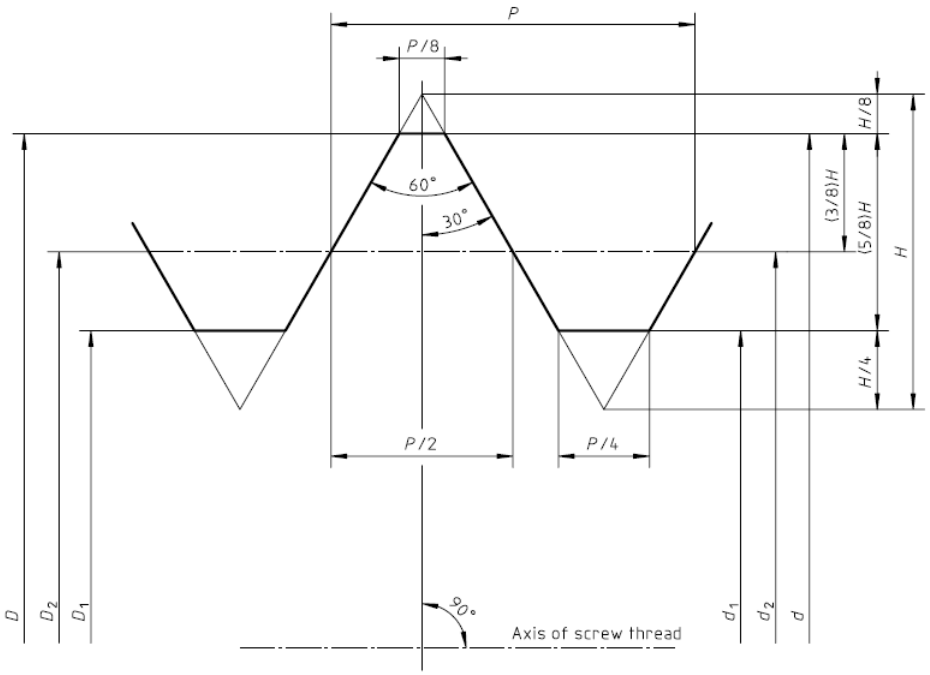

where

D	is the basic major diameter of internal thread (nominal diameter)
d	is the basic major diameter of external thread (nominal diameter)
D_2	is the basic pitch diameter of internal thread
d_2	is the basic pitch diameter of external thread
D_1	is the basic minor diameter of internal thread
d_1	is the basic minor diameter of external thread
H	is the height of fundamental triangle
P	is the pitch

Figure A.2: Geometrical definitions of metric screw thread [20]

B. *Formulas for design of threaded assemblies*

This appendix presents formulas for capacity calculations for threaded assemblies. All formuals along with dimensions are presented. The basis for these formulas is the work of Alexander [7].

Tensile stress area

$$A_s = \frac{\pi}{4} \cdot [d_2 + d_3]^2 \tag{B.1}$$

Shear stress area bolt

$$\begin{aligned} AS_b = \frac{LE - LB}{P} \cdot \pi \cdot D_1 \cdot \left[\frac{P}{2} + (d_2 - D_1) \cdot \frac{1}{\sqrt{3}} \right] \\ + \frac{LE}{P} \cdot \pi \cdot D_m \cdot \left[\frac{P}{2} + (d_2 - D_m) \cdot \frac{1}{\sqrt{3}} \right] \end{aligned} \tag{B.2}$$

The reason for the extended formula for the shear area of the bolt is bell-mouth shape of the nut. The bell-mouth shape reduce the overlap of the mating threads.

Shear stress area nut

$$AS_n = \frac{LE}{P} \cdot \pi \cdot d \cdot \left[\frac{P}{2} + (d_2 - D_1) \cdot \frac{1}{\sqrt{3}} \right] \tag{B.3}$$

This equation is shorter because the height of the bolt threads are constant over the length of threaded engagement. The nuts threads will therefor be sheared of at the same plane.

Length of threaded engagement

$$LE = m - (D_c - D_1 + T_{D1}) \cdot 0.6 \tag{B.4}$$

Allowing for 40 % of the effectiveness for countersink height.

Nut dialation

$$C_1 = \left[-(s/D)^2 + 3.8(s/D) - 2.61 \right] \tag{B.5}$$

Relative strength

$$C_2 = \begin{cases} 5.5946 - 13.682R_s + 14.107R_s^2 - 6.057R_s^3 + 0.9353R_s^4 & 1<R_s<2.2, \\ 0.897 & R_s \leq 1. \end{cases} \tag{B.6}$$

$$C_3 = \begin{cases} 0.728 + 1.769R_s - 2.896R_s^2 + 1.296R_s^3 & 0.4< R_s<1, \\ 0.897 & R_s \geq 1. \end{cases} \tag{B.7}$$

P	=	Pitch
m	=	Nut Height
LE	=	Length of threaded engagement
LB	=	Length of bell mouthed section of nut
As	=	Tensile stress area
H	=	Height of fundamental thread triangle
AS_b	=	Shear area bolt
AS_n	=	Shear area nut
D	=	Basic major diameter, Internal
D_1	=	Basic minor diameter, Internal
D_m	=	Mean diameter of bell mouth section
D_2	=	Basic Pitch Diameter, External
d	=	Basic major diameter, External
d_1	=	Basic minor diameter, External
d_2	=	Basic Pitch diameter, External
d_3	=	Minor diameter external threads = $d_1 - \frac{H}{6}$
σ_b	=	Bolt material ultimate strength
σ_n	=	Nut material ultimate strength
s	=	Width across flats
R_s	=	Strength ratio = $\frac{\sigma_n AS_n}{\sigma_b AS_b}$
T_{D1}	=	Tolerance for basic minor diameter, internal

Table B.1: Symbols

C. *Calculations of capacity*

This chapter presents calculations after Alexanders[7] formulas: The yield strength of the nut is set as 70% of the bolt, after results in Chapter 6.3.

SB-bolt

Tensile stress area

Pitch :	P	$= 2.0mm$
Height of fundamental trianlge :	$H = \sqrt{3}\frac{P}{2}$	$= 1.732mm$
Basic pitch diamter :	$d_2 = d - 2 \cdot \frac{3}{8}H$	$= 14.471mm$
Minor diameter external threads :	$d_3 = d_1$	$= 13.32mm$
Tensile stress area :	$A_s = \frac{\pi}{4} \cdot [d_2 + d_3]^2$	$= 151.63mm^2$

Thread shear area of bolt

Countersink diameter :	$D_c = 1.08 \cdot D$	$= 17.53mm$
Basic minor diamter, internal :	D_1	$= 14.08mm$
Basic major diamter, internal :	D	$= 16.22mm$
Tolerance for basic minor nut :	T_{D1}	$= 0.475mm$
Height of nut :	m	$= 14.59mm$
Length of thread engament :	$LE = m - (D_c - D_1 - T_{D1}) \cdot 0.6$	$= 12.805mm$
Length of bellmouth of nut :	$LB = \frac{m - 5 \cdot P}{2}$	$= 2.30mm$
Mean diameter of bell mouthed section :	$D_m = \frac{D + D_1}{2}$	$= 15.15mm$
Shear area of bolt :	$AS_b =$ Equation $B.2$	$= 404.9mm^2$

Thread shear area of nut

Major diameter, external :	d	$= 15.77mm$
Basic pitch diameter, internal :	$D_2 = D - 2 \cdot \frac{3}{8}H$	$= 14.921mm$
Shear area of bolt :	$AS_n =$ Equation $B.3$	$= 472.67mm^2$

Nut dialation

Width across flats :	s	$= 23.88mm$
Basic major diameter, internal :	D	$= 16.22mm$
Nut dialation factor :	$C_1 = \left[-(s/D)^2 + 3.8(s/D) - 2.61 \right]$	$= 0.817$

Relative strength

Ultimate stress bolt :	σ_b	$= 913MPa$
Ultimate stress nut :	σ_n	$= 640MPa$
Strength ratio :	$R_s = \frac{\sigma_n AS_n}{\sigma_b AS_b}$	$= 0.82$
	$Eq.B.6 \Longrightarrow C_2$	$= 0.897$
	$Eq.B.7 \Longrightarrow C_3$	$= 0.93$

Load capacities for SB-bolt

Bolt fracture :	$F_{bf} = \sigma_b \cdot A_s$	$= 138.4kN$
Bolt thread stripping :	$F_{bs} = \sigma_b \cdot AS_b \cdot C_1 \cdot C_2 \cdot 0.6$	$= 168.5kN$
Nut thread stripping :	$F_{ns} = \sigma_n \cdot AS_n \cdot C_1 \cdot C_3 \cdot 0.6$	$= 133.01kN$

HR-bolt

Tensile stress area

Pitch :	P	$= 2.0mm$
Height of fundamental trianlge :	$H = \sqrt{3}\frac{P}{2}$	$= 1.732mm$
Basic pitch diamter :	$d_2 = d - 2 \cdot \frac{3}{8}H$	$= 14.481mm$
Minor diameter external threads :	$d_3 = d_1$	$= 13.44mm$
Tensile stress area :	$A_s = \frac{\pi}{4} \cdot [d_2 + d_3]^2$	$= 153.07mm^2$

Thread shear area of bolt

Countersink diameter :	$D_c = 1.08 \cdot D$	$= 17.53mm$
Basic minor diamter, internal :	D_1	$= 14.15mm$
Basic major diamter, internal :	D	$= 16.91mm$
Tolerance for basic minor nut :	T_{D1}	$= 0.475mm$
Height of nut :	m	$= 14.64mm$
Length of thread engament :	$LE = m - (D_c - D_1 - T_{D1}) \cdot 0.6$	$= 12.897mm$
Length of bellmouth of nut :	$LB = \frac{m - 5 \cdot P}{2}$	$= 2.32mm$
Mean diameter of bell mouthed section :	$D_m = \frac{D + D_1}{2}$	$= 15.53mm$
Shear area of bolt :	$AS_b =$ Equation $B.2$	$= 302.6mm^2$

Thread shear area of nut

Major diameter, external :	d	$= 15.78mm$
Basic pitch diameter, internal :	$D_2 = D - 2 \cdot \frac{3}{8}H$	$= 15.61mm$
Shear area of bolt :	$AS_n =$ Equation $B.3$	$= 478.22mm^2$

Nut dialation

Width across flats :	s	$= 26.59mm$
Basic major diameter, internal :	D	$= 16.91mm$
Nut dialation factor :	$C_1 = \left[-(s/D)^2 + 3.8(s/D) - 2.61 \right]$	$= 0.90$

Relative strength

Ultimate stress bolt :	σ_b	$= 890MPa$
Ultimate stress nut :	σ_n	$= 890MPa$
Strength ratio :	$R_s = \dfrac{\sigma_n AS_n}{\sigma_b AS_b}$	$= 1.18$
	$Eq.B.6 \Longrightarrow C_2$	$= 0.96$
	$Eq.B.7 \Longrightarrow C_3$	$= 0.897$

Load capacities for HR-bolt

Bolt fracture :	$F_{bf} = \sigma_b \cdot A_s$	$= 136.3kN$
Bolt thread stripping :	$F_{bs} = \sigma_b \cdot AS_b \cdot C_1 \cdot C_2 \cdot 0.6$	$= 139.3kN$
Nut thread stripping :	$F_{ns} = \sigma_n \cdot AS_n \cdot C_1 \cdot C_3 \cdot 0.6$	$= 206.0kN$

Python/Abaqus script for 3D helix model

```
from part import *
from material import *
from section import *
from assembly import *
from step import *
from interaction import *
from load import *
from mesh import *
from optimization import *
from job import *
from sketch import *
from visualization import *
from connectorBehavior import *
m = mdb.models['Model-1']
SS = m.ConstrainedSketch(name='BoltBasis', sheetSize=200.0)
session.journalOptions.setValues(replayGeometry=COORDINATE,recoverGeom
etry=COORDINATE)
import numpy
from numpy import arange
from numpy import linspace
######################################################################
######################### Variables ##################################
######################################################################
### Model parameters ###
bomVelocity = 0.0266 # Velocity of upper grip in motion
t_fullSpeed = 20.0 # Time before full speed in smooth step function
(see BC)
simulationTime = 600.0 # Total simulation time in seconds
targetTimeIncrement = 0.001 # Target time increment for mass scaling
fricThreads = 0.2 # Friction coefficient between threads
fricGrip = 0.2 # Friction coefficient in grip zone
n_free_nut = 12.0 # Number of free threads (NB!! Remember to verify
the nut position visualy)
### Meshing ###
mesh_core_bolt = 0.4 # Mesh size of bolt core
mesh_midCore_bolt = 0.4 # Mesh size of mid core of bolt
mesh_thread_bolt = 0.4 # Mesh size for bolt threads
mesh_outer_nut = 0.6 # Mesh size of outer part of nut
mesh_thread_nut = 0.4 # Mesh size for nut threads
mesh_head = 4.0 # Mesh size for bolt head
mesh_shank = 1.5 # Mesh size for shank
mesh_grip = 4.0 # Mesh size of grip plate
### Bolt head ###
k = 10.2 # Head hight
w_flats = 23.7 # Width across flats
w_corners = 26.9 # Width across corners
### Unthreaded part of bolt ###
d_unthread = 16.0 # Diameter of unthreaded part
l_unthread = 73.5+4.0 # Length of unthreaded part (last part makes
the grip length correct)
l_chamfer = 2.8 # Length of chamfer
d_chamfer = 13.32 # Inner diameter of special thread
### Threaded part of bolt ###
d_inner = 13.32 # Inner diameter of threaded part
d_outer = 15.77 # Outer diameter of threaded part
p = 2.0 # Pitch size
n_p = 22.0 # Number of threads
l_thread = 44.0 # Length of threaded part
l_special = 0.8  # Length of special thread
l_tie = 10.0 # Length of untreaded part before tie constraint NB!
Check grip length if this is changed
### Nut ###
e = 27.3 # Witdh across corners
s = 23.9 # Width across flats
h_nut = 14.4 # Height of nut
d_inner_nut = 16.26 # Diameter of thread valley of nut
d_outer_nut = 14.08 # Diameter of thread "top" of nut
d_chamfer_nut = 17.5 # Diameter of top/bottom if chamfer part
l_chamfer_nut = 1.2 # Length of chamfer part
### Grip plate ###
d_ext_grip = 75.0 # External diameter of grip plate
d_int_grip = 18.0 # Internal diameter of grip plate
```

```
h_grip = 20.0 # Height of grip plate
### Other variables ###
eps = 0.001 # Small number to avoid numerical problems
tan30 = tan(pi/6) # Geometrical variable for sketching
cos30 = cos(pi/6) # # Geometrical variable for sketching
##################################################################
######################### Create parts ###########################
##################################################################

#################
### Bolt head ###
#################
mdb.models['Model-1'].ConstrainedSketch(name='__profile__',
sheetSize=200.0)
mdb.models['Model-1'].sketches['__profile__'].Line(point1=(0,
-w_corners/2), point2=
    (-cos30*w_corners/2, -w_corners/4))
mdb.models['Model-1'].sketches['__profile__'].Line(point1=(-cos30*w_co
rners/2, -w_corners/4),
    point2=(-cos30*w_corners/2, w_corners/4))
mdb.models['Model-1'].sketches['__profile__'].Line(point1=(-cos30*w_co
rners/2, w_corners/4), point2=
    (0.0, w_corners/2))
mdb.models['Model-1'].sketches['__profile__'].Line(point1=(0.0,
w_corners/2), point2=(
    cos30*w_corners/2, w_corners/4))
mdb.models['Model-1'].sketches['__profile__'].Line(point1=(cos30*w_cor
ners/2, w_corners/4),
    point2=(cos30*w_corners/2, -w_corners/4))
mdb.models['Model-1'].sketches['__profile__'].Line(point1=(cos30*w_cor
ners/2, -w_corners/4),
    point2=(0.0, -w_corners/2))
mdb.models['Model-1'].Part(dimensionality=THREE_D, name='Head', type=
    DEFORMABLE_BODY)
mdb.models['Model-1'].parts['Head'].BaseSolidExtrude(depth=k, sketch=
    mdb.models['Model-1'].sketches['__profile__'])
del mdb.models['Model-1'].sketches['__profile__']

###################################
### Unthreaded shaft and chamfer ###
###################################
mdb.models['Model-1'].ConstrainedSketch(name='__profile__',
sheetSize=200.0)
mdb.models['Model-1'].sketches['__profile__'].ConstructionLine(point1=
(0.0,
    -100.0), point2=(0.0, 100.0))
mdb.models['Model-1'].sketches['__profile__'].Line(point1=(0.0,
0.0), point2=(
    d_unthread/2, 0.0))
mdb.models['Model-1'].sketches['__profile__'].Line(point1=(d_unthread/
2, 0.0), point2=(
    d_unthread/2, l_unthread-l_chamfer-l_tie))
mdb.models['Model-1'].sketches['__profile__'].Line(point1=(d_unthread/
2, l_unthread-l_chamfer-l_tie), point2=(
    0.0, l_unthread-l_chamfer-l_tie))
mdb.models['Model-1'].sketches['__profile__'].Line(point1=(0.0,
l_unthread-l_chamfer-l_tie), point2=(
    0.0, 0.0))

# Finish up sketch and generate part
mdb.models['Model-1'].Part(dimensionality=THREE_D, name='Shank', type=
    DEFORMABLE_BODY)
mdb.models['Model-1'].parts['Shank'].BaseSolidRevolve(angle=360.0,
    flipRevolveDirection=OFF, sketch=
    mdb.models['Model-1'].sketches['__profile__'])
del mdb.models['Model-1'].sketches['__profile__']

####################
### Threaded part ###
####################
mdb.models['Model-1'].ConstrainedSketch(name='__profile__',
sheetSize=200.0)
```

```
mdb.models['Model-1'].sketches['__profile__'].ConstructionLine(point1=
(0.0,
    -100.0), point2=(0.0, 100.0))
mdb.models['Model-1'].sketches['__profile__'].Line(point1=(0.0,
-l_tie-l_chamfer), point2=(
    d_unthread/2, -l_tie-l_chamfer))
mdb.models['Model-1'].sketches['__profile__'].Line(point1=(d_unthread/
2, -l_tie-l_chamfer), point2=(
    d_unthread/2, -l_chamfer))
mdb.models['Model-1'].sketches['__profile__'].Line(point1=(d_unthread/
2, -l_chamfer), point2=(
    d_inner/2, 0.0))
mdb.models['Model-1'].sketches['__profile__'].Line(point1=(d_inner/2,
0.0), point2=(
    d_outer/2, 0.0))
mdb.models['Model-1'].sketches['__profile__'].Line(point1=(d_outer/2,
0.0), point2=(
    d_outer/2, l_thread))
mdb.models['Model-1'].sketches['__profile__'].Line(point1=(d_outer/2,
l_thread), point2=(
    0.0, l_thread))
mdb.models['Model-1'].sketches['__profile__'].Line(point1=(0.0,
l_thread), point2=(
    0.0, -l_tie-l_chamfer))
mdb.models['Model-1'].Part(dimensionality=THREE_D,
name='ThreadedShaft', type=
    DEFORMABLE_BODY)
mdb.models['Model-1'].parts['ThreadedShaft'].BaseSolidRevolve(angle=36
0.0,
    flipRevolveDirection=OFF, sketch=
    mdb.models['Model-1'].sketches['__profile__'])
del mdb.models['Model-1'].sketches['__profile__']

# Create a cutted helix from cylinder
# mdb.models['Model-1'].ConstrainedSketch(name='__profile__',
sheetSize=200.0)
#
mdb.models['Model-1'].sketches['__profile__'].CircleByCenterPerimeter(
center=(
    # 0.0, 0.0), point1=(d_outer/2, 0.0))
# mdb.models['Model-1'].Part(dimensionality=THREE_D,
name='ThreadedShaft', type=
    # DEFORMABLE_BODY)
#
mdb.models['Model-1'].parts['ThreadedShaft'].BaseSolidExtrude(depth=l_
thread,
    # sketch=mdb.models['Model-1'].sketches['__profile__'])
# del mdb.models['Model-1'].sketches['__profile__']

# Generate axis and datums for sketches
datum_core_XZ=mdb.models['Model-1'].parts['ThreadedShaft'].DatumPlaneB
yPrincipalPlane(offset=
    0.0, principalPlane=XZPLANE)
datum_core_YZ=mdb.models['Model-1'].parts['ThreadedShaft'].DatumPlaneB
yPrincipalPlane(offset=
    0.0, principalPlane=YZPLANE)
datum_core_XY=mdb.models['Model-1'].parts['ThreadedShaft'].DatumPlaneB
yPrincipalPlane(offset=
    0.0, principalPlane=XYPLANE)


x_axis=mdb.models['Model-1'].parts['ThreadedShaft'].DatumAxisByPrincip
alAxis(
    principalAxis=XAXIS)
y_axis=mdb.models['Model-1'].parts['ThreadedShaft'].DatumAxisByPrincip
alAxis(
    principalAxis=YAXIS)
z_axis=mdb.models['Model-1'].parts['ThreadedShaft'].DatumAxisByPrincip
alAxis(
    principalAxis=ZAXIS)

# Extrude thread valley
```

```
A = (d_outer-d_inner)/2*tan30                    # Height of inclined
part of thread
B = (p-2*A)/3                                    # Height of outer
part of thread (P/8 in ISO68)
C = 2*B                                          # Height of inner
part of thread  (P/4 in ISO68)

# Denne delen lager en vanlig utskjæring, som skjærer ut gjenger
over hele l_unthread
mdb.models['Model-1'].ConstrainedSketch(gridSpacing=2.72,
name='__profile__',
    sheetSize=109.02, transform=
    mdb.models['Model-1'].parts['ThreadedShaft'].MakeSketchTransform(

    sketchPlane=mdb.models['Model-1'].parts['ThreadedShaft'].datums[da
    tum_core_XY.id],
    sketchPlaneSide=SIDE1,

    sketchUpEdge=mdb.models['Model-1'].parts['ThreadedShaft'].datums[y
    _axis.id],
    sketchOrientation=RIGHT, origin=(0.0, 0.0, 0.0)))
mdb.models['Model-1'].parts['ThreadedShaft'].projectReferencesOntoSket
ch(
    filter=COPLANAR_EDGES, sketch=
    mdb.models['Model-1'].sketches['__profile__'])
mdb.models['Model-1'].sketches['__profile__'].Line(point1=(d_outer/2,
    A), point2=(d_inner/2, 0.0))
mdb.models['Model-1'].sketches['__profile__'].Line(point1=(d_inner/2,
    0.0), point2=(d_inner/2, -C))
mdb.models['Model-1'].sketches['__profile__'].Line(point1=(d_inner/2,
    -C), point2=(d_outer/2, -A-C))
mdb.models['Model-1'].sketches['__profile__'].Line(point1=(d_outer/2,
    -A-C), point2=(d_outer/2, -A-B-C))
mdb.models['Model-1'].sketches['__profile__'].Line(point1=(d_outer/2,
    -A-B-C), point2=(d_outer/2+eps, -A-B-C))
mdb.models['Model-1'].sketches['__profile__'].Line(point1=(d_outer/2+e
ps,
    -A-B-C), point2=(d_outer/2+eps, A))
mdb.models['Model-1'].sketches['__profile__'].Line(point1=(d_outer/2+e
ps,
    A), point2=(d_outer/2, A))
mdb.models['Model-1'].parts['ThreadedShaft'].CutRevolve(angle=(l_threa
d/p+2)*360.0,          # Endre vinkel på rotasjon her
    flipPitchDirection=ON, flipRevolveDirection=OFF,
    moveSketchNormalToPath=OFF
    , pitch=2.0,
    sketch=mdb.models['Model-1'].sketches['__profile__'],
    sketchOrientation=RIGHT, sketchPlane=

    mdb.models['Model-1'].parts['ThreadedShaft'].datums[datum_core_XY.
    id], sketchPlaneSide=
    SIDE1,
    sketchUpEdge=mdb.models['Model-1'].parts['ThreadedShaft'].datums[y
    _axis.id])
del mdb.models['Model-1'].sketches['__profile__']

# Utskjæring som lager en smooth overgang
mdb.models['Model-1'].ConstrainedSketch(gridSpacing=4.27,
name='__profile__',
    sheetSize=170.87, transform=
    mdb.models['Model-1'].parts['ThreadedShaft'].MakeSketchTransform(

    sketchPlane=mdb.models['Model-1'].parts['ThreadedShaft'].datums[da
    tum_core_XY.id],
    sketchPlaneSide=SIDE1,

    sketchUpEdge=mdb.models['Model-1'].parts['ThreadedShaft'].datums[y
    _axis.id],
    sketchOrientation=RIGHT, origin=(0.0, 0.0, 0.0)))
mdb.models['Model-1'].parts['ThreadedShaft'].projectReferencesOntoSket
ch(
    filter=COPLANAR_EDGES, sketch=
```

```
    mdb.models['Model-1'].sketches['__profile__'])
mdb.models['Model-1'].sketches['__profile__'].Line(point1=(d_inner/2,
0.0),
    point2=(d_outer/2, A))
mdb.models['Model-1'].sketches['__profile__'].Line(point1=(d_outer/2,
A), point2=(d_outer/2, 0.0))
mdb.models['Model-1'].sketches['__profile__'].Line(point1=(d_outer/2,
0.0), point2=(d_inner/2, 0.0))
mdb.models['Model-1'].parts['ThreadedShaft'].CutRevolve(angle=360.0,
    flipRevolveDirection=OFF, sketch=
    mdb.models['Model-1'].sketches['__profile__'],
    sketchOrientation=RIGHT,

    sketchPlane=mdb.models['Model-1'].parts['ThreadedShaft'].datums[da
    tum_core_XY.id],
    sketchPlaneSide=SIDE1, sketchUpEdge=
    mdb.models['Model-1'].parts['ThreadedShaft'].datums[y_axis.id])
del mdb.models['Model-1'].sketches['__profile__']

############
### Nut ###
############
# Make a circle
mdb.models['Model-1'].ConstrainedSketch(name='__profile__',
sheetSize=200.0)
mdb.models['Model-1'].sketches['__profile__'].CircleByCenterPerimeter(
center=(
    0.0, 0.0), point1=(0.0, e/2))
mdb.models['Model-1'].sketches['__profile__'].CircleByCenterPerimeter(
center=(
    0.0, 0.0), point1=(0.0, d_outer_nut/2))
mdb.models['Model-1'].Part(dimensionality=THREE_D, name='Nut', type=
    DEFORMABLE_BODY)
mdb.models['Model-1'].parts['Nut'].BaseSolidExtrude(depth=h_nut,
sketch=
    mdb.models['Model-1'].sketches['__profile__'])
del mdb.models['Model-1'].sketches['__profile__']

# Generate axis and datums for sketches
datum_nut_XZ=mdb.models['Model-1'].parts['Nut'].DatumPlaneByPrincipalP
lane(offset=
    0.0, principalPlane=XZPLANE)
datum_nut_YZ=mdb.models['Model-1'].parts['Nut'].DatumPlaneByPrincipalP
lane(offset=
    0.0, principalPlane=YZPLANE)

y_axis_nut=mdb.models['Model-1'].parts['Nut'].DatumAxisByPrincipalAxis
(
    principalAxis=YAXIS)
z_axis_nut=mdb.models['Model-1'].parts['Nut'].DatumAxisByPrincipalAxis
(
    principalAxis=ZAXIS)

# MAKE PARTITION: separate threads from outer part of nut for better
mesh
mdb.models['Model-1'].ConstrainedSketch(gridSpacing=1.85,
name='__profile__',
    sheetSize=74.13, transform=
    mdb.models['Model-1'].parts['Nut'].MakeSketchTransform(
    sketchPlane=mdb.models['Model-1'].parts['Nut'].faces.findAt((0.0,
    d_chamfer_nut/2+eps, 0.0), ), sketchPlaneSide=SIDE1,

    sketchUpEdge=mdb.models['Model-1'].parts['Nut'].edges.findAt((e/2,
     0.0,
    0.0), ), sketchOrientation=RIGHT, origin=(0.0, 0.0, 0.0)))
mdb.models['Model-1'].parts['Nut'].projectReferencesOntoSketch(filter=
    COPLANAR_EDGES,
    sketch=mdb.models['Model-1'].sketches['__profile__'])
mdb.models['Model-1'].sketches['__profile__'].CircleByCenterPerimeter(
center=(
    0.0, 0.0), point1=(0.0, d_chamfer_nut/2+3*mesh_thread_nut))
mdb.models['Model-1'].parts['Nut'].PartitionFaceBySketch(faces=
```

```
    mdb.models['Model-1'].parts['Nut'].faces.findAt(((0.0,d_chamfer_nu
    t/2+3*mesh_thread_nut,
    0.0), )), sketch=mdb.models['Model-1'].sketches['__profile__'],

    sketchUpEdge=mdb.models['Model-1'].parts['Nut'].edges.findAt((e/2,
     0.0, 0.0), ))
del mdb.models['Model-1'].sketches['__profile__']
mdb.models['Model-1'].parts['Nut'].PartitionCellByExtrudeEdge(cells=

    mdb.models['Model-1'].parts['Nut'].cells.findAt(((d_chamfer_nut/2+
    3*mesh_thread_nut +eps, 0.0, 0.0),
    )),
    edges=(mdb.models['Model-1'].parts['Nut'].edges.findAt((d_chamfer_
    nut/2+3*mesh_thread_nut, 0.0,
    0.0), ), ),
    line=mdb.models['Model-1'].parts['Nut'].datums[z_axis_nut.id],
    sense=
    FORWARD)

# Make threads
Anut = (d_inner_nut-d_outer_nut)/2*tan30                #Height of
inclined part of thread
Bnut = (p-2*Anut)/3                                     #Height of
outer part of thread (P/8 in ISO68)
Cnut = 2*Bnut                                           #Height of
inner part of thread  (P/4 in ISO68)

mdb.models['Model-1'].ConstrainedSketch(gridSpacing=2.3,
name='__profile__',
    sheetSize=92.33, transform=
    mdb.models['Model-1'].parts['Nut'].MakeSketchTransform(

    sketchPlane=mdb.models['Model-1'].parts['Nut'].datums[datum_nut_XZ
    .id],
    sketchPlaneSide=SIDE1,

    sketchUpEdge=mdb.models['Model-1'].parts['Nut'].datums[z_axis_nut.
    id],
    sketchOrientation=RIGHT, origin=(0.0, 0.0, 0.0)))
mdb.models['Model-1'].parts['Nut'].projectReferencesOntoSketch(filter=
    COPLANAR_EDGES,
    sketch=mdb.models['Model-1'].sketches['__profile__'])

# Constant for moving up cut: Makes better mesh, no infinite
elements that causes error
HeightNoErrorNut = 2*Anut+Bnut+Cnut # Ta bort +Cnut if SB-bolt

# Denne delen gir vanlig utskjæring av gjenger
mdb.models['Model-1'].sketches['__profile__'].Line(point1=(d_outer_nut
/2, Cnut+HeightNoErrorNut),
    point2=(d_outer_nut/2, 0.0+HeightNoErrorNut))
mdb.models['Model-1'].sketches['__profile__'].Line(point1=(d_outer_nut
/2, 0.0+HeightNoErrorNut),
    point2=(d_inner_nut/2, -Anut+HeightNoErrorNut))
mdb.models['Model-1'].sketches['__profile__'].Line(point1=(d_inner_nut
/2,
    -Anut+HeightNoErrorNut), point2=(d_inner_nut/2,
    -Anut-Bnut+HeightNoErrorNut))
mdb.models['Model-1'].sketches['__profile__'].Line(point1=(d_inner_nut
/2, -Anut-Bnut+HeightNoErrorNut),
    point2=(d_outer_nut/2,-2*Anut-Bnut+HeightNoErrorNut))
mdb.models['Model-1'].sketches['__profile__'].Line(point1=(d_outer_nut
/2, -2*Anut-Bnut+HeightNoErrorNut),
    point2=(d_outer_nut/2-eps, -2*Anut-Bnut+HeightNoErrorNut))
mdb.models['Model-1'].sketches['__profile__'].Line(point1=(d_outer_nut
/2-eps, -2*Anut-Bnut+HeightNoErrorNut),
    point2=(d_outer_nut/2, Cnut+HeightNoErrorNut))
mdb.models['Model-1'].parts['Nut'].CutRevolve(angle=360.0*(h_nut/p)-(4
60), flipPitchDirection=           # Endre vinkelen på rotasjon her
(+90 gir liten kutt)
    ON, flipRevolveDirection=OFF, moveSketchNormalToPath=OFF,
```

```
    pitch=2.0, sketch=
    mdb.models['Model-1'].sketches['__profile__'],
    sketchOrientation=RIGHT,

    sketchPlane=mdb.models['Model-1'].parts['Nut'].datums[datum_core_X
    Z.id], sketchPlaneSide=
    SIDE1,
    sketchUpEdge=mdb.models['Model-1'].parts['Nut'].datums[z_axis_nut.
    id])
del mdb.models['Model-1'].sketches['__profile__']

# Make chamfer
mdb.models['Model-1'].ConstrainedSketch(gridSpacing=2.34,
name='__profile__',
    sheetSize=93.72, transform=
    mdb.models['Model-1'].parts['Nut'].MakeSketchTransform(

    sketchPlane=mdb.models['Model-1'].parts['Nut'].datums[datum_nut_XZ
    .id],
    sketchPlaneSide=SIDE1,

    sketchUpEdge=mdb.models['Model-1'].parts['Nut'].datums[z_axis_nut.
    id],
    sketchOrientation=RIGHT, origin=(0.0, 0.0, 0.0)))
mdb.models['Model-1'].parts['Nut'].projectReferencesOntoSketch(filter=
    COPLANAR_EDGES,
    sketch=mdb.models['Model-1'].sketches['__profile__'])

diamCut = d_chamfer_nut/2-d_outer_nut/2
tan50 = tan(0.872665)
tan70 = tan(1.2217)

mdb.models['Model-1'].sketches['__profile__'].Line(point1=(d_chamfer_n
ut/2, h_nut), point2=
    (d_chamfer_nut/2-diamCut/2, h_nut-tan50*(diamCut/2)))
mdb.models['Model-1'].sketches['__profile__'].Line(point1=(d_chamfer_n
ut/2-diamCut/2, h_nut-tan50*(diamCut/2)), point2=
    (d_chamfer_nut/2-diamCut,
    h_nut-tan50*(diamCut/2)-tan70*(diamCut/2)))
mdb.models['Model-1'].sketches['__profile__'].Line(point1=(d_chamfer_n
ut/2-diamCut, h_nut-tan50*(diamCut/2)-tan70*(diamCut/2)), point2=
    (d_chamfer_nut/2-diamCut, h_nut))
mdb.models['Model-1'].sketches['__profile__'].Line(point1=(d_chamfer_n
ut/2-diamCut, h_nut), point2=
    (d_chamfer_nut/2, h_nut))
mdb.models['Model-1'].sketches['__profile__'].sketchOptions.setValues(
    constructionGeometry=ON)
mdb.models['Model-1'].sketches['__profile__'].assignCenterline(line=

    mdb.models['Model-1'].sketches['__profile__'].geometry.findAt((0.0
    ,
    h_nut/2), ))
mdb.models['Model-1'].parts['Nut'].CutRevolve(angle=360.0,
    flipRevolveDirection=OFF, sketch=
    mdb.models['Model-1'].sketches['__profile__'],
    sketchOrientation=RIGHT,

    sketchPlane=mdb.models['Model-1'].parts['Nut'].datums[datum_nut_XZ
    .id], sketchPlaneSide=
    SIDE1,
    sketchUpEdge=mdb.models['Model-1'].parts['Nut'].datums[z_axis_nut.
    id])
del mdb.models['Model-1'].sketches['__profile__']

mdb.models['Model-1'].ConstrainedSketch(gridSpacing=2.34,
name='__profile__',
    sheetSize=93.72, transform=
    mdb.models['Model-1'].parts['Nut'].MakeSketchTransform(

    sketchPlane=mdb.models['Model-1'].parts['Nut'].datums[datum_nut_XZ
    .id],
    sketchPlaneSide=SIDE1,
```

```
    sketchUpEdge=mdb.models['Model-1'].parts['Nut'].datums[z_axis_nut.
    id],
    sketchOrientation=RIGHT, origin=(0.0, 0.0, 0.0)))
mdb.models['Model-1'].parts['Nut'].projectReferencesOntoSketch(filter=
    COPLANAR_EDGES,
    sketch=mdb.models['Model-1'].sketches['__profile__'])
mdb.models['Model-1'].sketches['__profile__'].Line(point1=(d_chamfer_n
ut/2, 0.0), point2=
    (d_chamfer_nut/2-diamCut/2, tan50*(diamCut/2)))
mdb.models['Model-1'].sketches['__profile__'].Line(point1=(d_chamfer_n
ut/2-diamCut/2, tan50*(diamCut/2)), point2=
    (d_chamfer_nut/2-diamCut, tan50*(diamCut/2)+tan70*(diamCut/2)))
mdb.models['Model-1'].sketches['__profile__'].Line(point1=(d_chamfer_n
ut/2-diamCut, tan50*(diamCut/2)+tan70*(diamCut/2)), point2=
    (d_chamfer_nut/2-diamCut, 0.0))
mdb.models['Model-1'].sketches['__profile__'].Line(point1=(d_chamfer_n
ut/2-diamCut, 0.0), point2=
    (d_chamfer_nut/2, 0.0))
mdb.models['Model-1'].sketches['__profile__'].sketchOptions.setValues(
    constructionGeometry=ON)
mdb.models['Model-1'].sketches['__profile__'].assignCenterline(line=

    mdb.models['Model-1'].sketches['__profile__'].geometry.findAt((0.0
    ,
    h_nut/2), ))
mdb.models['Model-1'].parts['Nut'].CutRevolve(angle=360.0,
    flipRevolveDirection=OFF, sketch=
    mdb.models['Model-1'].sketches['__profile__'],
    sketchOrientation=RIGHT,

    sketchPlane=mdb.models['Model-1'].parts['Nut'].datums[datum_nut_XZ
    .id], sketchPlaneSide=
    SIDE1,
    sketchUpEdge=mdb.models['Model-1'].parts['Nut'].datums[z_axis_nut.
    id])
del mdb.models['Model-1'].sketches['__profile__']

# Make hexagonal shape
mdb.models['Model-1'].ConstrainedSketch(gridSpacing=1.99,
name='__profile__',
    sheetSize=79.6, transform=
    mdb.models['Model-1'].parts['Nut'].MakeSketchTransform(

    sketchPlane=mdb.models['Model-1'].parts['Nut'].faces.findAt((d_cha
    mfer_nut/2+eps,
    0.0, 0.0), ), sketchPlaneSide=SIDE1,

    sketchUpEdge=mdb.models['Model-1'].parts['Nut'].edges.findAt((d_ch
    amfer_nut/2, 0.0,
    0.0), ), sketchOrientation=RIGHT, origin=(0.0, 0.0, 0.0)))
mdb.models['Model-1'].parts['Nut'].projectReferencesOntoSketch(filter=
    COPLANAR_EDGES,
    sketch=mdb.models['Model-1'].sketches['__profile__'])
mdb.models['Model-1'].sketches['__profile__'].Line(point1=(0.0, e/2),
    point2=(-e/2*cos30, e/4))
mdb.models['Model-1'].sketches['__profile__'].Line(point1=(-e/2*cos30,

    e/4), point2=(-e/2*cos30, -e/4))
mdb.models['Model-1'].sketches['__profile__'].Line(point1=(-e/2*cos30,

    -e/4), point2=(0.0, -e/2))
mdb.models['Model-1'].sketches['__profile__'].Line(point1=(0.0,
    -e/2), point2=(e/2*cos30, -e/4))
mdb.models['Model-1'].sketches['__profile__'].Line(point1=(e/2*cos30,
    -e/4), point2=(e/2*cos30, e/4))
mdb.models['Model-1'].sketches['__profile__'].Line(point1=(e/2*cos30,
    e/4), point2=(0.0, e/2))
mdb.models['Model-1'].sketches['__profile__'].rectangle(point1=(-50.0,

    50.0), point2=(50.0, -50.0))
mdb.models['Model-1'].parts['Nut'].CutExtrude(flipExtrudeDirection=OFF
```

```
, sketch=
    mdb.models['Model-1'].sketches['__profile__'],
    sketchOrientation=RIGHT,

    sketchPlane=mdb.models['Model-1'].parts['Nut'].faces.findAt((d_cha
    mfer_nut/2+eps,
    0.0, 0.0), ), sketchPlaneSide=SIDE1, sketchUpEdge=

    mdb.models['Model-1'].parts['Nut'].edges.findAt((d_chamfer_nut/2,
    0.0, 0.0), ))
del mdb.models['Model-1'].sketches['__profile__']

###################
### Grip plate ###
###################
mdb.models['Model-1'].ConstrainedSketch(name='__profile__',
sheetSize=200.0)
mdb.models['Model-1'].sketches['__profile__'].CircleByCenterPerimeter(
    center=(0.0, 0.0), point1=(0.0, d_ext_grip/2))
mdb.models['Model-1'].sketches['__profile__'].CircleByCenterPerimeter(
    center=(0.0, 0.0), point1=(0.0, d_int_grip/2))
mdb.models['Model-1'].Part(dimensionality=THREE_D, name='GripPlate',
type=
    DEFORMABLE_BODY)
mdb.models['Model-1'].parts['GripPlate'].BaseSolidExtrude(depth=h_grip
,
    sketch=mdb.models['Model-1'].sketches['__profile__'])
del mdb.models['Model-1'].sketches['__profile__']

#################################################################
########################## Partition ############################
#################################################################

# Merk at noen partisjoner er laget under "parts". Dette er merket
med MAKE PARTITION

#############
### Bolt ###
#############

# Underside of bolt head (for contact whith grip plate and tie
control)
x_axis_head=mdb.models['Model-1'].parts['Head'].DatumAxisByPrincipalAx
is(
    principalAxis=XAXIS)

mdb.models['Model-1'].ConstrainedSketch(gridSpacing=1.12,
name='__profile__',
    sheetSize=44.82, transform=
    mdb.models['Model-1'].parts['Head'].MakeSketchTransform(
    sketchPlane=mdb.models['Model-1'].parts['Head'].faces.findAt((
    0.0, 0.0, 0.0), ), sketchPlaneSide=SIDE1,

    sketchUpEdge=mdb.models['Model-1'].parts['Head'].datums[x_axis_hea
    d.id],
    sketchOrientation=RIGHT, origin=(0.0, 0.0, 0.0)))
mdb.models['Model-1'].parts['Head'].projectReferencesOntoSketch(
    filter=COPLANAR_EDGES, sketch=
    mdb.models['Model-1'].sketches['__profile__'])
mdb.models['Model-1'].sketches['__profile__'].CircleByCenterPerimeter(
center=(
    0.0, 0.0), point1=(0.0,d_int_grip/2))
mdb.models['Model-1'].parts['Head'].PartitionFaceBySketch(faces=

    mdb.models['Model-1'].parts['Head'].faces.findAt(((d_int_grip/2-ep
    s,
    0.0, 0.0), )),
    sketch=mdb.models['Model-1'].sketches['__profile__'],

    sketchUpEdge=mdb.models['Model-1'].parts['Head'].datums[x_axis_hea
    d.id])
```

```
mdb.models['Model-1'].ConstrainedSketch(gridSpacing=1.12,
name='__profile__',
    sheetSize=44.82, transform=
    mdb.models['Model-1'].parts['Head'].MakeSketchTransform(
    sketchPlane=mdb.models['Model-1'].parts['Head'].faces.findAt((
    0.0, 0.0, 0.0), ), sketchPlaneSide=SIDE1,

    sketchUpEdge=mdb.models['Model-1'].parts['Head'].datums[x_axis_hea
    d.id],
    sketchOrientation=RIGHT, origin=(0.0, 0.0, 0.0)))
mdb.models['Model-1'].parts['Head'].projectReferencesOntoSketch(
    filter=COPLANAR_EDGES, sketch=
    mdb.models['Model-1'].sketches['__profile__'])
mdb.models['Model-1'].sketches['__profile__'].CircleByCenterPerimeter(
center=(
    0.0, 0.0), point1=(0.0,d_unthread/2))
mdb.models['Model-1'].parts['Head'].PartitionFaceBySketch(faces=

    mdb.models['Model-1'].parts['Head'].faces.findAt(((d_unthread/2-ep
    s,
    0.0, 0.0), )),
    sketch=mdb.models['Model-1'].sketches['__profile__'],

    sketchUpEdge=mdb.models['Model-1'].parts['Head'].datums[x_axis_hea
    d.id])

############
### Nut ###
############
mdb.models['Model-1'].parts['Nut'].PartitionCellByDatumPlane(cells=

    mdb.models['Model-1'].parts['Nut'].cells.getByBoundingBox(-1000.0,
    -1000.0,-1000.0,1000.0,1000.0,1000.0), datumPlane=
    mdb.models['Model-1'].parts['Nut'].datums[datum_nut_XZ.id])
mdb.models['Model-1'].parts['Nut'].PartitionCellByDatumPlane(cells=

    mdb.models['Model-1'].parts['Nut'].cells.getByBoundingBox(-1000.0,
    -1000.0,-1000.0,1000.0,1000.0,1000.0), datumPlane=
    mdb.models['Model-1'].parts['Nut'].datums[datum_nut_YZ.id])

##################
### Grip plate ###
##################
# Generate axis and datums for sketches
z_axis_grip=mdb.models['Model-1'].parts['GripPlate'].DatumAxisByPrinci
palAxis(
    principalAxis=ZAXIS)
y_axis_grip=mdb.models['Model-1'].parts['GripPlate'].DatumAxisByPrinci
palAxis(
    principalAxis=YAXIS)

# Make circular hole for nut contact
mdb.models['Model-1'].ConstrainedSketch(gridSpacing=1.12,
name='__profile__',
    sheetSize=44.82, transform=
    mdb.models['Model-1'].parts['GripPlate'].MakeSketchTransform(

    sketchPlane=mdb.models['Model-1'].parts['GripPlate'].faces.findAt(
    (
    d_ext_grip/2-eps, 0.0, 0.0), ), sketchPlaneSide=SIDE1,

    sketchUpEdge=mdb.models['Model-1'].parts['GripPlate'].datums[y_axi
    s_grip.id],
    sketchOrientation=RIGHT, origin=(0.0, 0.0, 0.0)))
mdb.models['Model-1'].parts['GripPlate'].projectReferencesOntoSketch(
    filter=COPLANAR_EDGES, sketch=
    mdb.models['Model-1'].sketches['__profile__'])
mdb.models['Model-1'].sketches['__profile__'].CircleByCenterPerimeter(
center=(
    0.0, 0.0), point1=(0.0, max(w_corners/2,e/2)))
mdb.models['Model-1'].parts['GripPlate'].PartitionFaceBySketch(faces=
```

```
    mdb.models['Model-1'].parts['GripPlate'].faces.findAt(((d_ext_grip
    /2-eps,
    0.0, 0.0), )),
    sketch=mdb.models['Model-1'].sketches['__profile__'],

    sketchUpEdge=mdb.models['Model-1'].parts['GripPlate'].datums[y_axi
    s_grip.id])
mdb.models['Model-1'].parts['GripPlate'].PartitionCellByExtrudeEdge(ce
lls=

    mdb.models['Model-1'].parts['GripPlate'].cells.findAt(((d_int_grip
    /2+eps,
    0.0, 0.0), )), edges=(

    mdb.models['Model-1'].parts['GripPlate'].edges.findAt((max(w_corne
    rs/2,e/2), 0.0, 0.0),
    ), ),
    line=mdb.models['Model-1'].parts['GripPlate'].datums[z_axis_grip.i
    d], sense=
    FORWARD)

##################################################################
########################## Material ##############################
##################################################################
# Material ikke redusert for HV
mdb.models['Model-1'].Material(name='SteelTest')
mdb.models['Model-1'].materials['SteelTest'].Density(table=((7.8e-09,
), ))
mdb.models['Model-1'].materials['SteelTest'].Elastic(table=((210000.0,
 0.3), ))

# Material for mutter om redusert materialegeskaper basert på HV
mdb.models['Model-1'].Material(name='SteelTestReducedHV')
mdb.models['Model-1'].materials['SteelTestReducedHV'].Density(table=((
7.85e-09, ), ))
mdb.models['Model-1'].materials['SteelTestReducedHV'].Elastic(table=((
210000.0, 0.3), ))

##################################################################
######################### Create Sections ########################
##################################################################
# Generate sections (Use this if nut material is NOT reduced)
#
mdb.models['Model-1'].HomogeneousSolidSection(material='SteelTest',
name=
    # 'BoltThreadSection', thickness=None)
#
mdb.models['Model-1'].HomogeneousSolidSection(material='SteelTest',
name=
    # 'BoltSection', thickness=None)
#
mdb.models['Model-1'].HomogeneousSolidSection(material='SteelTest',
name=
    # 'NutSection', thickness=None)
#
mdb.models['Model-1'].HomogeneousSolidSection(material='SteelTest',
name=
    # 'GripPlateSection', thickness=None)

# Generate sections (Use this if nut material is reduced)
mdb.models['Model-1'].HomogeneousSolidSection(material='SteelTest',
name=
    'BoltThreadSection', thickness=None)
mdb.models['Model-1'].HomogeneousSolidSection(material='SteelTest',
name=
    'BoltSection', thickness=None)
mdb.models['Model-1'].HomogeneousSolidSection(material='SteelTestReduc
edHV', name=
    'NutSection', thickness=None)
mdb.models['Model-1'].HomogeneousSolidSection(material='SteelTest',
name=
    'GripPlateSection', thickness=None)
```

```
############
### Bolt ###
############
# Bolt head
mdb.models['Model-1'].parts['Head'].SectionAssignment(offset=0.0,
    offsetField='', offsetType=MIDDLE_SURFACE, region=Region(

    cells=mdb.models['Model-1'].parts['Head'].cells),sectionName='Bolt
    Section'
    , thicknessAssignment=FROM_SECTION)

# Bolt shank
mdb.models['Model-1'].parts['Shank'].SectionAssignment(offset=0.0,
    offsetField='', offsetType=MIDDLE_SURFACE, region=Region(

    cells=mdb.models['Model-1'].parts['Shank'].cells),sectionName='Bol
    tSection'
    , thicknessAssignment=FROM_SECTION)

# Threaded part
mdb.models['Model-1'].parts['ThreadedShaft'].SectionAssignment(offset=
0.0,
    offsetField='', offsetType=MIDDLE_SURFACE, region=Region(

    cells=mdb.models['Model-1'].parts['ThreadedShaft'].cells),sectionN
    ame='BoltThreadSection'
    , thicknessAssignment=FROM_SECTION)

############
### Nut ###
############
mdb.models['Model-1'].parts['Nut'].SectionAssignment(offset=0.0,
    offsetField='', offsetType=MIDDLE_SURFACE, region=Region(

    cells=mdb.models['Model-1'].parts['Nut'].cells),sectionName='NutSe
    ction', thicknessAssignment=FROM_SECTION)

###################
### Grip Plate ###
###################
mdb.models['Model-1'].parts['GripPlate'].SectionAssignment(offset=0.0,

    offsetField='', offsetType=MIDDLE_SURFACE, region=Region(

    cells=mdb.models['Model-1'].parts['GripPlate'].cells),sectionName=
    'GripPlateSection'
    , thicknessAssignment=FROM_SECTION)

#########################################################################
######################## Create surfaces ########################
#########################################################################

############
### Bolt ###
############
# Underside of bolt head
mdb.models['Model-1'].parts['Head'].Surface(name='BoltUnderHeadSurface
', side1Faces=

    mdb.models['Model-1'].parts['Head'].faces.findAt(((d_int_grip/2+ep
    s, 0.0, 0.0), )))

############
### Nut ###
############
# Bottom surface against grip plate
mdb.models['Model-1'].parts['Nut'].Surface(name='NutUnderContactSurfac
e', side1Faces=

    mdb.models['Model-1'].parts['Nut'].faces.findAt(((d_chamfer_nut/2+
    eps, eps,
```

```
    0.0), ), ((d_chamfer_nut/2+eps, -eps, 0.0), ),
    ((-d_chamfer_nut/2-eps, eps,
    0.0), ), ((-d_chamfer_nut/2-eps, -eps, 0.0), ),
    ((d_chamfer_nut/2+3*mesh_thread_nut+eps, -eps, 0.0), ),
    ((d_chamfer_nut/2+3*mesh_thread_nut+eps, +eps, 0.0), ),
    ((-d_chamfer_nut/2-3*mesh_thread_nut-eps, -eps, 0.0), ),
    ((-d_chamfer_nut/2-3*mesh_thread_nut-eps, eps, 0.0), ), ),)

##################
### Grip Plate ###
##################
# Surface against bolt head and nut
mdb.models['Model-1'].parts['GripPlate'].Surface(name='GripUnderContac
tSurface', side1Faces=

    mdb.models['Model-1'].parts['GripPlate'].faces.findAt(((max(w_corn
    ers/2,e/2)-eps, 0.0, 0.0), )))

#########################################################################
########################## Create sets ##################################
#########################################################################
# Creating set for fixed grip (BC)
mdb.models['Model-1'].parts['GripPlate'].Set(faces=

    mdb.models['Model-1'].parts['GripPlate'].faces.findAt(((d_ext_grip
    /2-eps,
    eps, h_grip), ), ((d_ext_grip/2-eps, -eps, h_grip), ),
    ((-d_ext_grip/2+eps,
    -eps, h_grip), ), ((-d_ext_grip/2+eps, eps, h_grip), ), ), name=
    'FixedGripSet')

# Creating set for moving grip (BC)
mdb.models['Model-1'].parts['GripPlate'].Set(faces=

    mdb.models['Model-1'].parts['GripPlate'].faces.findAt(((d_ext_grip
    /2-eps,
    eps, h_grip), ), ((d_ext_grip/2-eps, -eps, h_grip), ),
    ((-d_ext_grip/2+eps,
    -eps, h_grip), ), ((-d_ext_grip/2+eps, eps, h_grip), ), ), name=
    'MovingGripSet')

#########################################################################
########################## Assembly #####################################
#########################################################################
mdb.models['Model-1'].rootAssembly.DatumCsysByDefault(CARTESIAN)

# Include and position shaft
mdb.models['Model-1'].rootAssembly.Instance(dependent=ON,
name='Shank-1', part=
    mdb.models['Model-1'].parts['Shank'])

# Include and position threaded shaft
mdb.models['Model-1'].rootAssembly.Instance(dependent=ON, name=
    'ThreadedShaft-1',
    part=mdb.models['Model-1'].parts['ThreadedShaft'])
mdb.models['Model-1'].rootAssembly.translate(instanceList=('ThreadedSh
aft-1', )
    , vector=(0.0, l_unthread, 0.0))

# Include and position bolt head
mdb.models['Model-1'].rootAssembly.Instance(dependent=ON,
name='Head-1', part=
    mdb.models['Model-1'].parts['Head'])
mdb.models['Model-1'].rootAssembly.rotate(angle=-90.0,
axisDirection=(-1.0, 0.0,
    0.0), axisPoint=(1.0, 0.0, 0.0), instanceList=('Head-1', ))

nutPos = -0.3 # Moving the nut and grip place in place (tighten up)

# Include and position nut
mdb.models['Model-1'].rootAssembly.Instance(dependent=ON,
name='Nut-1', part=
```

```
    mdb.models['Model-1'].parts['Nut'])
mdb.models['Model-1'].rootAssembly.rotate(angle=90.0,
axisDirection=(-1.0, 0.0,
    0.0), axisPoint=(1.0, 0.0, 0.0), instanceList=('Nut-1', ))
mdb.models['Model-1'].rootAssembly.translate(instanceList=('Nut-1',
), vector=(
    0.0, l_unthread+(n_free_nut)*p-p/2+nutPos, 0.0))
    #########-->Position the nut here (last numer for finer movement)

# Include and position lower grip (Grip to nut)
mdb.models['Model-1'].rootAssembly.Instance(dependent=ON,
name='GripPlate-1',
    part=mdb.models['Model-1'].parts['GripPlate'])
mdb.models['Model-1'].rootAssembly.rotate(angle=-90.0,
axisDirection=(-1.0, 0.0,
    0.0), axisPoint=(1.0, 0.0, 0.0), instanceList=('GripPlate-1', ))
mdb.models['Model-1'].rootAssembly.translate(instanceList=('GripPlate-
1', )
    , vector=(0.0, l_unthread+(n_free_nut)*p-p/2-eps+nutPos, 0.0))
    ###########-->Position the lower grip here

# Include and position upper grip (Grip to bolt head)
mdb.models['Model-1'].rootAssembly.Instance(dependent=ON,
name='GripPlate-2',
    part=mdb.models['Model-1'].parts['GripPlate'])
mdb.models['Model-1'].rootAssembly.rotate(angle=90.0,
axisDirection=(-1.0, 0.0,
    0.0), axisPoint=(1.0, 0.0, 0.0), instanceList=('GripPlate-2', ))
mdb.models['Model-1'].rootAssembly.translate(instanceList=('GripPlate-
2', )
    , vector=(0.0, eps, 0.0))          ################-->Position
    the upper grip here

##################################################################
############################## Step ##############################
##################################################################
mdb.models['Model-1'].ExplicitDynamicsStep(name='BomDisplacement',
previous=
    'Initial')
mdb.models['Model-1'].steps['BomDisplacement'].setValues(timePeriod=si
mulationTime)
mdb.models['Model-1'].steps['BomDisplacement'].setValues(massScaling=(
(
    SEMI_AUTOMATIC, MODEL, AT_BEGINNING, 0.0, targetTimeIncrement,
    BELOW_MIN, 0, 0, 0.0, 0.0,
    0, None), ))

##################################################################
############################ Contact #############################
##################################################################
# Contact PROPERTIES for steel to steel in threads
mdb.models['Model-1'].ContactProperty('SteelThreadProperty')
mdb.models['Model-1'].interactionProperties['SteelThreadProperty'].Tan
gentialBehavior(
    dependencies=0, directionality=ISOTROPIC,
    elasticSlipStiffness=None,
    formulation=PENALTY, fraction=0.005, maximumElasticSlip=FRACTION,
    pressureDependency=OFF, shearStressLimit=None,
    slipRateDependency=OFF,
    table=((fricThreads, ), ), temperatureDependency=OFF)
mdb.models['Model-1'].interactionProperties['SteelThreadProperty'].Nor
malBehavior(
    allowSeparation=ON, constraintEnforcementMethod=DEFAULT,
    pressureOverclosure=HARD)

# Contact PROPERTIES for steel to steel in grip
mdb.models['Model-1'].ContactProperty('SteelGripProperty')
mdb.models['Model-1'].interactionProperties['SteelGripProperty'].Tange
ntialBehavior(
    dependencies=0, directionality=ISOTROPIC,
    elasticSlipStiffness=None,
    formulation=PENALTY, fraction=0.005, maximumElasticSlip=FRACTION,
```

```
    pressureDependency=OFF, shearStressLimit=None,
    slipRateDependency=OFF,
    table=((fricGrip, ), ), temperatureDependency=OFF)
mdb.models['Model-1'].interactionProperties['SteelGripProperty'].Norma
lBehavior(
    allowSeparation=ON, constraintEnforcementMethod=DEFAULT,
    pressureOverclosure=HARD)

# INTERACTION: General contact (Special for thread to thread, grip
to nut and grip to head)
# mdb.models['Model-1'].ContactExp(createStepName='BomDisplacement',
name=
    # 'ThreadToThreadGeneralContact')
#
mdb.models['Model-1'].interactions['ThreadToThreadGeneralContact'].inc
ludedPairs.setValuesInStep(
    # addPairs=((
    #
    mdb.models['Model-1'].rootAssembly.instances['Nut-1'].surfaces['Nu
    tThreadSurface'],
    #
    mdb.models['Model-1'].rootAssembly.instances['ThreadedShaft-1'].su
    rfaces['BoltThreadSurface']),
    # (
    #
    mdb.models['Model-1'].rootAssembly.instances['GripPlate-1'].surfac
    es['GripUnderContactSurface'],
    #
    mdb.models['Model-1'].rootAssembly.instances['Nut-1'].surfaces['Nu
    tUnderContactSurface']),
    # (
    #
    mdb.models['Model-1'].rootAssembly.instances['GripPlate-2'].surfac
    es['GripUnderContactSurface'],
    #
    mdb.models['Model-1'].rootAssembly.instances['Head-1'].surfaces['B
    oltUnderHeadSurface']))
    # , stepName='BomDisplacement', useAllstar=OFF)
#
mdb.models['Model-1'].interactions['ThreadToThreadGeneralContact'].con
tactPropertyAssignments.appendInStep(
    # assignments=((GLOBAL, SELF, 'SteelThreadProperty'), (
    #
    mdb.models['Model-1'].rootAssembly.instances['ThreadedShaft-1'].su
    rfaces['BoltThreadSurface'],
    #
    mdb.models['Model-1'].rootAssembly.instances['Nut-1'].surfaces['Nu
    tThreadSurface'],
    # 'SteelThreadProperty'), (
    #
    mdb.models['Model-1'].rootAssembly.instances['GripPlate-1'].surfac
    es['GripUnderContactSurface'],
    #
    mdb.models['Model-1'].rootAssembly.instances['Nut-1'].surfaces['Nu
    tUnderContactSurface'],
    # 'SteelGripProperty'), (
    #
    mdb.models['Model-1'].rootAssembly.instances['GripPlate-2'].surfac
    es['GripUnderContactSurface'],
    #
    mdb.models['Model-1'].rootAssembly.instances['Head-1'].surfaces['B
    oltUnderHeadSurface'],
    # 'SteelGripProperty')), stepName='BomDisplacement')

# INTERACTION: General contact (NO special interaction between
surfaces, everything GENERAL)
mdb.models['Model-1'].ContactExp(createStepName='BomDisplacement',
name=
    'GeneralContact')
mdb.models['Model-1'].interactions['GeneralContact'].includedPairs.set
ValuesInStep(
    stepName='BomDisplacement', useAllstar=ON)
```

```
mdb.models['Model-1'].interactions['GeneralContact'].contactPropertyAs
signments.appendInStep(
    assignments=((GLOBAL, SELF, 'SteelThreadProperty'), ), stepName=
    'BomDisplacement')

##########################################################################
############################## BC ########################################
##########################################################################
# Make smooth step function at beginning of displacement
mdb.models['Model-1'].SmoothStepAmplitude(data=((0.0, 0.0),
(t_fullSpeed, 1.0)),
    name='SmoothStepStartDisplacement', timeSpan=STEP)

# Lower grip fixed
mdb.models['Model-1'].DisplacementBC(amplitude=UNSET, createStepName=
    'Initial', distributionType=UNIFORM, fieldName='', fixed=OFF,
    localCsys=
    None, name='FixedGripBC', region=

    mdb.models['Model-1'].rootAssembly.instances['GripPlate-1'].sets['
    FixedGripSet']
    , u1=0.0, u2=0.0, u3=0.0, ur1=0.0, ur2=0.0, ur3=0.0)

# Upper grip in motion
mdb.models['Model-1'].VelocityBC(amplitude='SmoothStepStartDisplacemen
t',
    createStepName='BomDisplacement', distributionType=UNIFORM,
    fieldName='',
    localCsys=None, name='MovingGripBC', region=

    mdb.models['Model-1'].rootAssembly.instances['GripPlate-2'].sets['
    MovingGripSet']
    , v1=0.0, v2=-bomVelocity, v3=0.0, vr1=0.0, vr2=0.0, vr3=0.0)

##########################################################################
############################## Mesh ######################################
##########################################################################

#################
### Bolt head ###
#################
mdb.models['Model-1'].parts['Head'].seedPart(deviationFactor=0.1,
    minSizeFactor=0.1, size=mesh_head)

mdb.models['Model-1'].parts['Head'].setMeshControls(elemShape=TET,
regions=
    mdb.models['Model-1'].parts['Head'].cells
    , technique=FREE)

mdb.models['Model-1'].parts['Head'].setElementType(elemTypes=(ElemType
(
    elemCode=UNKNOWN_HEX, elemLibrary=EXPLICIT), ElemType(
    elemCode=UNKNOWN_WEDGE, elemLibrary=EXPLICIT),
    ElemType(elemCode=C3D10M,
    elemLibrary=EXPLICIT, secondOrderAccuracy=OFF,
    distortionControl=DEFAULT)),
    regions=(mdb.models['Model-1'].parts['Head'].cells, ))

mdb.models['Model-1'].parts['Head'].generateMesh()

#############################
### Untreaded part of bolt ###
#############################
# Element size
mdb.models['Model-1'].parts['Shank'].seedPart(deviationFactor=0.1,
    minSizeFactor=0.1, size=mesh_shank)

# Mesh technique
mdb.models['Model-1'].parts['Shank'].setMeshControls(algorithm=MEDIAL_
AXIS,

    regions=mdb.models['Model-1'].parts['Shank'].cells.findAt(((1.0419
```

```
    69, 0.0,
    7.259574), )))

# Element type
mdb.models['Model-1'].parts['Shank'].setElementType(elemTypes=(ElemTyp
e(
    elemCode=C3D8R, elemLibrary=EXPLICIT, secondOrderAccuracy=OFF,
    kinematicSplit=AVERAGE_STRAIN, hourglassControl=ENHANCED,
    distortionControl=DEFAULT, elemDeletion=ON),
    ElemType(elemCode=C3D6,
    elemLibrary=EXPLICIT), ElemType(elemCode=C3D4,
    elemLibrary=EXPLICIT)),
    regions=(mdb.models['Model-1'].parts['Shank'].cells, ))

mdb.models['Model-1'].parts['Shank'].generateMesh()

############################
### Threaded part of bolt ###
############################
# Circular PARTITION for structured mesh
mdb.models['Model-1'].ConstrainedSketch(gridSpacing=1.12,
name='__profile__',
    sheetSize=44.82, transform=
    mdb.models['Model-1'].parts['ThreadedShaft'].MakeSketchTransform(

    sketchPlane=mdb.models['Model-1'].parts['ThreadedShaft'].faces.fin
    dAt((
    0.0, -l_tie-l_chamfer, 0.0), ), sketchPlaneSide=SIDE1,

    sketchUpEdge=mdb.models['Model-1'].parts['ThreadedShaft'].datums[x
    _axis.id],
    sketchOrientation=RIGHT, origin=(0.0, 0.0, 0.0)))
mdb.models['Model-1'].parts['ThreadedShaft'].projectReferencesOntoSket
ch(
    filter=COPLANAR_EDGES, sketch=
    mdb.models['Model-1'].sketches['__profile__'])
mdb.models['Model-1'].sketches['__profile__'].CircleByCenterPerimeter(
center=(
    0.0, 0.0), point1=(0.0, d_inner/2-4*mesh_thread_bolt))
mdb.models['Model-1'].parts['ThreadedShaft'].PartitionFaceBySketch(fac
es=

    mdb.models['Model-1'].parts['ThreadedShaft'].faces.findAt(((d_inne
    r/2-4*mesh_thread_bolt-eps,
    -l_tie-l_chamfer, 0.0), )),
    sketch=mdb.models['Model-1'].sketches['__profile__'],

    sketchUpEdge=mdb.models['Model-1'].parts['ThreadedShaft'].datums[x
    _axis.id])
mdb.models['Model-1'].parts['ThreadedShaft'].PartitionCellByExtrudeEdg
e(cells=

    mdb.models['Model-1'].parts['ThreadedShaft'].cells.findAt(((d_inne
    r/2-4*mesh_thread_bolt-eps,
    -l_tie-l_chamfer, 0.0), )), edges=(

    mdb.models['Model-1'].parts['ThreadedShaft'].edges.findAt((d_inner
    /2-4*mesh_thread_bolt, -l_tie-l_chamfer, 0.0),
    ), ),
    line=mdb.models['Model-1'].parts['ThreadedShaft'].datums[y_axis.id
    ], sense=
    FORWARD)

# Assign tetrahedal elements to all cells
mdb.models['Model-1'].parts['ThreadedShaft'].setMeshControls(elemShape
=TET,
    regions=mdb.models['Model-1'].parts['ThreadedShaft'].cells,
    technique=FREE)
mdb.models['Model-1'].parts['ThreadedShaft'].setElementType(elemTypes=
(
    ElemType(elemCode=UNKNOWN_HEX, elemLibrary=EXPLICIT), ElemType(
    elemCode=UNKNOWN_WEDGE, elemLibrary=EXPLICIT),
```

```
    ElemType(elemCode=C3D10M,
    elemLibrary=EXPLICIT, secondOrderAccuracy=OFF,
    distortionControl=DEFAULT,
    elemDeletion=ON)), regions=(
    mdb.models['Model-1'].parts['ThreadedShaft'].cells, ))

# Meshing bolt threads
mdb.models['Model-1'].parts['ThreadedShaft'].seedPart(deviationFactor=
0.1,
    minSizeFactor=0.1, size=mesh_thread_bolt)

# mdb.models['Model-1'].parts['ThreadedShaft'].generateMesh()

############
### Nut ###
############
# Assign tetrahedal elements to all cells
mdb.models['Model-1'].parts['Nut'].setMeshControls(elemShape=TET,
    regions=mdb.models['Model-1'].parts['Nut'].cells, technique=FREE)
mdb.models['Model-1'].parts['Nut'].setElementType(elemTypes=(
    ElemType(elemCode=UNKNOWN_HEX, elemLibrary=EXPLICIT), ElemType(
    elemCode=UNKNOWN_WEDGE, elemLibrary=EXPLICIT),
    ElemType(elemCode=C3D10M,
    elemLibrary=EXPLICIT, secondOrderAccuracy=OFF,
    distortionControl=DEFAULT,
    elemDeletion=ON)), regions=(
    mdb.models['Model-1'].parts['Nut'].cells, ))

# Global element size for outer part (big element size)
mdb.models['Model-1'].parts['Nut'].seedPart(deviationFactor=0.1,
    minSizeFactor=0.1, size=mesh_outer_nut)

# Meshing threads of nut in smaller elements
mdb.models['Model-1'].parts['Nut'].seedEdgeBySize(constraint=FINER,

    edges=mdb.models['Model-1'].parts['Nut'].edges.getByBoundingCylind
    er((0.0, 0.0, -eps),(0.0, 0.0,
    h_nut+eps),(d_chamfer_nut/2+3*mesh_thread_nut+eps)), size=
    mesh_thread_nut)

# mdb.models['Model-1'].parts['Nut'].generateMesh()

##################
### Grip Plate ###
##################
# Make partition into 4 slices for better meshing
datum_grip_YZ=mdb.models['Model-1'].parts['GripPlate'].DatumPlaneByPri
ncipalPlane(offset=
    0.0, principalPlane=YZPLANE)
datum_grip_XZ=mdb.models['Model-1'].parts['GripPlate'].DatumPlaneByPri
ncipalPlane(offset=
    0.0, principalPlane=XZPLANE)

mdb.models['Model-1'].parts['GripPlate'].PartitionCellByDatumPlane(cel
ls=
    mdb.models['Model-1'].parts['GripPlate'].cells, datumPlane=
    mdb.models['Model-1'].parts['GripPlate'].datums[datum_grip_XZ.id])
mdb.models['Model-1'].parts['GripPlate'].PartitionCellByDatumPlane(cel
ls=
    mdb.models['Model-1'].parts['GripPlate'].cells, datumPlane=
    mdb.models['Model-1'].parts['GripPlate'].datums[datum_grip_YZ.id])

# Assign quadratic elements to all cells
mdb.models['Model-1'].parts['GripPlate'].setMeshControls(algorithm=
    ADVANCING_FRONT, regions=
    mdb.models['Model-1'].parts['GripPlate'].cells, technique=SWEEP)
mdb.models['Model-1'].parts['GripPlate'].setElementType(elemTypes=(Ele
mType(
    elemCode=C3D8R, elemLibrary=EXPLICIT, secondOrderAccuracy=OFF,
    kinematicSplit=AVERAGE_STRAIN, hourglassControl=DEFAULT,
    distortionControl=DEFAULT), ElemType(elemCode=C3D6,
    elemLibrary=EXPLICIT),
```

```
    ElemType(elemCode=C3D4, elemLibrary=EXPLICIT)), regions=(
    mdb.models['Model-1'].parts['GripPlate'].cells, ))

# Seed element size of grip plate
mdb.models['Model-1'].parts['GripPlate'].seedPart(deviationFactor=0.1,

    minSizeFactor=0.1, size=mesh_grip)

mdb.models['Model-1'].parts['GripPlate'].generateMesh()

##################################################################
###################### Tie bolt togheter ########################
##################################################################

# Make surface on bolt head
mdb.models['Model-1'].parts['Head'].Surface(name='BoltHeadTieConstrain
tSurface', side1Faces=
    mdb.models['Model-1'].parts['Head'].faces.findAt(((0.0, 0.0,
    0.0), )))

# Make surfaces on shaft
mdb.models['Model-1'].parts['Shank'].Surface(name=
    'ShankToHeadTieConstraintSurface', side1Faces=
    mdb.models['Model-1'].parts['Shank'].faces.findAt(((0.0, 0.0,
    0.0), )))

mdb.models['Model-1'].parts['Shank'].Surface(name=
    'ShankToThreadTieConstraintSurface', side1Faces=
    mdb.models['Model-1'].parts['Shank'].faces.findAt(((0.0,
    l_unthread-l_tie-l_chamfer,
    0.0), )))

# Make surface on threaded shaft
mdb.models['Model-1'].parts['ThreadedShaft'].Surface(name=
    'ThreadToShankTieConstraintSurface', side1Faces=
    mdb.models['Model-1'].parts['ThreadedShaft'].faces.findAt(((0.0,
    -l_tie-l_chamfer,
    0.0), ), ((d_inner/2+eps, -l_tie-l_chamfer, 0.0), ), ))


# Tie constraint between head and shaft (y=l_unthread)
mdb.models['Model-1'].rootAssembly.regenerate()
mdb.models['Model-1'].Tie(adjust=ON,
constraintEnforcement=SURFACE_TO_SURFACE,
    master=

    mdb.models['Model-1'].rootAssembly.instances['Shank-1'].surfaces['
    ShankToHeadTieConstraintSurface']


    , name='ShankToHeadTieConstraint',
    positionToleranceMethod=COMPUTED, slave=

    mdb.models['Model-1'].rootAssembly.instances['Head-1'].surfaces['B
    oltHeadTieConstraintSurface']
    , thickness=ON, tieRotations=ON)

# Tie constraint between shaft and threaded shaft (y=0)
mdb.models['Model-1'].Tie(adjust=ON,
constraintEnforcement=SURFACE_TO_SURFACE,
    master=

    mdb.models['Model-1'].rootAssembly.instances['ThreadedShaft-1'].su
    rfaces['ThreadToShankTieConstraintSurface']
    , name='ThreadToShankTieConstraint',
    positionToleranceMethod=COMPUTED,
    slave=

    mdb.models['Model-1'].rootAssembly.instances['Shank-1'].surfaces['
    ShankToThreadTieConstraintSurface']
    , thickness=ON, tieRotations=ON)
mdb.models['Model-1'].constraints['ThreadToShankTieConstraint'].swapSu
```

```
rfaces() # Changing master/slave due to warning message

##################################################################
############################ Output ##############################
##################################################################
# Output data for visualize fracture
mdb.models['Model-1'].fieldOutputRequests['F-Output-1'].setValues(vari
ables=(
    'S', 'SVAVG', 'PE', 'PEVAVG', 'PEEQ', 'PEEQVAVG', 'LE', 'U',
    'V', 'A',
    'RF', 'CSTRESS', 'DMICRT', 'EVF', 'STATUS'))

# Total force
mdb.models['Model-1'].HistoryOutputRequest(createStepName='BomDisplace
ment',
    name='TotalForce', rebar=EXCLUDE, region=

    mdb.models['Model-1'].rootAssembly.allInstances['GripPlate-1'].set
    s['FixedGripSet']
    , sectionPoints=DEFAULT, timeInterval=0.5, variables=('RF2', ))

##################################################################
############################ Job #################################
##################################################################
```